EFFICIENT SYNTHESIS OF NOVEL NEAR IR EMITTING DISTYRYL-BORADIAZAINDACENE SENSITIZERS FOR PHOTODYNAMIC THERAPY

A THESIS SUBMITTED TO
THE GRADUATE SCHOOL OF NATURAL AND APPLIED SCIENCES
OF
THE MIDDLE EAST TECHNICAL UNIVERSITY

BY

ZEYNEP DOST

IN PARTIAL FULFILLMENT OF THE REQUIREMENTS
FOR
THE DEGREE OF MASTER OF SCIENCE
IN
THE DEPARTMENT OF CHEMISTRY

JUNE 2006

Approval of the Graduate School of Natural and Applied Sciences

_____

Prof. Dr. Canan Özgen
Director

I certify that this thesis satisfies all requirements as a thesis for the degree of Master of Science.

_____

Prof. Dr. Hüseyin İşçi
Chairmen of the Department

This is to certify that we have read this thesis and in our opinion, it is fully adequate, in scope and quality, as a thesis for the degree of Master of Science.

_____

Prof. Dr. Engin U. Akkaya
Supervisor

Examining Committee Members

Prof. Dr. İdris M. Akhmedov (METU, CHEM) _____

Prof. Dr. Engin Umut Akkaya (METU, CHEM) _____

Prof. Dr. Metin Zora (METU, CHEM) _____

Prof. Dr. Deniz Üner (METU, CHE) _____

Asst. Prof. Dr. Neslihan Şaki (KOCAELİ UNI., CHEM) _____

I hereby declare that all information in this document has been obtained and presented in accordance with academic rules and ethical conduct. I also declare that, as required by these rules and conduct, I have fully cited and referenced all material and results that are not original to this work.

Name, Last name : Zeynep DOST

Signature :

To my aunt and my grandmother

ABSTRACT

EFFICIENT SYNTHESIS OF NOVEL NEAR IR EMITTING DISTYRYL-BORADIAZAINDACENE SENSITIZERS FOR PHOTODYNAMIC THERAPY

ZEYNEP DOST

M. S., Department of Chemistry

Supervisor: Prof. Dr. Engin U. AKKAYA

June 2006, 91 pages

Photodynamic therapy (PDT) is a noninvasive method of treating malignant tumors and age-related macular degeneration. Current practice of PDT is limited to a few functionalized porphyrins, however these compounds are not considered to be ideal drugs for use in PDT. Among the limitations, the most prominent is the low extinction coefficient of porphyrins in the body's therapeutic window. Therefore, there is a significant impetus to develop novel and better efficiency sensitizers for use in PDT.

Boradiazaindacenes (BODIPY dyes or difluoroboradipyrrines) are well known fluorescent dyes. We discovered novel distyryl-derivatized boradiazaindacene dyes. These dyes have strong absorptions beyond 650nm. In order to transform these novel dyes into potential PDT reagents, bromine substituents were placed and then heavy atom effect was showed. We also demonstrated that on red-light excitation, singlet oxygen trap 1,3-diphenyl-*iso*-benzofuran is rapidly degraded.

Keywords: sensitizer,boradiazaindacenes dyes, singlet oxygen, photodynamic therapy.

ÖZ

FOTODİNAMİK TERAPİDE KULLANIMA YÖNELİK YENİ YAKIN IR EMİSYONU OLAN DİSTİRİLBORADİAZA-İNDASENLERİN ETKİN SENTEZİ

ZEYNEP DOST
Yüksek Lisans, Kimya Bölümü
Tez Yöneticisi: Prof. Dr. Engin U. AKKAYA

Haziran 2006, 91 sayfa

Fotodinamik terapi (PDT) kötü huylu tümörlerin ve yaşlılıkla ilişkili maküler dejenerasyon tedavisinde kullanılan non-invazif bir yöntemdir. PDT'nin bugünkü uygulanışı bir kaç porfirin türevi ile sınırlıdır. Ancak porfirinlerin PDT için ideal ilaçlar olmadığı bilinmektedir. Porfirinlerle ilgili sorunlardan belki de en önemlisi, bu maddelerin vücudun terapötik penceresi olarak bilinen spektral bölgede zayıf soğurma katsayılarına sahip olmalarıdır. Bu nedenle yeni ve daha etkin PDT reaktifleri geliştirmek için güçlü bir motivasyon vardır.

Boradiazaindasenler (BODIPY ya da difloroboradiprinler olarak da bilinirler) çok iyi bilinen floresan boyar maddelerdir. Bu çalışma sırasında distirilboradiazaindasenlerin bir sentez yöntemini geliştirdik. Bu boyar maddelerin 650 nm'nin ilerisinde kuvvetli absorbsiyonları vardır. Bu yeni boyar maddeleri potansiyel PDT reaktiflerine dönüştürmek için boradizaindasen sisteme ağır atom etkisi oluşturan Brom atomları yerleştirdik. Ayrıca kırmızı ışık ile uyararak siglet oksijen tuzağı 1,3-difenilizobenzofuran hızla azaldığını göstermiş bulunuyoruz.

Anahtar kelimeler: sensitizer, boradiazaindasen boyar maddeleri, singlet oksijen, fotodinamik terapi.

ACKNOWLEDGEMENTS

I would like to express my deep gratitude to my supervisor Prof Dr. Engin U. Akkaya for his guidance, support and patience during the course of this research as well as his unlimited knowledge and experience that I have benefited from greatly.

I wish to thank to our laboratory members Erhan, Serdar, Ali, Deniz, Burçak, Handan, Ceyda, Bora, İlker, Ruslan, Seçil for their help and friendship.

I want to express my sincere thanks to my parents and my fiancé for their continuous support, confidence and encouragement that make this work possible.

TABLE OF CONTENTS

LIST OF TABLES

TABLES

LIST OF FIGURES

FIGURES

CHAPTER I

INTRODUCTION

1.1. Supramolecular Chemistry

In 1978, Jean-Marie Lehn introduced the modern concept of supramolecular chemistry, which he defined as the "...chemistry of molecular assemblies and of the intermolecular bond,"[1] although the term itself made a much earlier appearance (in *Webster's Dictionary* in 1903). Traditionally, phrases such as "chemistry beyond the molecule," "the chemistry of the non-covalent bond," and "non-molecular chemistry" or even "Lego chemistry" were also used to describe the field. In the beginning, supramolecules mainly comprised two components, a host a guest, which interact with one another in a noncovalent fashion (Fig.1). The area rapidly evolved to encompass molecular devices and molecular assemblies. More recently (2002), Lehn added a further functional definition: "Supramolecular Chemistry aims at developing highly complex chemical systems from components interacting by non-covalent intermolecular forces."[2] The current emphasis is thus on increasing complexity and, hence, increasingly sophisticated functionality, and on the information stored in molecular components that allows this complexity to be achieved.

Fundamentally, supramolecular chemistry concerns the mutual interaction of molecules or molecular entities with discrete properties. This interaction is usually of a noncovalent type (an "intermolecular bond," such as a hydrogen bond, dipolar interaction or ππ-stacking). Key to many definitions of supramolecular chemistry is a sense of modularity. Supramolecules, in the broad sense, are aggregates in which a number of components (of one or more type) come together, either spontaneously or by design, to form a larger entity with properties derived from its components.

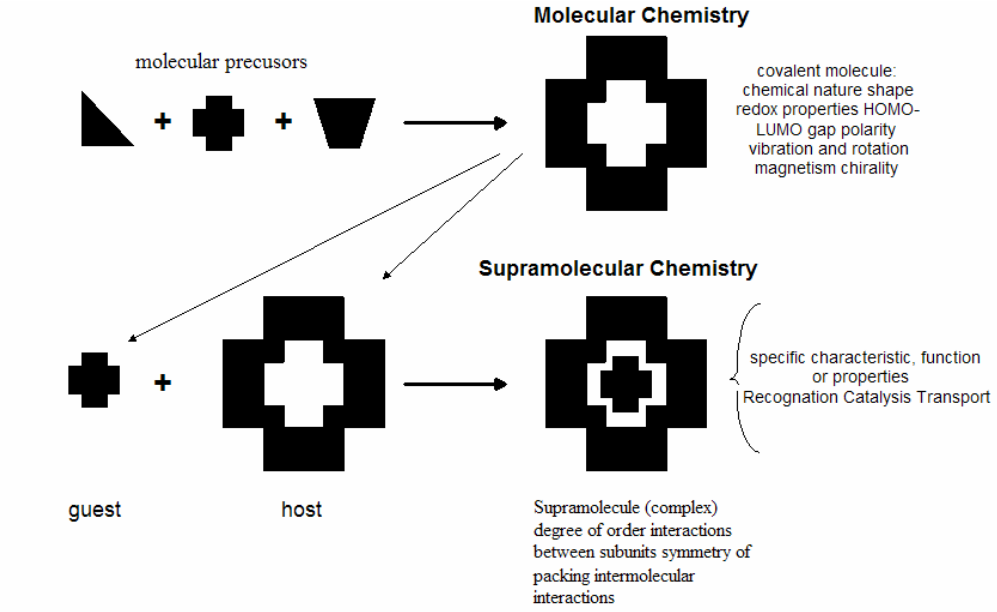

Figure 1: Comparison between the scope of molecular and supramolecular chemistry according to Lehn [2].

These aggregates can be of the host-guest type in which one molecule encapsulates the other, or self-complementary, components of similar size, in which there is no host or guest (Fig. 2).

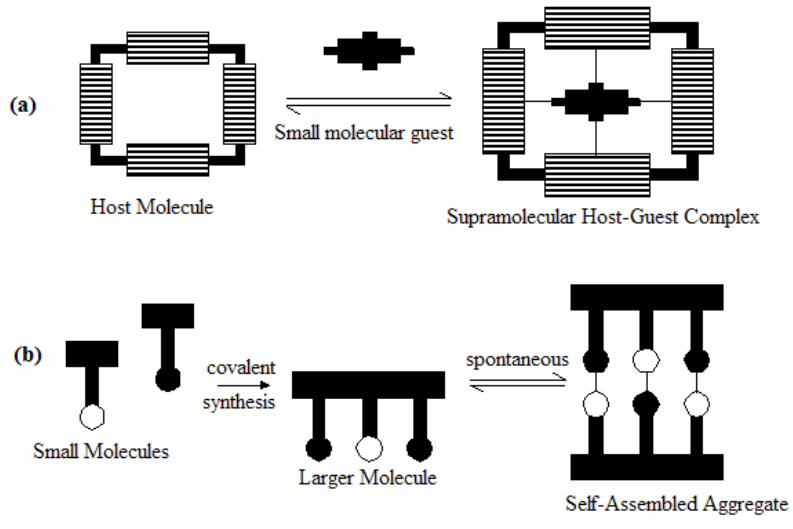

Figure 2: The development of a supramolecular system from molecular building blocks. **(a)** Host-guest complexation and **(b)** Assembly between complementary species (circles represent binding sites).

1.2. Photodynamic Therapy

Photodynamic therapy (PDT) is one of the noninvasive ways of treating malignant tumors or macular degeneration.[3] PDT is based on the delivery of a photosensitizer (PS) to the target tissue, after the administration of PS, Photoirradiation by appropriate laser light generates highly reactive oxygen species, such as singlet oxygen, which results in the oxidative destruction of target tissue. There are several kinds of already developed PSs for the clinical evaluation of their photodynamic efficacy. Most of the conventional PSs have large π-conjugation domains to extend their absorption cross sections and basically have hydrophobic characteristics. Therefore, PSs form aggregates easily, which produce the self-quenching of the excited state, in aqueous medium because of their π-π interaction and hydrophobic characteristics. To improve the photodynamic efficacy, the efficient delivery of PSs and high quantum yield of the singlet oxygen generation are significantly important.

Photodynamic therapy (PDT) has been developed as a cancer therapy over the last 25 years and has regulatory approval in many countries for cancers of the lung, digestive tract, and genitourinary tract using Photofrin as a photosensitizer.[4-7] PDT with Photofrin is also being evaluated as a protocol for treating cancers of the head and neck region [8] and for treating pancreatic cancer.[9] An ideal photodynamic reagent should possess these qualities: high extinction coefficient beyond 630 nm, good singlet oxygen yield, low dark toxicity, constant composition (no isomeric mixtures), straightforward synthesis, appropriate solution behavior. The development of second generation photosensitizers is a very active research field and many non-porphyrin reagents are proposed. Among these, phthalocyanines and naphtocyanines [10, 11], texaphyrins [12], squarines [13, 14], azadipyromethanes [15, 16] should be mentioned.

1.2.1. History of PDT

The effect was discovered in the winter semester of 1897-98 at the Ludwig-Maximillian University in Munich where Oscar Raab was a medical student. He observed, using law concentrations of acridine (Figure 3) as the photosensitizer, that

the paramecia which are unicellular organisms of the Protista class were killed in the presence of daylight, but that in darkness they survived. The result was published in 1900 and stimulated much further activity, so that by 1903 von Tappeiner and Jodlbauer were proposing various dermatological applications for photosensitizers (such as eosin Figure 4) some of which they demonstrated. In 1904, von Tappeiner and Jodlbauer used the term "photodynamische wirkung" for the first time, emphasizing the requirement for oxygen in the process. This German term has been generally translated as "photodynamic action".

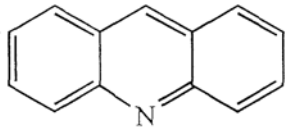

Figure 3: Structure of Acridine

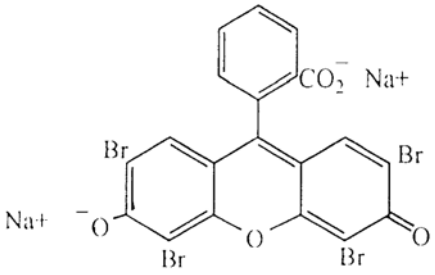

Figure 4: Structure of Eosin Y

Experiments followed in rapid succession extending the variety of living systems and photosensitizers studied. Clearly the subject had caught the scientific imagination. Using the photohaemolysis of erythrocytes as a model, Hasselbach showed in 1909 that the photosensitizer increased the rate of the photoreaction only in the presence of oxygen, confirming the earlier conclusions of von Tappeiner and Jodlbauer. In Hans Fischer's organic research laboratory in Munich (1912) it was shown that haematoporphyrin had a strong photodynamic effect in the mouse

Friedrich Meyer-Betz had become familiar with the phototoxicity of haematoporphyrin in the mouse. Working In the medical clinic at Königsberg he carried out a remarkable experiment on himself.

Between 5.45 am and 6.15 am on October 14th 1912 Meyer-Betz injected himself intravenously with 200 mg of haematoporphyrin. (The porphyrin was dissolved in 10 ml of 0.1 M NaOH, and diluted with 300 ml of physiological saline, the whole being heat and filter sterilized). The next day was overcast, and nothing spectacular occurred. However October 16th 1912 was a sunny day in Königsberg and a photosensitized reaction set in - a prickling and burning sensation, with those regions of his body which had been exposed to sunlight developing erythema (reddening) and oedema (swelling), which intensified. Meyer-Betz had exposed the right side of his face more than the left side. By October 19th the swelling had receded somewhat, but the photosensitivity remained for several weeks until the haematoporphyrin (which was probably not a pure substance) had worked its way out of his body. In the gloom of the Königsberg winter the effects were not observed, and by the spring of 1913 the sensitization had disappeared. In modern health and safety terms this has to be regarded as a very foolhardy experiment (especially with such a massive dose), but nonetheless, at a time when such heroic experiments were not regarded as unexceptionable, it did demonstrate very clearly the photodynamic effect of porphyrin sensitizers in human beings.

In 1920s, Policard noted that tumor tissue was inherently more fluorescent than healthy tissue [17].

Between 1940 and 1960, Figger et al [18-20] and Rasmussen-Taxdal et al administered natural porphyrins to patients and tumor-bearing animals, an attempt to more accurately detect tumor tissue by fluorescence.

During the 1960s Winkelman used synthetic porphyrins (tetraphenyl porphyrines) to detect tumor tissue [21-24].

Throughout the 20th century a few attempts were made to treat tumor tissue with nonporphyrin photosensitizers.

Weishaupt et al identified the cytotoxic product of the photochemical reaction to be singlet oxygen [25].

Porphyrin photosensitizers were then examined as photosensitizers because they can efficiently generate singlet oxygen and have absorption maxima in the red

portion of the electromagnetic spectrum. Eventually Dougherty rediscovered Schwartz's haematoporphyrin derivative, which by then was known to have a high singlet oxygen quantum yield, an absorption maximum in the red, and is selectively retained in tumor tissue [25]. After several years spent isolating and identifying the active fractions of HpD, a purified version named photofrin, was produced. In the following years, photofrin was approved for use in the United States against early- and late-stage lung cancers and esophageal cancers and dysplasias with other indications pending. Nearly 10000 patients in some countries have been used for this work.

Since Photofrin has gained legal status many of mechanisms by which PDT works have been elucidated, many new photosensitizers have been created [26, 27] and research and development continues.

1.2.2. Cancer

The phototherapy of cancer is essentially photodynamic therapy, requiring visible light, a photosensitizer and oxygen. Photodynamic therapy (PDT) involves the use of photochemical reactions mediated through the interaction of photosensitizing agents, light, and oxygen for the treatment of malignant or benign diseases. PDT is a 2-step procedure. In the first step, the photosensitizer is administered to the patient by one of several routes (e.g. topical, oral, intravenous), and it is allowed to be taken up by the target cells. The second step involves the activation of the photosensitizer in the presence of oxygen with a specific wavelength of light directed toward the target tissue. Because the photosensitizer is preferentially absorbed by hyperproliferative tissue and the light source is directly targeted on the lesional tissue, PDT achieves dual selectivity, minimizing damage to adjacent healthy structures.

PDT is mediated by oxygen-dependent photochemical reactions. Upon absorption of photons of light, the photosensitizer is excited to a short-lived singlet state followed by a transition to the reactive triplet state. From its triplet state in the presence of oxygen, reactive free radicals and singlet oxygen species ensue. These, in turn, react with cell membranes, causing direct damage to the mitochondria, endoplasmic reticulum, and/or plasma membranes [28-30].

1.3. Photodynamic Action

Photodynamic action refers to the damage or destruction of living tissue by visible light in the presence of a photosensitizer and oxygen. In principal, light in the very near infrared region could be employed, but photosensitizers absorbing there are rather uncommon, and in most cases irradiation is visible light. The light source may be incoherent (e.g. a tungsten lamp) or coherent (e.g. a laser): the sensitizer must absorb the light and the excited sensitizer then activates oxygen in some way.

1.3.1. Light

In order to come to an appreciation of the nature electromagnetic radiation, of which visible light is a small part, it is necessary to be able to think of it as a form of energy which can be expressed both as a wave and as a particle (quantum, photon). The wave approach allows a treatment of light propagation, refraction, diffraction and polarization, whereas the particle approach is suited for an understanding of absorption and emission phenomena.

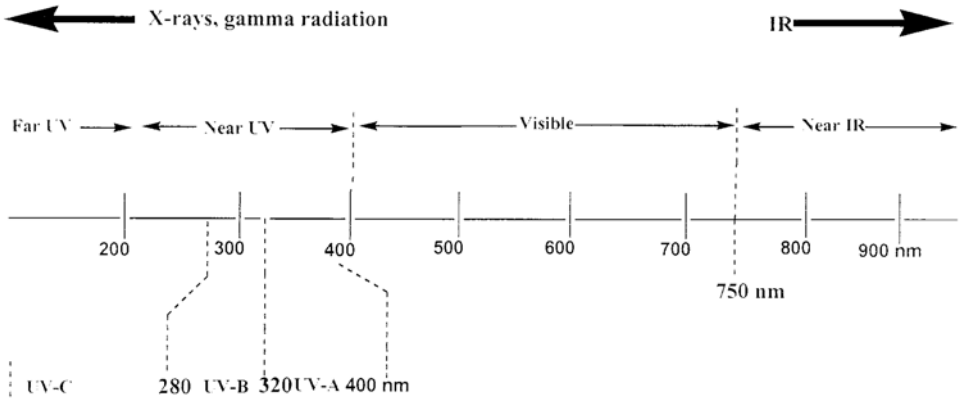

Figure 5: The Electromagnetic Spectrum, showing particularly the Near-UV, Visible and Near-IR Regions in which occur The Principal Electronic Transitions of Interest in Phototherapy.

The place of visible light in the electromagnetic spectrum is shown in Figure 5. Electromagnetic radiation can be interpreted in terms of a transverse plane of

wavelength λ associated with electric and magnetic fields, the vectors of which are in planes perpendicular to one another and to the direction of propagation. The wavelength of visible light falls in the range 400-750 nm: 400 nm we see as indigo, and 750 nm we see as red.

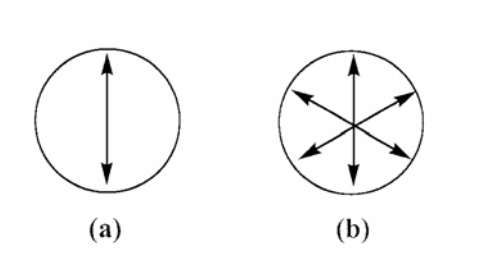

Figure 6: Representation of electromagnetic radiation in terms of sinusoidal electric and magnetic fields, the vectors of which are at right angles to one another and to the direction of propagation. For simplicity, plane polarized light is shown. The circles represent the transverse wave in (a) polarized and (b) unpolarized light, looking down the axis of propagation.

At higher energies the near ultra-violet region extends to 200 nm beyond which vacuum spectrometers are required because of absorption by air. Photobiologists divide the near ultraviolet region into three parts, thus;

UV-A	320-400 nm
UV-B	280-320 nm
UV-C	< 280 nm

This division in terms of photobiology is useful in relation to photodamage to living tissue. Energy per mole of photons (called an einstein) increases from A to C. Thus whereas UV-A is relatively harmless, by the point at which UV-B is reached a sunburn reaction occurs in humans, and this is the region that sun creams are designed. The DNA bases and certain α-amino acid side chains (e.g. tryptophan and tyrosine) have broad absorption maxima in the UV -C/UV -B region. Irradiation here does not penetrate far into tissue, but it can cause skin cancer. In the near infrared (~750-2000 nm) we find mainly vibrational and rotational transitions, but some

extended organic chromophores (e.g. naphthalocyanines) show electronic transitions as far out as this.

The wavelength (λ) of light may be expressed in various units. The wavelength can be used as nanometers (nm, 10^{-9} m, 10^{-7} cm). The Angstrom unit (A^0, 10^{-10}m) is also employed. Because of the relationship:

$$\nu = c / \lambda$$

Where *c* is the velocity of light ($3.00x10^{-10}$ cm s^{-1}) and *v* is the frequency (waves or cycles per second), it is also possible to refer to the light in terms of its frequency (units s^{-1}, or waves s^{-1}= Hertz, Hz). A variant is to employ wave numbers, another frequency unit (represented by *v).* This is reciprocal wavelength (1/λ), the units being $length^{-1}$, and generally cm^{-1}: hence it specifies the number of waves per centimeter.

It is a matter of custom and convenience which of these units is used, and they are readily interconverted. For example, the wavelength of 400 nm is equivalent to that is $0.75x10^{15}$ waves per second in frequency units; or 25000 waves for each centimeter, in wave number units.

Another way of talking about wavelength is in terms of energy, visualized as the energy of the corresponding photon. This is a switch to the quantum approach, and illustrates the intermingling of the wave and particle concepts. Energy is given by the equation:

$$E = h\upsilon = \frac{hc}{\lambda}$$

Where E is the energy of the h is Planck's constant ($6.626x\ 10^{-34}$ Js). Continuing with the example of light at 400 nm, and expressing the result on a molar basis. The energy of the Avogadro number of photons at a given wavelength is sometimes referred to as the *Einstein*. Thus an Einstein of light of wavelength 400 nm is 299 kJ.

Several other energy units are employed, particularly kcal and electron volts: some workers prefer to use frequency units, which are linear with energy. When speaking of peak widths (e.g. width at half height) and peak separations (e.g. the separation of Bands I and III in porphyrin spectra; the Stokes shift) it makes sense to

use frequency units (usually cm^{-1}) so that if energetic regularities exist, they can emerge clearly. With these exceptions, we shall use kJ mol^{-1} for energy and nm for wavelength.

The total amount of light energy employed in a given photoprocess and the rate at which it is applied to the system are important parameters in both photochemistry and photomedicine. In chemistry it is the amount of light (number of quanta) absorbed which is important in deriving quantities such as quantum yield. In photobiology and photomedicine it is generally the amount of light arriving at the surface of a given object (referred to as light dose, precisely analogous to drug dose) that is measured, usually with a commercial light meter. (Sometimes the light is fractionated, that is, given as a series of short exposures with short dark intervals-a few seconds, perhaps). The quantities recorded are usually *fluence* and *fluence rate* but other terms are also employed.

Fluence is the total radiant energy traversing a small transparent imaginary spherical target containing the point under consideration, divided by the cross sectional area of the target.

Fluence rate (irradiance, power density) is the rate of *fluence.* Units: W cm^2. So *fluence* is the total energy arriving at a unit surface area, while *fluence rate* is the corresponding power or rate of energy (Power unit: 1 Watt = 1 Joule per second). Thus, in using m- THPC as a photosensitizer in cancer treatment, the *fluence* ('light dose') at 652 nm may typically be 20 Jcm^{-2} and the *fluence rate* is 100 $mWcm^{-2}$ (= 0.1 $Js^{-1}cm^{-2}$). The time of treatment is therefore 20/0.1 = 200 s, or just over three minutes.

1.3.2. Light Sources

Any light source either coherent (e.g. laser) or incoherent (e.g. nonlaser light) with suitable spectral characteristics and high output at an absorption maximum of the photosensitizer can be used in PDT.

1.3.2.1. Sunlight

It is evident from everyday observation that solar energy maintains life on Earth, and it is commonly thought to have been a key factor in the generation of that life. Photobiology is a rich subject, and much of it is related to sunlight but for the phototherapeutic purposes to be considered here, sunlight is neither convenient nor reliable enough for routine use.

1.3.2.2. Incandescent Lamps

These depend on a filament (e.g. tungsten) which is heated in an evacuated glass envelope by an electric current. Such lamps are inexpensive and have been used in PDT. In the phototherapy of neonatal hyperbilirubinemia fluorescent tubes have commonly been used but Ohmeda have recently developed a woven fiber optic pad (the Biliblanket^{R}) which wraps around the infant and which is supplied with light from a 100w quartz halogen bulb. Infrared and ultraviolet light are filtered out with filters and a dichroic reflector to give illumination in the required 400-550 nm region (bilirubin λ_{max} 450 nm).

1.3.2.3. Arc Lamps

The mercury arc lamp is the workhorse of organic photochemistry, and has some applications in photomedicine. There are three main types.

l- The low-pressure mercury arc operates at room temperature and about 10^{-3} mm pressure: the main emission is a single line at 253.7 nm.

2- Medium-pressure mercury lamps operate at about 1 atmosphere: the emission contains a number of lines, of which 366 nm and 546 nm are the principal ones.

3- The high-pressure mercury arc operates at ~100 atmospheres and is an intense source. Such lamps must be cooled, and even then have a short life.

Where it is desired to generate a narrow wavelength band from lamps (such as the xenon lamp just referred to, or the incandescent lamp), this can be done by using a monochromator or by using commercial filters. Water cuts out much of the infrared: 2mm of Pyrex glass effectively removes ultraviolet below ~300 nm. In

those cases where light has to be delivered to an internal site, the light is carried through a guide such as a fiber optic or a plastic tube full of liquid.

1.3.2.4. Light Emitting Diodes

Light-emitting diodes (LEDs) are III-IV semiconductor-based devices driven by an electric current. The emission is not coherent (this is not a laser source), and is low power, so not much heat is produced. Wavelength can be adjusted by changing the semiconductor, and the devices are small, but they can be bunched together to fit a particular structure. They are finding increasing application. Thus, the LED system recently announced by Diomed consists of a close-packed array of LEDs in a water-cooled head which is designed to be kept in contact with the area of treatment. The irradiation wavelength is 635 nm or 652 nm, with a fluence rate of up to 200 mW cm^{-2}.

1.3.2.5. Lasers

Laser is acronym for "light amplification by stimulated emission of radiation". "Stimulated" emission means the release of a photon by electronically excited species S^* on interaction with a photon,

$$S^* + h\upsilon \rightarrow S + 2h\upsilon$$

Laser emission has special properties some of which are important in photomedicine. The beam emerging from the laser is

(i) ***intense***. This leads to uses in laser surgery (e.g. the carbon dioxide laser emitting at 10600 nm) for cutting, abiating, and sealing. High intensity is not needed for PDT, however.

(ii) ***coherent***. This means all the waves, besides being of the same wavelength, are in phase.

(iii) ***deliverable in some cases in pulses of short duration*.** Pulses down to the femtosecond (10^{-15}s) range have allowed the study of initial events in photochemical and photobiological processes.

(iv) ***monochromatic***. This is a very useful characteristic, especially in tunable lasers where, for example, the wavelength can be set to the maximum of an intense absorption band of a photosensitizer.

(v) ***parallel beam.*** Further collimation is not required, and the beam can be conducted into and along a fiber optic, for example in an endoscope, with little loss of intensity.

Many lasers emit light at too long a wavelength for photochemical use, but the technique of *frequency doubling* can be employed to get into the useful UV-VIS region. Essentially, these are two-photon absorption processes, sequential not simultaneous, and require materials with non-linear optical properties. Thus, the emission from a ruby laser (694 nm) on passage through a range of the dye. Rhodamine 6G (Figure 7) is an example of such a dye: its fluorescence emission occurs over the range 570-620 nm and the dye laser is tunable over this region.

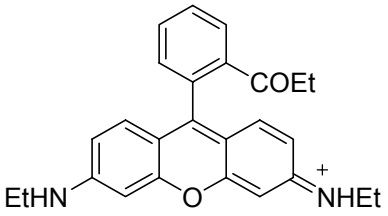

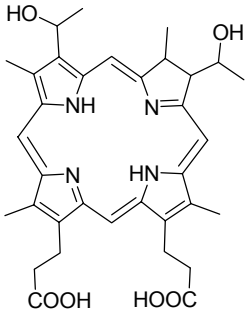

Figure 7: Structure of Rhodamine 6G **Figure 8:** Structure of Haematoporphyrin

One of the problems with conventional lasers is that they are expensive, they also need expert technical supervision and maintenance. The diode lasers which are now emerging are smaller and much cheaper, and look promising. They are based on semiconductors *(n - p* junctions activated electrically) and although most examples emit in the infrared, the range is rapidly being extended to the red region of the visible, which is needed for PDT applications. Thus, Diomed have produced diode lasers adapted for δ-ALA (AlGalnP~ 635 nm), mTHPC (InGaAIP, 652 nm), and lutetium texaphyrin (AlGaAs, 730 nm).

1.3.3. Light Absorption

1.3.3.1. The Beer-Lambert Law

The intensity of a light absorption band of a given substance in a stated solvent follows two laws. Lambert's law states that the fraction of light absorbed is independent of the incident radiant power; while Beer's Law relates that the amount of light absorbed is directly proportional to the concentration of the solution. Put together (Beer-Lambert law) in mathematical form this becomes:

$$\log_{10} \frac{P_0}{P} = A = \varepsilon cl = \log_{10} \frac{I_0}{I}$$

where P_0 and P are the incident and transmitted radiant powers (in common parlance called intensities, and represented by I_0 and I), *A* is the absorbance, ε is the molar absorption coefficient (also called by same the molar or molecular extinction coefficient), *c* is the concentration (mol l^{-1}) and *l* is the path length (in centimeters, so this is conveniently unity when the common 10mm cuvettes are used). The units of ε are therefore 1 mol^{-1} cm^{-1} (although they are often not stated).

Beer's Law usually holds well for dilute solution, but it breaks down in concentrated solution or under limiting solubility conditions when aggregation occurs.

1.3.3.2. Excitation

1.3.3.2.1. Multiplicity

Light absorption in the ultraviolet and visible region involves electronic transitions: a photon of a given energy interacts with the substrate molecule in its ground state (S_0) to cause an electron to be promoted from a bonding or non-bonding orbital to a higher energy orbital, normally an unoccupied antibonding orbital in organic molecules. The molecule is energized from its ground state to an electronically excited state.

Such excitation can formally result in two electronic configurations, which differ in multiplicity. Multiplicity is defined as 2S + 1, where *S* is the total spin of the system (Σ+/-1/2). The configurations in question are excited singlet and triplet states, and are shown in figure 9.

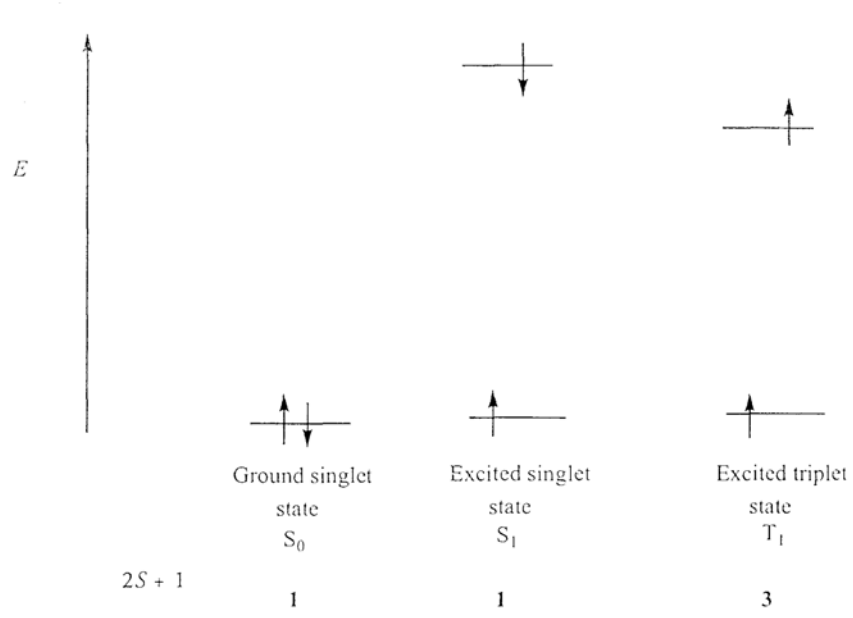

Figure 9: Multiplicity of ground and exited state: configuration of outer electrons shown.

1.3.3.2.2. Probability

The energy of a given transition is determined by its wavelength: the molar absorption coefficient gives the probability or allowedness of the transition. This is related to the area under the absorption band, but is commonly spoken of in terms of the value of ε_{max}. There are various features which cause a transition to be 'forbidden' i.e. less probable, so lowering ε:

(i) ***Spin****:* transitions involving a change in multiplicity (S → T, or T → S) are forbidden. This restriction can be relaxed in the presence of heavy atoms, paramagnetic species, and by spin-orbit coupling. Nevertheless the transition So → T_1 is strongly forbidden.

(ii) ***Space****:* orbitals involved in the transition need to overlap: they do so for the $\pi \rightarrow \pi^*$ transition of the carbonyl group, but not for the $n \rightarrow \pi^*$ transition, which is forbidden.

(iii) ***Symmetry****:* if the sign of the wavefunction changes on reflection through a centre of symmetry, then the symmetry is referred to as *ungerade* denoted *u:* if it is unchanged, it is termed *gerade* (German: even, direct) denoted *g*. Then $u \rightarrow g$ and $g \rightarrow u$ transitions are allowed, while $u \rightarrow u$ and $g \rightarrow g$ transitions are forbidden. Thus the $\pi \rightarrow \pi^*$ transition of the C = C double bond: is an allowed transition on the symmetry criterion. It occurs as an intense band at about 165 nm in ethylene.

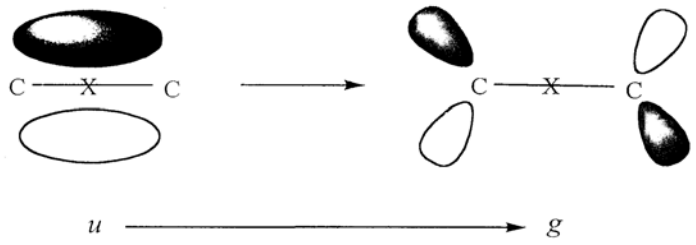

Figure 10: u → g transition

(iv) ***Momentum****:* transitions which cause a large change in linear or angular momentum of the molecule are forbidden.

1.3.4. Emission

Subsequent to excitation, the excited state, be it singlet or triplet, can do one or more of four things:

(i) It can emit a photon.

(ii) It can convert to a different state. Changes between states of the same multiplicity are called *internal conversion* (e.g. $S_1 \rightarrow So^v$, vibrationally excited ground state) while changes between states of different multiplicity (which are formally spin forbidden) are called *intersystem crossing* (e.g. $S_1 \rightarrow T_1$).

(iii) It can undergo a chemical reaction.

(iv) It can pass on its excitation to another (ground state) molecule (electronic excitation transfer).

Emission of a photon from the excited singlet state is called fluorescence, while emission from the triplet state is called phosphorescence. In both cases the wavelength of the light emitted is longer than the exciting wavelength, and in both cases the ground state, S_o, is reached. Since the change from the triplet, say $T_1 \rightarrow S_o$, is spin forbidden, this emission, and the triplet itself, are long-lived (typically ms -*s*): the $S_1 \rightarrow S_o$ emission is not spin forbidden, and fluorescence lifetimes, and lifetimes of the excited singlet state, are short (typically < μs).Because the triplet excited state is longer lived, it tends to be important in many photochemical reactions. Although fluorescence is easily observed in solution, phosphorescence is not: T_1 is sufficiently long lived to be deactivated by collision. Therefore phosphorescence has usually to be observed at low temperature in glasses such as EPA (ether: isopentane: ethanol = 5:5:2) which forms a transparent glass at 77 K.

The measurement of fluorescence is particularly important, since it is used both for detection and analysis. Fluorescence is measured with a spectrofluorimeter, which consists of a light source with a monochromator to provide the *excitation* wavelength. The cuvette is polished on all four sides since (unlike the cuvette in absorption spectroscopy where the beam is transmitted through the sample) in this case the emission is measured at right angles to the incident beam. The emitted beam is passed through a second monochromator and on to a detection device to generate the fluorescence spectrum.

Two types of spectrum can be obtained: the *excitation spectrum* is obtained by scanning the incident wavelengths for a set emission wavelength, while for the *emission spectrum* the dispersion of the emitted light is measured for a set exciting wavelength. Although fluorimetry is a very sensitive technique (metal-free porphyrins can be analyzed at 10^{-8} M) it has some drawbacks which need to be recognized. Chief among these is the quenching of the emission, which effect increases with concentration *(concentration quenching).* Variable emission also occurs on aggregation (which always reduces fluorescence) and on interaction with other chromophores, so that direct measurements *in vivo* are particularly subject to error. The best way to analyze for photosensitizer in tissue is to extract it into solvent, thus getting rid of the bulk of tissue components, before making the

fluorescence measurements. This is time consuming, and destroys the tissue: because of its sensitivity, convenience and non-invasive nature, direct fluorimetry *in vivo* is likely to remain popular in photobiology, in spite of its inherent ambiguities.

A last point on fluorescence, whereas compounds of the porphyrin photosensitizer class generally show strong red fluorescence. This is considerably reduced if a substituent with a high atomic number (such as iodine) is present *(heavy atom effect)*. In general, halogen substitution is found to increase ϕ_{isc} leading to enhanced yields of the triplet (and therefore high ϕ_{Δ}, as in eosin Y and rose bengal). For metalloporphyrins, fluorescence is quenched where the metal has an incomplete *d* shell, since the empty orbitals here offer a pathway for the rapid deactivation of the excited states. Thus, whereas zinc(II) porphyrins *(d_{10})* show strong orange-red fluorescence, complexes of the first transition series (including haems, of course) show no fluorescence to the naked eye.

1.3.5. Quantum Efficiency

Following the excitation process, the reaction process follows. The reaction process is actually a dark process which happens to the electronically excited species ie another photon is not required. Thus for substrate XYZ we have:

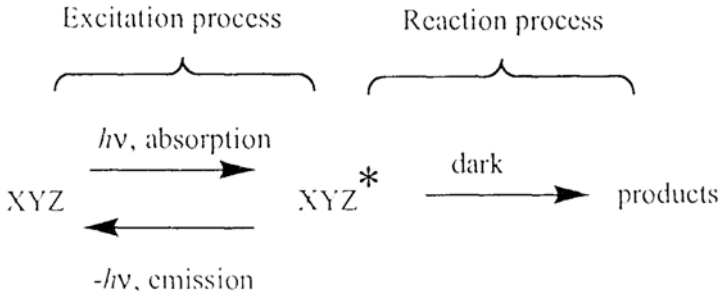

For practical purposes it is usually necessary to know the percentage yields of products in the conventional way i.e. based on the mass of XYZ. However, from a photochemical point of view it is also important to know how efficiently the product is generated in terms of the photons absorbed. This is given by the *quantum yield* which may be defined as

$$\phi_{\text{product}} = \frac{\text{number of molecules of product fromed per ml. per second}}{\text{number of quanta absorbed per ml. per second}}$$

Since quantum yield varies with wavelength, this quantity is most meaningfully measured with monochromatic light. $\phi_{product}$ cannot be greater than unity, and is sometimes very low. These results in long irradiation times, but these may still be acceptable if the overall chemical yield is good.

The idea of quantum yield can be usefully applied to the photophysical 'products' of the excitation process. Thus we have quantum yield of fluorescence ϕ_t. quantum yield of phosphorescence ϕ_p, quantum yield of intersystem crossing ϕ_{isc}. quantum yield of singlet ϕ_s and quantum yield of triplet ϕ_T. Again $\sum\phi_x < 1$. The ratio ϕ_p/ϕ_f covers an extensive range: > 1000 (ie efficient intersystem crossing) shown by dromatic kerones, for example; and < 1, shown by polycydic aromatic hydrocarbons. This is significant for the problem now to be considered.

1.3.6. Singlet Oxygen Quantum Yields

One of the ways in which singlet oxygen is generated is by electronic excitation transfer from suitable sensitizers, and it is this sort of photosensitizer that is used in photodynamic therapy. The process can be summarized as follows (Sens = Sensitizer):

$$\text{Sens } (S_o) \xrightarrow{hv} \text{Sens } (S_1) \xrightarrow{isc} \text{Sen } (T_1)$$

$$\text{Sen } (T_1) + {}^3O_2 \longrightarrow \text{Sens } (S_o) + {}^1O_2$$

This last equation is spin allowed, since the total spin is the same before and after reaction (Wigner rule), thus:

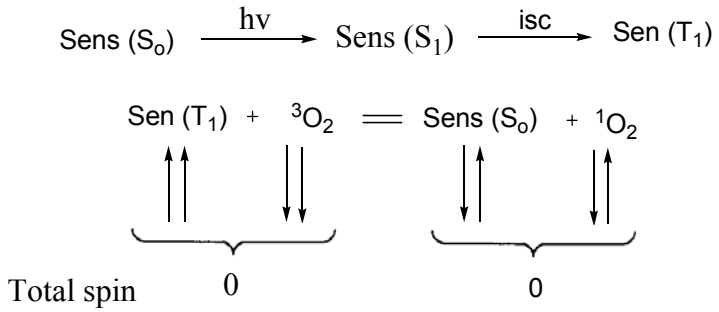

But to proceed effectively the energy of the T_1 state must be above 94 kJ mol^{-1}, the energy of singlet oxygen above its ground state.

The photochemical efficiency with which various photosensitizers generate singlet oxygen is the singlet oxygen quantum yield, denoted by ϕ_Δ. If singlet oxygen is derived only from the triplet of the sensitizer, it follows that ϕ_Δ must be less than ϕ_T; but in fact dioxygen is a very efficient quencher of many of these triplet states, and ϕ_Δ values are often not far short of ϕ_T. The ϕ_Δ values are substantial (>0.3) for many of the compounds quoted. However, for 8-methoxypsolen the quantum yield of singlet oxygen is low (0.009), and this substance is thought to act mainly by cycloaddition, not via production of singlet oxygen.

In principle, it is possible for the singlet oxygen quantum yield to reach a higher value than unity. This becomes feasible, for example, if both the $S_1 \rightarrow T_1$ and the $T_1 \rightarrow S_0$ energy gaps are about or somewhat larger than 94 kJ mol^{-1}, thus permitting the spin allowed in 1.4.2 processes:

1.4. Mechanism of Photodynamic Action

There are two broad mechanistic categories by which light, in the presence of a photosensitizer and dioxygen, can promote chemical reaction in a substrate, including damage to living tissue. They are referred to as Type I and Type II processes.

1.4.1. The Type I Mechanism-Electron Transfer

In this mechanism the excited state generates a radical species, for example by electron transfer from (or to) a substrate, or by hydrogen atom abstraction from a

substrate. The radical species then reacts with ground state oxygen so that overall the reaction is a photodynamically initiated autoxidation, thus:

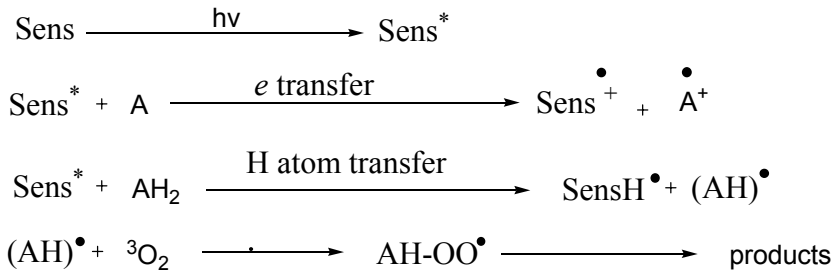

1.4.2. The Type II Mechanism-Energy Transfer

In this mechanism electronic excitation energy is transferred from the triplet of the sensitizer to triplet dioxygen, to give the sensitizer in its ground and singlet oxygen, thus:

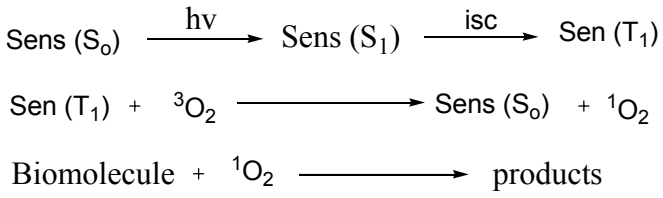

1.4.3. Distinguishing between Type I and Type II Photooxygenation Process

The distinction between the two mechanistic types is not easily made. And some of the so-called distinguishing tests (such as lifetime in deuteriated solvents, quenching by azide, detection of spin-trapped hydroxyl radical) do not reliably distinguish between singlet oxygen and superoxide and superoxide intermediates.

Once a molecule has absorbed energy in the form of electromagnetic radiation, there are a number of routes by which it can return to ground state (the statistically most common energy state for room temperature chemical species). The following graphic, termed a Jablonski diagram, shows a few of these processes.

If the photon emission (shown in as a short wavelength, that is downward pointing, "long" green line in the diagram) occurs between states of the same spin state (e.g. $S_1 \rightarrow S_0$) this is termed fluorescence. If the spin state of the initial and final

energy levels are different (e.g. $T_1 \rightarrow S_0$), the emission (loss of energy) is called phosphorescence. In the diagram this is depicted by a longer wavelength (lower energy) and therefore shorter length line. Since fluorescence is statistically much more likely than phosphorescence, the lifetimes of fluorescent states are very short (1×10^{-5} to 10^{-8} seconds) and phosphorescence somewhat longer (1×10^{-4}+ seconds to minutes or even hours; think about glow-in-the-dark flying disks).

Three nonradiative deactivation processes are also significant here: internal conversion (IC), intersystem crossing (ISC) and vibrational relaxation. Examples of the first two can be seen in the diagram. Internal conversion is the radiationless transition between energy states of the same spin state (compare with fluorescence-a radiative process). Intersystem crossing is a radiationless transition between different spin states (compare to phosphorescence). Vibrational relaxation, the most common of the three-for most molecules, occurs very quickly ($<1 \times 10^{-12}$ seconds) and is enhanced by physical contact of an excited molecule with other particles with which energy, in the form of vibrations and rotations, can be transferred through collisions. This means that most excited state molecules never emit any energy because in liquid samples the solvent or, in gas phase samples, other gas phase molecules that are present "steal" the energy before other deactivation processes can occur.

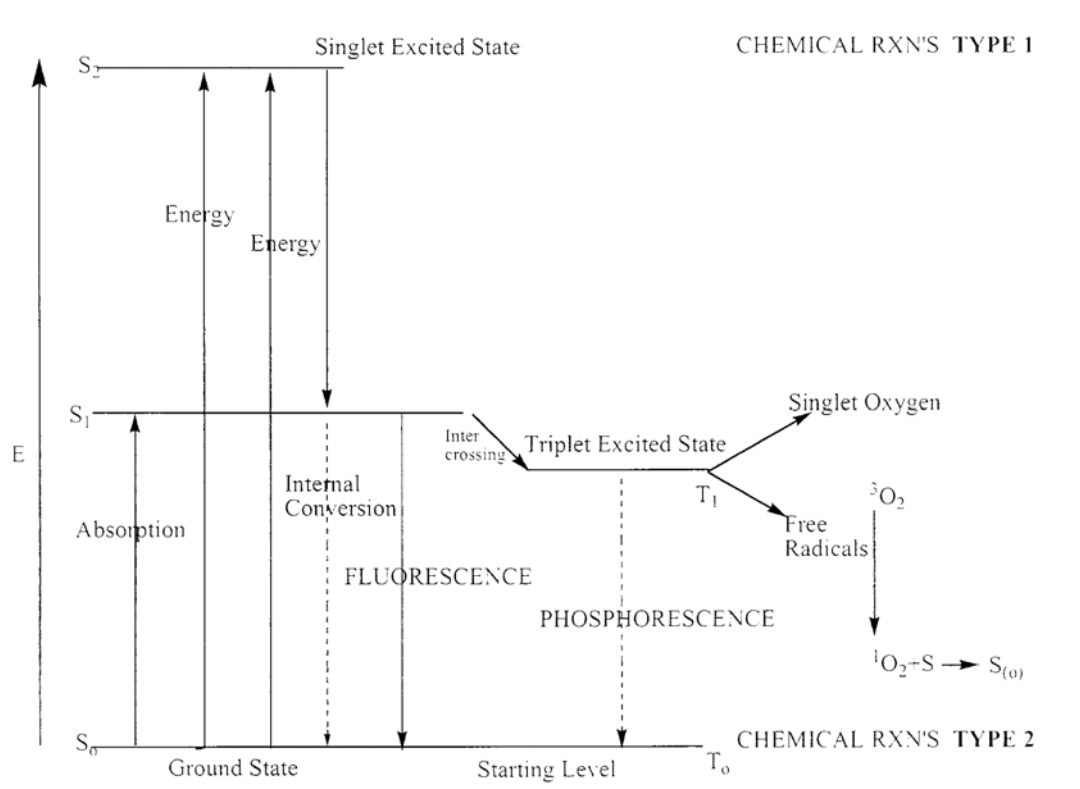

Figure 11: Jablonski Diagram- Showing origin of Type I and Type II photooxygenation processes.

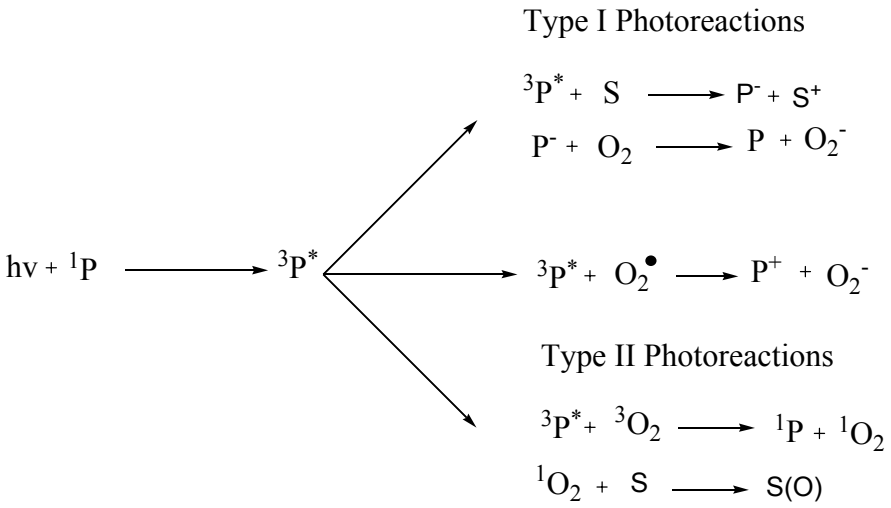

Although TypeII photoreactions are commonly associated with singlet oxygen production some other compounds have triplet-ground states and can be involved in Type-II photoreactions, among these are nitric oxide and vitamin A [28]. Although

Type II reactions are reported to dominate during PDT [29], foote has suggested Type-I reactions may become more dominant under conditions where the photosensitizers are highly concentrated, and especially under conditions [28].

1.5. Oxygen in PDT

1.5.1. Singlet Oxygen

Singlet oxygen, the predominant cytotoxic agent produced during PDT [33] is highly reactive form of oxygen that is produced by inverting the spin of one of the outermost electrons. Normally, groundstate oxygen has two unpaired electrons residing separately in the outermost antibonding orbitals. In the absence of a magnetic field the electronic configuration is indistinguishable, however in a magnetic field (fluorescence) the spins of the electrons can be revealed to be in one of three possible configurations, both spins aligned up, both spins aligned down, or one up and down [34]. When the spins are both aligned up the oxygen molecule will deflect down in a magnetic field, when both spins are aligned down they will deflect the molecule upwards in a magnetic field, and when the spins are anti-parallel the molecule will pass unperturbed through the magnetic field. Because of these three possible states the ground state of oxygen is called a triplet state. Any molecule with such a valance electron configuration is considered to be in a triplet state [34, 35].

In figure 12, the extreme reactivity of singlet oxygen arises from the pairing of two electrons into one of the π_{2p^*} antibonding orbitals. In the ground state the outermost electrons are distributed, according to Hund's rule. in the P_x and P_y antibonding orbitals [34]. Since the orbitals are degenerated and the electrons have aligned spins, the quantum numbers of each electron are identical and thus are forced to occupy separate orbitals to comply with the Pauli Exclusion Principle [36]. During an interaction with the excited photosensitizer the spin of one electron inverts, making its quantum numbers unique, allowing them to pair together into the antibonding orbital which destabilizes the molecule. Although singlet oxygen is often depicted as diradical, it is actually a highly polarized zwitter ion (Figure 12) [36].

Singlet oxygen is so reactive that it has a lifetime that ranges from 10-100μs in organic solvents. In an aqueous environment singlet oxygen's lifetime is reduced

to approximately 2μs because the energy of oxygen-hydrogen (O-H) stretching in water molecules nearly equals the excited-state energies of singlet oxygen. The energy is dissipated as heat by the stretching and vibrational motions of water molecules. Because singlet oxygen reacts so rapidly, PDT-induced oxidative damaged is highly localized to regions no larger in diameter than the thickness of a cell membrane. Photodynamic damage is probably confined to targets near to or within hydrophobic regions of the cell due to the hydrophobic character of most photosensitizers.

In tissue oxygenation, the importance of tissue oxygenation in PDT was demonstrated by several researchers [37, 38]. Hypoxic cells, those with less than 5% oxygenation, were found to be resistant to PDT. Henderson et al have reported that oxygen consumption depends on the fluence rate of the light [39], and that tissue destruction might be enhanced by using lower fluence rates. Lower fluence rates do not deplete the tissue's oxygen supply as rapidly and as a result the tissue is exposed to singlet oxygen far a longer time during treatment [37, 40].

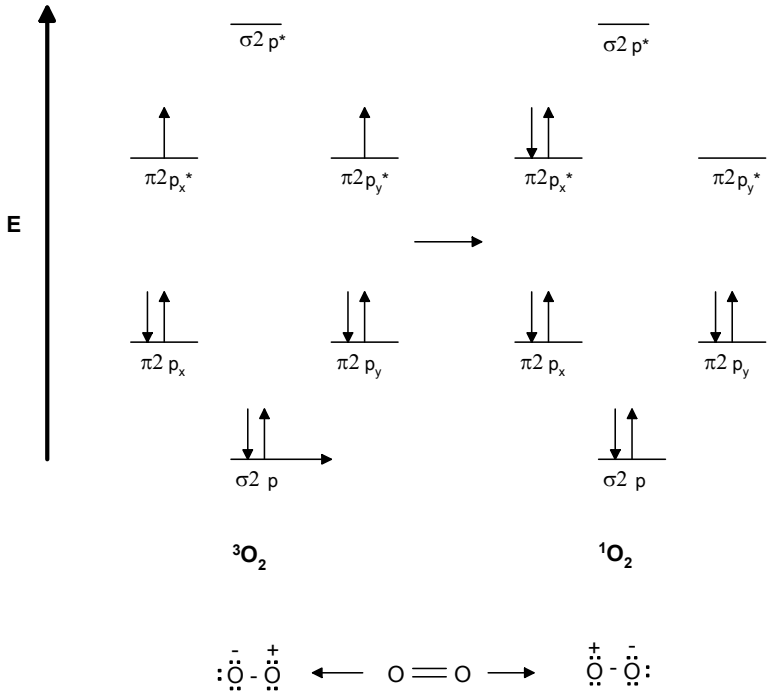

Figure 12: Molecular Orbital Diagrams showing the electron distribution in triplet and singlet oxygen (top). Lewis structure depicting the zwitterionic character of singlet oxygen (bottom).

1.5.2. Properties of Singlet Oxygen

1.5.2.1. Electronic Structure of Singlet Oxygen

Molecular oxygen has two low-lying singlet excited states $1\Delta g$ and $1\sigma g^+$ above triplet state. Electronic configurations of these states differently by the structure of the π-antibonding orbitals. The configuration of the molecular orbitals of the first excited state, $l\Delta g$, is as follows: $O_2KK(2\sigma_g)^2(2\sigma_u)^2(3\sigma_g)^2(l\pi_u)^4(1\pi_g^+)(1\pi_g^+)$. In the second excited state, $l\sigma_g^+$, the electronic configuration is identical to that the ground state, except that the last two electrons have antiparallel spins like below;

State	*Orbital Assignment*
$1\sigma g^+$	$\uparrow \pi \quad \downarrow \pi$
$1\Delta g$	$\uparrow\downarrow \pi$
$1\sigma g^+$	$\uparrow \pi \quad \uparrow \pi$

Primitive representations of molecular oxygen lowest singlet and triplet states

1.5.2.2. Quenching of $^1O_2$

Once dioxygen is in its singlet excited state, it can be deactivated by other species to return to its ground state. This quenching can take place in two major ways like;

(i) Physical Quenching: $^1O_2+A \rightarrow {}^{kp3}O_2+A$, in which interaction leads only to deactivation of singlet oxygen with no O_2 consumption or product formation.

(ii) Chemical Quenching: $^1O_2+A \rightarrow$ kcp, where the quencher reacts with singlet oxygen to give a new product.

Early work with singlet oxygen found that this active species could oxidize substrates that were unaffected by oxygen in its normal energy state. Oxygen is more oxidizing in its singlet excited state and is therefore significantly more electrophilic, reacting rapidly with unsaturated carbon-carbon bonds, neutral nucleophiles such as sulfides and amines, and as well as with anions.

Singlet oxygen, due to its high electrophilicity, is capable of oxidizing phenols, sulfides, and amines.

The reaction of singlet oxygen with phenol results in the formation of peroxides that dehydrate to form p-benzoquinones: Sulfides are generally oxidized to sulfoxides, while disulfides react to form thiosulfinates. Amines with low ionization potentials can be oxidized by singlet oxygen, possibly through a charge transfer intermediate.

The singlet oxygen generation efficiency will be determined experimentally for the synthesize perylenediimide derivatives.

1.6. First Generation Photosensitizers

1.6.1. Haematoporphyrin and Photofrin

The first sensitizer used in clinical PDT was haematoporphyrin (figure 8) derivative and its purified fraction, Photofrin®. HpD (figure was first described by *Lipson et al* in 1961 and is prepared by acetylation of haematoporphyrin (Hp), followed by neutralisation prior to alkaline hydrolysis. The resulting mixture is known to contain haematoporphyrin, hydroxyethylvinyldeuteroporphyrin (HVD) and protoporphyrin (Pp), as well as a complex dimeric and oligomeric fraction containing ester, ether and carbon-carbon linkages of haematoporphyrin. HpD is typically 45% monomeric/dimeric porphyrins and 55% oligomeric material, the latter being accountable for the tumour localising activity of HpD *in vivo*. This fraction has been partly purified in the commercial development of Photofrin®, which has been reported to be around 85% oligomeric material. The same compound was prepared in Leeds under the name Polyhaematoporphyrin or PHP. Investigations using HpD have highlighted several criteria that an ideal photosensitizer should fulfill.

Although the higher molecular mass fraction is responsible for tumor localization in vivo, it has a low fluorescent quantum yield and a low efficiency in generation of reactive oxygen species.

Photofrin®-mediated PDT has proved curative for a range of cancers, but there are well-documented drawbacks to treatment with this photosensitizer. Because the compound is a complex mixture, there are questions concerning the identity of the active components and also the reproducibility of the synthetic process. Photofrin® is excited clinically with red light at 630 nm. This wavelength can only penetrate tissue to a depth of a few mm, making Photofrin® unsuitable for the treatment of deep-seated tumors.

1.7. Design Criteria for Second Generation Photosensitizers

1.7.1. Dark Toxicity

It is clearly desirable that the photosensitizer has zero or very low cytotoxicity in the absence of light. This means that tumor or damage can be controlled by the light dose for a given drug dose. It has occasionally been suggested that the tumor-targetting properties of some porphyrins could be used to transport antimetabolities (such as nitrogen mustards, covalently attached) to the tumor site, but this idea does not appear to have been efficiently developed.

1.7.2. Composition

The photosensitizer should be of constant composition, and preferably a substance which does not have chiral centers (unlike haematoporphyrin, which has two). If the presence of one or more chiral centers is allowed, then the optical isomers may be expected to locate differently in cells, and the photodynamic effects will be different; it may be anticipated that regulatory authorities will ask for test results on such stereoisomers. The need for a single substance is, in fact, an overriding requirement, for the simple reason that there are far more variables in photodynamic therapy than there are in convertional pharmacology. Each component

may respond differently to each variable, and logical analysis, of biological results from a photosensitizer which is a complex mixture becomes very difficult indeed.

1.7.3. Synthesis

The synthesis should be as straightforward and as high-yielding as possible.

1.7.4. Solution Behaviour

What is needed is a substance which has some selectivity for the tumor, but which is rapidly cleared from the body after phototherapy, so that general photosensitization is minimized. It has emerged that photosensitizers with these features are often amphiphilic, that is, they have a blend of lipophilic and hydrophilic properties. Since the macrocyclic nuclei (porphyrins, phyhalocyanines etc.) on which many of the photosensitizers are based, are themselves hydrophobic, this means that hydrophylic substituents are needed to achieve the correct amphiphilic balance. Hydroxyl, sulphonic acid, and quarternary ammonium groups have been most used for this purpose.

1.8. Second Generation Photosensitizers

New photosensitizers have been synthesized that have better properties than HpD. Single substances are preferred because they allow simplified studies into the relationship between photosensitizer and effect, and clinical approval is easier to obtain. The increased absorbance in the red region of the spectrum and the increased molar absorption coefficients give rise to more excited photosensitizer at deeper tissue sites and hence more tumor damage. However, photosensitizer properties (aggregation, ionic charge, solubility, partition between aqueous and lipid) are also important and should promote selectivity without long term retention.

Following the success of PDT a number of so called "second generation" photosensitizers have been developed. These include modified porphyrins, chlorins, bacteriochlorins, phthalocyanines, naphthalocyanines, pheophorbides and purpurins. These photosensitizers show increased efficacy in PDT for many

different reasons, such as improved photophysical properties as demonstrated by their activation wavelengths, thus increasing tissue penetration.

1.8.1. Haematoporphyrin Derivative and Other Porphyrin Photosensitizers

HpD (figure 8) was the first photosensitizer to receive regulatory approval in Canada in 1993 and has received subsequent approval in the U.S., Europe, and Japan for a number of indications including cervical cancer, endobronchial cancer, esophageal cancer, bladder cancer, and gastric cancers.[41] As successful as HpD has been, it still suffers from many drawbacks, which have stimulated subsequent research for better photosensitizers. HpD is a mixture of compounds that include the hematoporphyrin monomer, dimer, and oligomers.[42] Partial purification of this mixture gives the commercial product porfimer sodium or Photofrin (Axcan Pharma, Montreal, Canada).[43] This "purified" product still consists of many Porphyrin containing compounds (about 60), which makes reproducibility difficult in their manufacture. Photofrin and other porphyrin-related sensitizers have weak absorbance in the red region of the spectrum (≥600 nm where penetration of light in tissue is optimal) and induce longlasting skin photosensitivity (4-6 weeks) through retention in cutaneous tissue. [44, 45] The band I absorption maximum of Photofrin is at 630 nm with a weak molar extinction coefficient, ε of 1170 M^{-1} cm^{-1}.

The quest for HpD-related photosensitizers has focused on derivatives that are synthetically accessible in pure form and on derivatives that have longer wavelengths of absorption. [46] Porphyrin-related chromophores all tend to be efficient producers of $^1O_2$, which makes them additionally attractive as photosensitizers.

The tetraarylporphyrins were the first easily prepared, easily purified porphyrins to be evaluated as photosensitizers. Tetraphenylporphyrin (TPP) Figure 13 has a band I absorption maximum of 630 nm and is an efficient generator of $^1O_2$ but has limited solubility. Sulfonation of TPP gives the tetrasulfonate $TPPS_4$ Figure 14, which remains an excellent producer of $^1O_2$ [quantum yield for $^1O_2$ generation, $\phi(^1O_2)$, of 0.71, [47] has excellent water solubility, and was once viewed as a promising photosensitizer for PDT. [48] $TPPS_4$ is membranepermeable, displays lysosomal accumulation in cells, accumulates in tumors, and is effective both in vitro

and in vivo. However, clinical ambitions for $TPPS_4$ ended after reported neurotoxicity in mice exposed to high doses of $TPPS_4$. [48, 50]

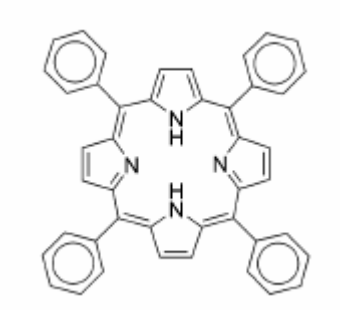

Figure 13: Structure of TPP

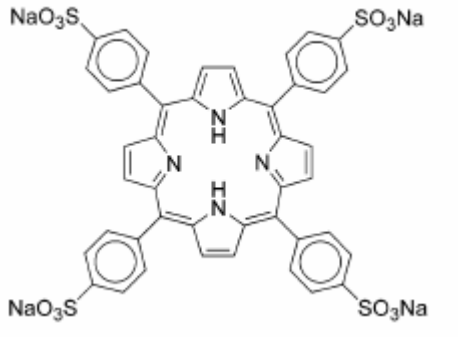

Figure 14: Structure of $TPPS_4$

Recent work with porphyrin derivatives suggests some novel approaches to porphyrin delivery. Dendrimeric porphyrin derivatives with a porphyrin ring as the dendrimer core (Figure 15) have been prepared.[51] The porphyrin chromophore is buried inside a hydrophobic shell. While these molecules can look protein-like, surface modifications of the dendrimer periphery have provided cationic and anionic surfaces for zinc porphyrins with up to 32 charged groups that have been touted as effective photosensitizers in vitro. [52]

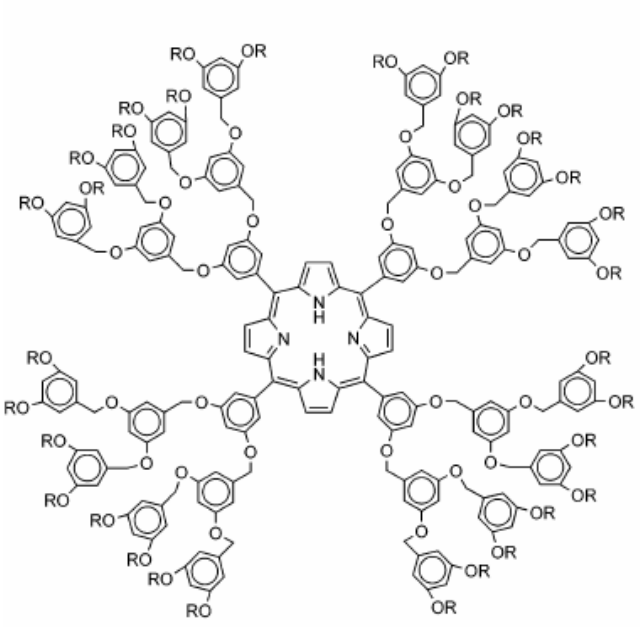

Figure 15: Structure of Dendrimeric Porphyrins

1.8.2. Chlorin and Bacteriochlorin Derivatives from Naturally Occurring Sources

The porphyrin and phthalocyanine cores are oxidatively stable, which has allowed numerous derivatives to be prepared and examined. [46] However, the porphyrin core absorbs wavelengths of light too short for optimal penetration in tissue. Reduction of a pyrrole double bond on the porphyrin periphery gives the chlorin core, and further reduction of a second pyrrole double bond on the chlorin periphery gives the bacteriochlorins (Figure 16). Both of these classes of molecules have band I absorption maxima at longer wavelengths (λ_{max} =650-670 nm for chlorins and (λ_{max} = 730-800 nm for bacteriochlorins) than the porphyrins and yet still remain efficient generators of $^1O_2$. [53] Several chlorins and bacteriochlorins are in various stages of evaluation for PDT.

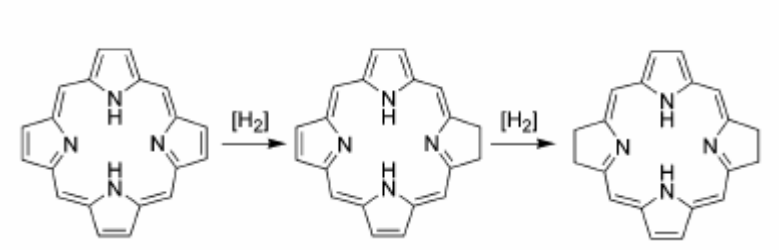

Fıgure 16: Structures of Porphyrin, Chlorin and Bacteriochlorin

One of the first chlorins to be evaluated was the naturally occurring chlorin *e*6 (**Figure 17**). Chlorin *e*6 is derived from oxidation of chlorophyll *a* and has a band I absorption maximum of 654 nm with a value of ε near 40 000M^{-1} cm^{-1}. Unfortunately, chlorin *e*6 shows long-term skin photosensitization [44] and requires high doses to be effective. Alkyl esters of chlorin *e*6 and derivatives such as mono-L-aspartyl chlorin *e*6 (**Figure 17**) have been found to be more bioavailable and more effective at lower doses and are being evaluated for topical delivery.[54]

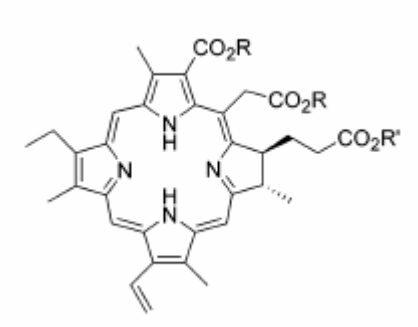

a) Chlorin e_6, R=R'=H
b)Chlorin e_6 Trimethyl Ester, R=R'=Me
c)mono-L-aspartyl Chlorin e_6, R=H,
R'= (L)-NHCH(CO_2H)CH_2CO_2H

Figure 17: Structures of Chlorin e_6 and Chlorin e_6 Trimethyl Ester

Metalated chlorin and bacteriochlorin cores have also given useful photosensitizers. Tin etiopurpurin (SnET2) (Figure 18) is a metal chlorin derivative that is currently being evaluated for the treatment of cutaneous metastatic breast cancer and basal cell carcinoma. [41] SnET2 has a band I absorption maximum of 660 nm with E of 28 000M^{-1} cm^{-1}. [44] However, SnET2 treatment also imparts long-term skin photosensitization, which limits its general utility. [44]

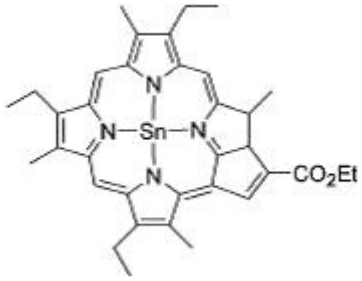

Figure 18: Structure of SnET2

Mono- L-aspartyl chlorin e_6 (Npe_6 or MACE) (Figure 17) is a highly water soluble chlorin-type photosensitizer. It has an absorbance peak at 654 nm (ε of 40 000 $M^{-1}cm^{-1}$) and is effective in vitro and in vivo.

1.8.3. Synthetic Chlorins

The synthetic chlorin 5,10,15,20-tetra(3-hydroxyphenyl)-2,3dihydroporphyrin (*m*THPC) (Figure 19) is perhaps the most useful photosensitizer of the synthetic

chlorins. *m*THPC (Foscan, Biolitec Pharma, Scotland, U.K.) has been approved in Europe for use against head and neck cancer, and additional indications have been filed for prostate and pancreatic tumors. [41] *m*THPC has also been used effectively in recurrent breast cancer for chest wall lesions with patients receiving 0.10 mg kg^{-1} and 5Jcm^{-2} of 652nm light. [55] However, *m*THPC shows long-term skin photosensitization of up to 6 weeks, which is one drawback to its use.

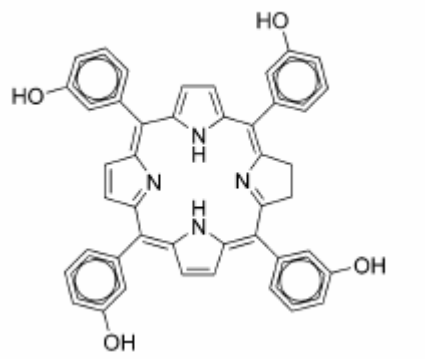

Figure 19: Structure of *m*THPC

1.8.4. Phthalocyanines

Phthalocyanines [Figure 20] are highly coloured compounds which have found widespread commercial application. Recently phthalocyanines have been developed as photosensitizing agents for PDT.

The pyrrole groups in phthalocyanines are conjugated to benzene rings and bridged by aza nitrogens rather than methine carbons. This causes the absorption spectrum to shift to longer wavelengths and the Q bands to become more intense than the Soret peak. The shift of this red absorption peak permits the use of longer wavelength light with increased tissue penetration to excite these compounds (typically around 680 nm), compared with the 630 nm light used to excite porphyrins.

A long-life triplet state is required for efficient photosensitization and this criterion may be fulfilled by the incorporation of a diamagnetic metal such as Zn or Al into the phthalocyanine macrocycle. Metal-free compounds and phthalocyanines

containing paramagnetic metals such as Cu, Co and Fe have a much shorter triplet lifetime and display minimal phototoxicity.

Phthalocyanines are generally hydrophobic compounds although water-soluble derivatives can be readily synthesized through substitution of the ring with moieties such as sulphonic acid, carboxylic acid and amino groups. The sulphonated compounds, have received the most attention with regard to photodynamic efficacy. Purification of these derivatives can be a problem and the final product is typically a mixture of mono- di- tri- and tetrasulphonated derivatives. Furthermore, these compounds have been observed to aggregate at relatively low concentrations in aqueous media which results in loss of photochemical activity.

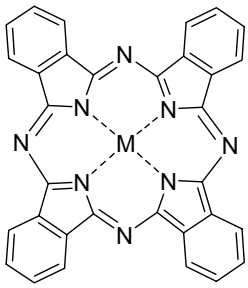

Figure 20: Structure of Phthalocyanine

1.8.5. Benzoporphyrin Derivate

Benzoporphyrin derivative mono-acid A (BPD) is another chlorin-type molecule that has been developed by QuadraLogic Technologies. [Figure 21] It is a hydrophobic molecule that is distinguished by the presence of a mono-acid at either position 3 or 4 of the porphyrin ring. The absorbance peak for PDT occurs at 650 nm with an extinction coefficient of 34 000 $M^{-1}cm^{-1}$. Phase I and II clinical trials have shown it has rapid tumor accumulation and reduced skin photosensitivity**.**

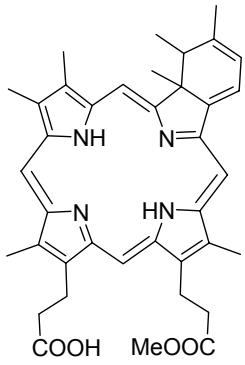

Figure 21: Structure of Benzoporphyrin derivate

1.9. Other Photosensitizers

1.9.1 Cyanine Dyes

They were originally developed another part of applied photosensitization that of photographic sensitizers: any critical application may be regarded as a bonus.

1.9.1.1. Merocyanine 540

It has already been advanced as a phototherapeutic agent against malignant haemopoietic cells, for the extracorpereal purging of bone marrow in leukemia cases. Although it localizes in leukemia cells, the phototoxicity does not appear to be sufficiently selective. Comparative studies in two myeloid leukemia cell lines in the mouse have revealed: (i) that m-THPC (Figure 19) is significantly more potent and more selective in photokilling leukemia cells than is meracyanine 540 and (ii) that both m- THPC and merocyanine 540 will induce apoptosis in leukemia cells, with the m- THPC being observed to kill virtually all the cells in this way.

1.9.1.2. Indocyanine Green

The significant point about indocyanine green is that it has already been approved for clinical administration, for example, in the determination of plasma volume. This means that if it were a useful PDT sensitizer, the route to regulatory approval would be much easier because of existing clinical experience. The PDT

effect on keratinoytes in cell culture has been investigated: the dye is taken up by the cells, and a photodynamic effect is observed. This effect is quenched by sodium azide, but a singlet oxygen mechanism seems rather unlikely since the Q_T value is only ~0.01. The dye has an extended delocalized system, with λ_{max} at 805 nm, but the absorption in the visible region is weak, which is an additional advantage.

1.9.2. Hypericin

It is a naturally-occurring extended quinone: It has λ_{max} 590 nm (ε 41600) in ethanol, and ϕ_Δ falls to 0.02, possibly due to aggregation. This substance has PDT activity against mammary carcinoma implants in athymic mice. In a single case (mesothelioma) where it was applied superficially, it was not effective by itself, but appeared to act synergistically with HpD given subcutaneously.

1.9.3. Phenothiazines:

Many of them typified by methylene blue and toluidine blue, are commercially available, and there is a considerable literature on the use of these dyes, and especially toluidine blue to stain and cancerous lesions in vivo as an aid diagnosis. They have photomicrobicidal properties, and have activity as PDT agents in *in vitro* experiments with cancer cell lines. Nevertheless, in spite of being good singlet oxygen sources, the phenothiazinium dyes have not emerged as good PDT against cancer. This is because when injected they tend to be rapidly excreted and lack selectivity.

1.9.4. Porphycenes

They are isomers of porphyrins that, like the porphyrins, posses an 18π aromatic system. The compounds were first described in 1986 by Vogel and hic colleagues (Cologne), and are synthesized by McMurry coupling of bipyrrole dialdehydes. Although the syntheses are often low-yielding from uncommon starting materials, the novelty of the system provides interest from the intellectual property point of view and many novel compounds have been prepared with PDT in mind.

Cytopharm Inc (Menlo Park, Califomia) in association with Glaxo-Wellcome is thought to be developing compounds of this series for PDT applications.

1.9.5. Texaphyrins

They have an expanded coordination with five nitrogen atoms, and it is metal complexes rather than the free base which appear to be making the running. They readily form complexes with metal ions, including those with larger ionic radii can be readily accommodated by porphyrins. These complexes have a strong absorption band in the 600-900 nm regions, the position of which can be varied by suitable choice of substituent (including metal).

1.9.6. Xanthenes

The xanthene dyes, for example, fluorescein, eosin, and rose bengal are excellent photosensitizers for singlet oxygen formation and are perhaps the most commonly used compounds where singlet oxygen is required in organic synthesis. Fluorescein is prepared by the condensation of phthalic anhydride and resorcinol, and eosin Y is made by direct bromination of the two activated aromatic rings. The earliest clinical experiments in this field were carried out by Jesionek and von Tappeiner with eosin (in 1903 and 1905) and in 1974 Dougherty started his PDT studies with fIuorescein. However, he quickly moved on to HpD because it was much more effective. The available xanthenes are too water soluble to give a good clinical result, except perhaps by topical application.

1.9.7. Squaraines

Squaraine dyes (1,3-dicondensation products of squaric acid and electron-rich molecules) [56] are currently the object of intense investigation as molecular components for a number of technological applications. Among them, electrophotography, optical data storage, solar cells, ion sensing, and nonlinear optics especially benefit from their peculiar photophysical and photochemical properties, namely, a sharp red near-IR absorption band and an extremely high extinction

coefficient. [57] Recently, squaraines have been proposed by Ramaiah et al. as a possible new class of photosensitizers for photodynamic therapy (PDT). [58]

Recently, *Pagani et al.* have designed and synthesized representative members of three new classes of squaraines, the intrinsic tailored nature of which allows the stepwise fulfillment of some of the many demanding requirements associated with the development of new photosensitizers for PDT: (a) all new dyes display absorption bands in the biological window; (b) the introduction of a triethyleneglycol chain results in significant solubility enhancement and achievement of high water solubility for **1c** and **2a**; (c) a qualitative estimate of singlet oxygen generation quantum yield shows that all of the derivatives possess intrinsic triplet yield. [59]

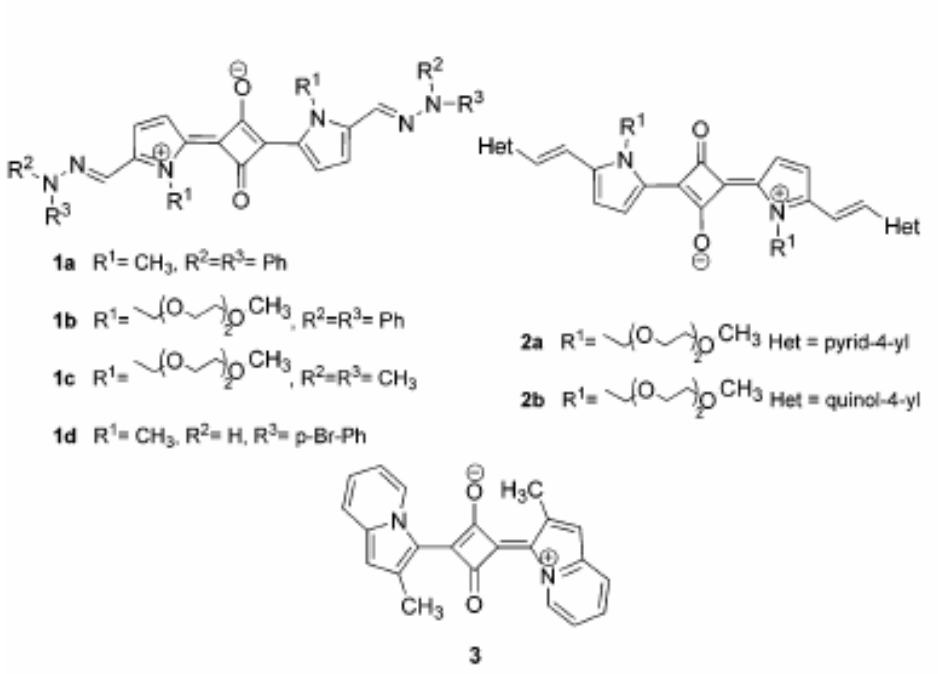

Figure 22: Structures of 1a, 1b, 1c, 1d, 2a, 2b

Class **1** derivatives were chosen to evaluate the substituent effect on different aspects connected with PDT absorption wavelength, water solubility, and the singlet oxygen production. Arylhydrazonomethylpyrroles represent a class of versatile electron-rich derivatives possessing a number of favorable features relevant for PDT.

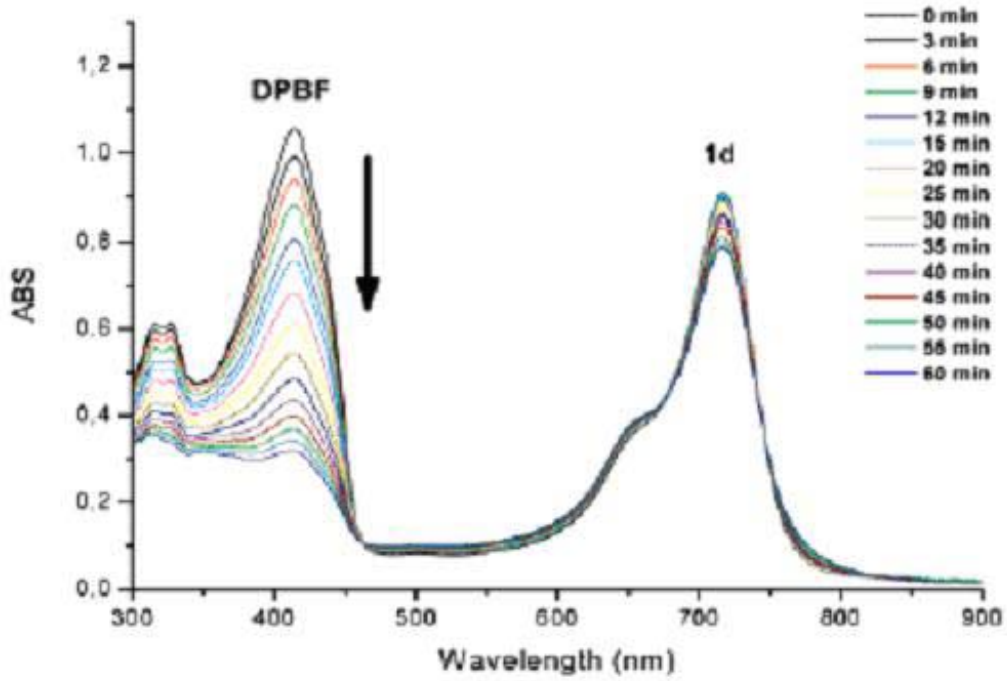

Figure 23: Time evolution of the UV-vis spectrum of a DPBF (50μM) and **1d** (5 μM) in CH_2Cl_2 solution.

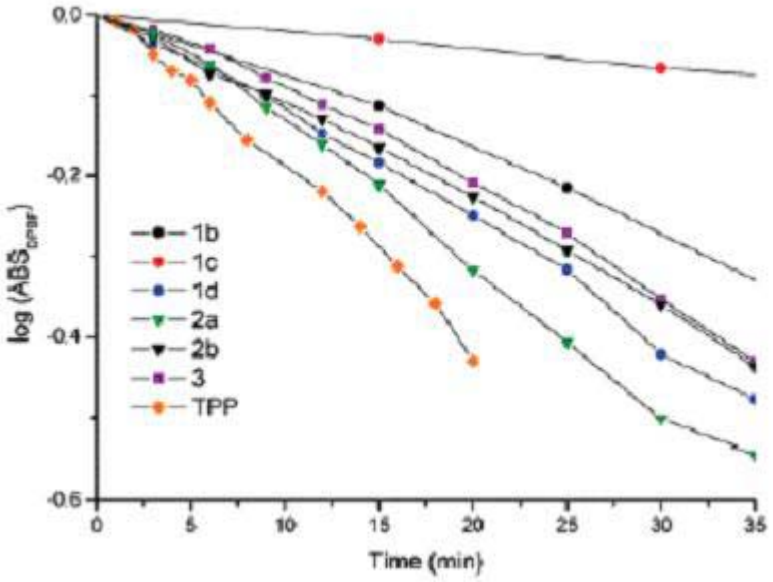

Figure 24: Comparative singlet oxygen generation of squaraines **1d**, **1c**, **1b**, and **4** in CH_2Cl_2 at 5 μM concentration.

Figure 24 plots the decrease of DPBF absorption at 415 nm as a function of illumination time for each sensitizer compared to that of *meso*-tetraphenylporphyrin (TPP), a well-known and very efficient singlet oxygen generator. They restricted the analysis to the first 30 min because, during this time, the photosensitizer did not show any appreciable degradation. A first general analysis shows that, despite the reported [60] low intersystem crossing efficiency of other squarainic derivatives, these squaraines do possess some inherent singlet oxygen generation abilities. In particular, within class **1** derivatives, the brominated compound **1d** shows peak performances, in accord with the anticipated heavy atom effect.

1.9.8. Perylenediimide Dyes

Perylenediimides (PDIs) are highly versatile dyes and pigments which find applications in diverse fields, such as organic light-emitting diodes,7 molecular switches and wires, light-harvesting arrays, photoreactive thin films, solar cells, and dye lasers, among others. One important problem to be addressed in many applications is solubility. Substitution at the bay region (positions 1, 6, 7, and 12) is known to increase solubility in organic solvents. [61] Water solubility is a more challenging problem [62] as these dyes have a strong tendency to aggregate even at very low concentrations in aqueous solutions. Yet, for potential biological applications, it is highly desirable to obtain water-soluble PDIs, especially with long wavelength absorption and emission. Simple substitutions at the imide groups do not change the spectral characteristics significantly, and extending the perylene core to form higher rylenes [63] reduces the chances of water solubility even further. The breakthrough came in 1999, when Wasielewski showed [64] that amine substitutions at the bay region resulted in remarkable green chromophores with absorptions in the desired region of the spectrum. Emission characteristics were also reported recently. [65]

Yukruk et al. synthesized 3 different PDIs. In pH 7.4 buffer solutions, the absorption spectra of compounds **1**-**3** show broad and red-shifted charge-transfer peaks centered at 676, 649, and 642 nm for compounds **1**, **2**, and **3**, respectively. The extinction coefficients in the same buffer solutions were near 20 000 M^{-1} cm^{-1}, which is considerably higher than that of porphyrins in the same spectral region.

Fluorescence emission (near 750 nm), as expected, was barely detectable in aqueous solutions. [66]

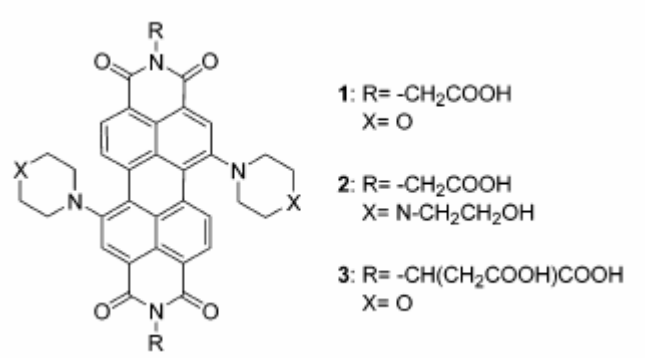

Figure 25: Structures of synthesized PDIs

Singlet oxygen generation capacities of these novel water-soluble PDI dyes were studied in 2-propanol. The experiments were performed in such a way that the requirements of both the red light and PDI sensitizers were unequivocally established. Red light from 240 W tungsten lamps, filtered to remove light with $\lambda <$ 600 nm was used to excite PDI dyes. The fluence rate was determined to be 11 mW/cm^2. Thus, Figure 26 shows the change in the absorbance of the selective [67] singlet oxygen trap 1,3-diphenyl-*iso*-benzofuran (50.0 *i*M) in the presence of 5.0 μM of PDI dyes (**1**-**3**). [66]

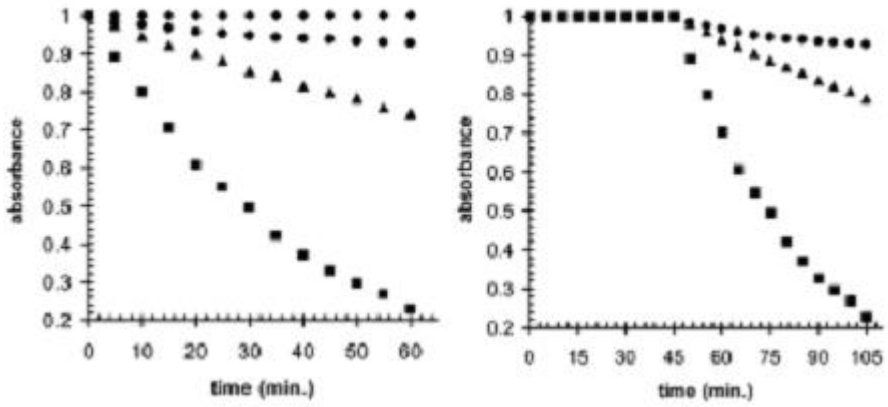

Figure 26: (A) (left) The change in the absorbance (at 415 nm) of 1,3 diphenylisobenzofuran (50 μM) in 2-propanol under red-light illumination in the

presence of 5.0 μM dyes (circles, **1**; triangles, **2**; squares, **3**; and diamonds, no added dye. (B) (right) Same concentration of dyes (circles, **1**; triangles, **2**; squares, **3**) and DPBF; illumination starts after 45 min dark treatment.

1.9.9. Boradiazaindacenes (BODIPY) dyes

Boradiazaindacenes (BODIPY dyes or difluoroboradipyrrines) are well known fluorescent dyes [68] with emerging applications in light harvesting systems and chemosensors. In recent years, there have been exciting reports [69] demonstrating their versatile chemistry.

Nagano et al. report a novel photosensitizer, which is highly efficient, photostable, and usable in both lipophilic and aqueous environments. To develop this photosensitizer, they focused on the boron dipyrromethene (BODIPY) fluorophore since BODIPYs generally have high extinction coefficients (ε) and high quantum efficiencies of fluorescence (ϕ_f), which are relatively insensitive to environment (i.e., solvent polarity or pH), and they are also resistant to photobleaching. Thus, they hypothesized that the BODIPY fluorophore can be transformed into a general photosensitizing chromophore without loss of its unique characteristics by attaching heavy atoms directly onto the chromophore, making use of the so-called internal heavy-atom effect. [68, 70]

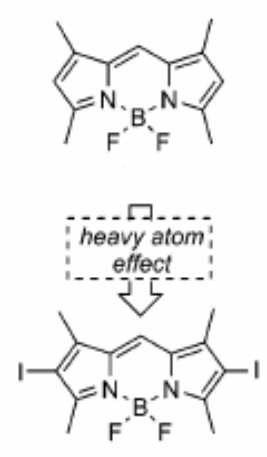

Figure 27: Structures of BODIPY and 2I-BODIPY

They examined the ability of 2I-BODIPY to generate $^1O_2$ in various solvents. This was achieved experimentally by following the disappearance of the 410 nm absorbance band of 1,3- diphenylisobenzofuran (DPBF), a known $^1O_2$ scavenger, at the initial concentration of $2x10^{-5}$ M in each solvent in the presence of $1x10^{-6}$ M photosensitizer under light illumination. Table 1 shows the rate of DPBF consumption at the initial stage (i.e., the slope), which corresponds to the efficiency of $^1O_2$ generation. 2IBODIPY generated $^1O_2$ in all of the solvents in Table 1 almost equally. The lower efficiency of $^1O_2$ generation in MeOH and aqueous solution probably reflects the shorter lifetime of $^1O_2$ in them as compared with other solvents. [69] On the other hand, RB could not be used in nonpolar solvents, including CH_2Cl_2 and $CHCl_3$, because of its low solubility. These results demonstrate that 2I-BODIPY can generate $^1O_2$ in various environments, suggesting that it would offer considerable flexibility as an experimental tool.

	2I-BODIPY						**RB**
	Aqueous solution	CH_3CN	CH_3OH	Acetone	CH_2Cl_2	$CHCl_3$	CH_3OH
Slope($x10^4s^{-1}$)	45	128	44	130	129	142	29
relative number of absorbed photons	0.09	0.11	0.12	0.12	0.096	0.086	0.13
relative efficiency of $^1O_2$ generation	0.048	0.11	0.037	0.11	0.14	0.17	0.022

Table 1: Singlet oxygen generation by 2I-BODIPY in various solvents

1.9.10. Conjugated Photosensitizers

It is the biochemical usage of conjugated photosensitizers that is required here. Conjugation in this sense may be defined as the covalent attachment of the

principal molecule to a second molecule, which may be small or large, and which confers some particular (usual1y beneficial) property on the principal molecule.

All of these classes of compounds are highly efficient singlet oxygen generators. The efficiency of production of singlet-oxygen is an empirically determined quantity called the singlet-oxygen quantum yield (ϕ). The singlet oxygen quantum yield describes the number of singlet oxygen molecules that are formed per photon of energy absorbed.

CHAPTER II

EXPERIMENTAL

2.1. Instrumentation

The compounds were characterized and analyzed by Nuclear Magnetic Resonance Spectroscopy (NMR), UV/Vis Spectroscopy, and Fluorescence Spectroscopy. ^{1}H and ^{13}C Nuclear Magnetic Resonance spectra of all compounds were recorded in $CDCl_3$ with Bruker Gmbh DPX-400, 400 MHz High Performance Digital FT-NMR Spectrometer. UV/VIS spectra were recorded by Varian Bio 100 UV/VIS Spectrophotometer. Fluorescence spectra were recorded using Varian Cary Eclipse Fluorescence Spectrophotometer. All solvents were distilled over $CaCl_2$ before use. *tert*-Butyl 2-(4-formylphenoxy)acetate was synthesized according to literature.[1] All chemicals were obtained from Aldrich, unless noted otherwise. Merck Silica Gel 60 F_{254} TLC Aluminum Sheets were used in monitoring reactions by thin layer chromatography. Merck Silica Gel 60 (particle size 0.040-0.0963 mm, 230-400 mesh ASTM) used in column chromatography. Elemental analyses were performed by METU-Central Labs or TUBITAK-ATAL. FAB and ESI mass spectrometry analyses were performed by Kent Mass Spectrometry Service, Darford, U.K.

2.2. Synthesis of 2,6-Dibromo-1,3,5,7-tetramethyl-8-phenyl-4,4'-difluoroboradiazaindacene (8)

8-Phenyl-BODIPY (**5**, 0.33 g, 1.02 mmol), AIBN (0.335 g, 2.04 mmol) and NBS (0.363 g, 2.04 mmol) were refluxed for 30 minutes in CCl_4 (15 mL). Crude product was then concentrated under vacuum, and purified by silica gel column chromatography (Hexane-EtOAc, 3:1). The red colored fraction was collected and

the solvent was removed under reduced pressure to yield the desired compound (**5**) (393.3 mg, 80%).

^{1}H NMR (400 MHz, $CDCl_3$), δ [ppm]: 1.37 (s, 6H), 2.56 (s, 6H), 7.15-7.2 (m, 2H), 7.42-7.48 (m, 3H).

^{13}C NMR (100 MHz, $CDCl_3$), δ [ppm]: 153.9, 142.1, 140.6, 134.4, 130.5, 129.5, 129.4, 129.2, 127.8, 28.0, 13.6.

Elemental analysis: Found: C, 47.45; H, 3.62; N, 5.99. $C_{19}H_{17}BBr_2F_2N_2$ requires, C, 47.35, H, 3.56, N, 5.81. ESI-MS (m/z); 482 [M^+].

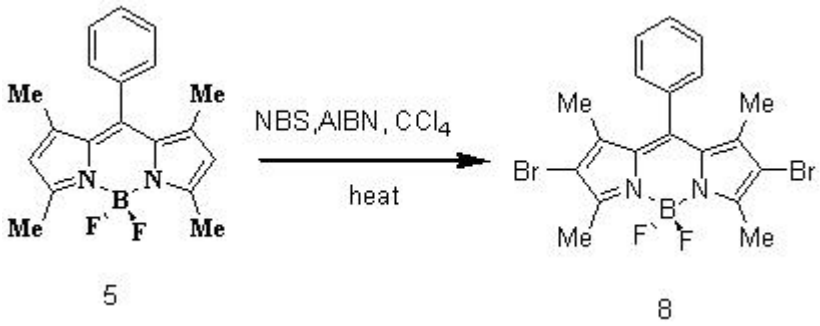

Figure 28: Synthesis of 2,6-Dibromo-1,3,5,7-tetramethyl-8-phenyl-4,4' difluoroboradiazaindacene **(8)**

2.3. Synthesis of monostyryl and distyryl-BODIPY dyes (10 and 11)

Compound **8** (500 mg, 1.037 mmol) and *tert*-butyl 2-(4-formylphenoxy) acetate (**2**, 0,245 g, 1.037 mmol) were refluxed in a mixture of toluene (50 ml), glacial acetic acid (0.77 ml) and piperidine (0.94 ml). Any water formed during the reaction was removed azeotropically by heating overnight in a Dean-Stark apparatus. Crude product was then concentrated under vacuum, and purified by silica gel column chromotagraphy (EtOAc-Hexane, 1:4). The blue colored fraction was collected and the solvent was removed under reduced pressure to yield the bright red fluorescent compound **10** (145 mg, 20%).

^{1}H NMR (400 MHz, $CDCl_3$), δ [ppm]: 1.29 (s, 3H), 1.32 (s, 3H), 1.42 (s, 9H), 2.56 (s, 3H), 4.5 (s, 2H), 6.84 (d, *J*= 8.7 Hz, 2H), 7.16-7.22 (m, 2H), 7.42-7.54 (m, 6H), 8.00 (d, *J*= 16.6 Hz, 1H). [1]

^{3}C NMR *(*100 MHz, $CDCl_3$), δ [ppm]: 167.1, 159.0, 154.0, 148.5, 141.5, 140.6, 140.1, 138.5, 134.6, 131.3, 131.0, 130.5, 129.5, 129.4, 129.1, 128.0, 118.2, 116.3, 115.0, 110.1, 109.7, 82.5, 65.7, 28.0, 13.8, 13.6, 10.6.

Elemental analysis: Found: C, 54.71; H, 4.58; N, 3.93. $C_{32}H_{31}BBr_2F_2N_2O_3$ requires, C, 54.89, H, 4.46, N, 4.00. ESI-MS (m/z) 707 [M^+].

The green colored fraction was collected and the solvent was removed under reduced pressure to yield the distryl dye **11** (300 mg, 32%).

^{1}H NMR (400 MHz, $CDCl_3$), δ [ppm]: 1.37 (s, 6H), 1.42 (s, 18H), 4.5 (s, 4H), 6.88 (d, *J*= 8.8 Hz, 4H), 7.23 (dd, *J*= 2.1 Hz, *J*= 5.8 Hz, 2H), 7.42-7.47 (m, 3H), 7.51-7.58(m, 6H), 8.01 (d, *J*= 16.6 Hz , 2H).

^{13}C NMR (100 MHz, $CDCl_3$), δ [ppm]: 168.6, 159.8, 149.3, 141.9, 139.9, 139.5, 135.7, 132.9, 131.4, 130.4, 130.3, 130.2, 129.9, 129.2, 117.3, 115.8, 83.5, 66.5, 29.0, 14.6.

Elemental analysis: Found: C, 58.82; H, 5.01; N, 2.98. $C_{45}H_{45}BBr_2F_2N_2O_6$ requires, C, 58.85, H, 4.94, N, 3.05. ESI-MS (m/z); 918 [M^+].

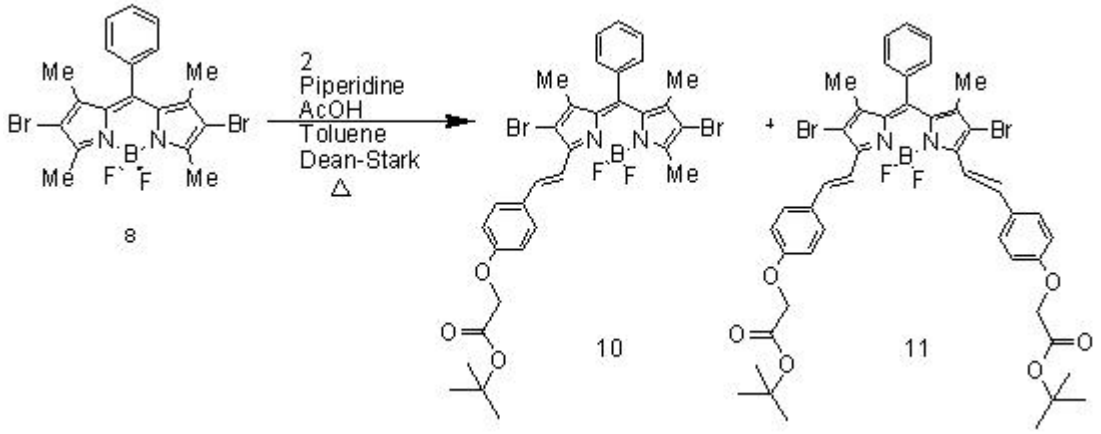

Figure 29: Synthesis of monostyryl and distyryl-BODIPY dyes **(10 and 11)**

2.4. Synthesis of 2,6-Diethyl-1,3,5,7-tetramethyl-8-(4-*t* butoxycarbonylmethyloxyphenyl)-4,4'-difluoroboradiazaindacene (7)

2,4-Dimethyl-3-ethylpyrrole (**4**, 0.81 g, 6.55 mmol) and *tert*-butyl 2-(4-formylphenoxy)acetate (**2**, 0.75 g, 3.18 mmol) were dissolved in absolute CH_2Cl_2 (200 mL) under N_2 atmosphere, one drop of TFA was added and the solution was stirred at rt until TLC analysis showed the complete comsumption of the aldehyde. At this point, a solution of tetrachlorobenzoquinone (0.81 g, 3.18 mmol) in CH_2Cl_2 (150 mL) was added, stirring was continued for 15 min. Then, Et_3N (9.96 mL) and, BF_3 .OEt_2 (9.96 mL) were added. After stirring for another 12 h, crude product was washed three times with water, dried over Na_2SO_4 and evaporated to dryness. The residue was chromatographed on silica gel ($CHCl_3$: MeOH, 96:4) to afford 324 mg (yield: 20%) **7** in the form of orange needles.

^{1}H NMR (400 MHz, $CDCl_3$), δ [ppm]: 0.90 (t, *J*= 7.5 Hz, 6H), 1.25 (s, 6H), 1.42 (s, 9H), 2.13-2.26 (q, *J*= 7.5 Hz, 4H), 2.47 (S, 6H) 4.50 (s, 2H), 6.94 (d, *J*= 8.5 Hz, 2H), 7.1 (d, *J*=8.5 Hz, 2H).

^{13} C NMR (100 MHz, $CDCl_3$), δ [ppm]: 165.9, 156.6, 151.8, 138.2, 136.6, 130.9, 129.3, 127.87, 127.0, 113.4, 80.7, 64.1 26.2, 15.2, 12.8, 10.7, 10.0.

Elemental analysis: Found: C, 68.35; H, 7.39; N, 5.40. $C_{29}H_{37}BF_2N_2O_3$ requires, C, 68.24; H, 7.31, N, 5.49. ESI-MS (m/z); 510 [M^+].

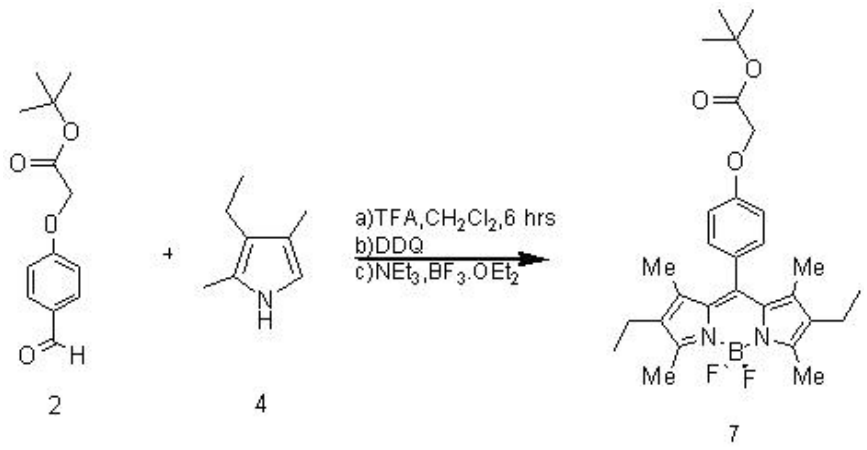

Figure 30: Synthesis of 2,6-Diethyl-1,3,5,7-tetramethyl-8-(4-*t* butoxycarbonylmethyloxyphenyl)-4,4'-difluoroboradiazaindacene **(7)**

2.5. Synthesis of monostyryl and distyryl-BODIPY dyes (14 and 15)

A similar procedure was followed in the synthesis of these monostyryl and distyryl dyes, thus, the BODIPY dye **7** (0.2662 g, 0.5215 mmol), and the aldehyde **2** (0.246 g, 1.043 mmol), piperidine (0.47 mL) and acetic acid (0.39 mL) were used in this reaction. The desired compounds were purified by silica gel column chromotagraphy ($CHCl_3$-Hexane (5:1). The blue colored fraction was collected and the solvent was removed under reduced pressure to yield the monostyryl compound **14** (50 mg, 13%).

^{1}HNMR *(*400 MHz, $CDCl_3$), δ [ppm]: 0.92 (t, *J*= 7.3 Hz, 3H), 1.04-1.09 (t, *J*= 7.3 Hz, 3H), 1.30 (s, 6H), 1.42 (S, 18H), 2.26 (q, 7.5 Hz, 2H), 2.50 (s+q, 5H), 4.46 (s, 2H), 4.52 (s, 2H), 6.84 (d, *J*=8.5 Hz, 2H), 6.94 (d, *J*= 9.6 Hz, 2H), 7.03-7.22 (m, 3H), 7.34 (d, *J*= 6.7 Hz, 2H), 7.48 (d, *J*= 9.6 Hz, 1H).
^{13}C NMR (100 MHz, $CDCl_3$), δ [ppm]: 167.8, 167.7, 158.5, 158.3, 155.0, 149.2, 139.1, 138.7, 138.5, 134.5, 133.5, 132.8, 132.1, 131.2, 129.7, 128.9, 128.5, 118.4, 115.2, 114.9, 82.5, 82.4, 65.9, 65.8, 28.1, 28.0, 18.3, 17.1, 14.5, 14.1, 12.7, 11.9, 11.5.

Elemental analysis: Found: C, 69.34; H, 7.01; N, 3.95. $C_{42}H_{51}BF_2N_2O_6$ requires, C, 69.23; H, 7.05, N, 3.84. ESI-MS (m/z); 728 [M^+].

The green colored fraction was collected and then the solvent was removed under reduced pressure to yield the distyryl compound **15** (90 mg, 18%).

^{1}H NMR (400 MHz, $CDCl_3$), δ [ppm]: 1.08 (t, *J*=7.3 Hz, 6H), 1.30 (s, 6H), 1.42 (s, 27H), 2.48-2.58 (q, *J*= 7.3 Hz, 4H), 4.49 (s, 4H), 4.52 (s, 2H), 6.86 (d, *J*= 8.6 Hz, 4H), 6.95 (d, *J*= 8.5 Hz, 2H), 7.09-7.2 (m, 4H), 7.49 (d, *J*= 8.6 Hz, 4H), 7.59 (d, *J*= 16.7 Hz, 2H).

^{13}C NMR (100 MHz, $CDCl_3$), δ [ppm]: 166.8, 166.7, 157.5, 157.4, 149.4, 137.8, 134.1, 132.6, 132.3, 130.1, 128.9, 128.1, 127.7, 117.6, 114.3, 113.9, 111.3, 81.6, 81.5, 64.9, 64.8, 27.1, 27.0, 17.4, 13.1, 10.7.

Elemental analysis: Found: C, 69.88; H, 6.98; N, 2.99. $C_{55}H_{65}BF_2N_2O_9$ requires, C, 69.76, H, 6.92, N, 2.96. ESI-MS (m/z); 946 [M^+].

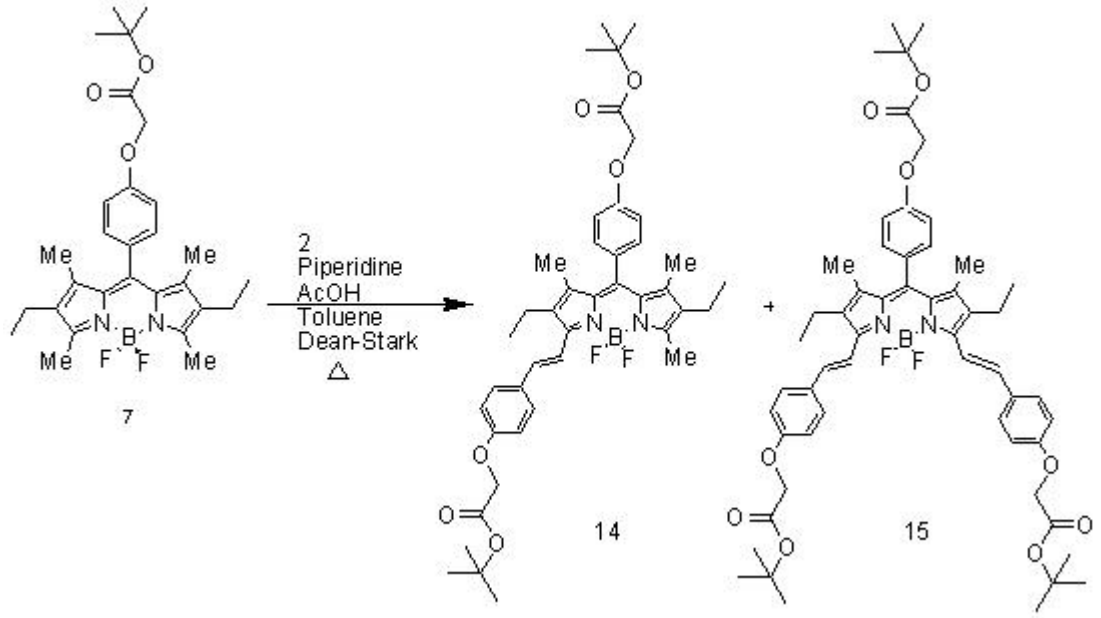

Figure 31: Synthesis of monostyryl and distyryl-BODIPY dyes **(14 and 15)**

2.6. Synthesis of BODIPY dye 6

A procedure very similar to the synthesis of compound **7** was applied in the synthesis of this BODIPY dye. Thus,. *tert*-butyl 2-(4-formylphenoxy)acetate (**2**, 1.5 g, 6.35 mmol), 2.4-dimethylpyrrole (**3**, 1.25 g, 13.1mmol), Et_3N (9.96 mL), $BF_3.OEt_2$ (9.96 mL) and 1.62 g of DDQ were used in this reaction. The residue was chromatographed on silica gel ($CHCl_3$:MeOH, 95:5) to afford 0.784 g compound **6** in the form of orange needles. Yield: 27%.

^{1}HNMR (400 MHz, $CDCl_3$), δ [ppm]: 1.35 (s, 6H), 1.42 (s, 9H), 2.48 (s, 6H), 4.55 (s, 2H), 5.88 (s, 2H), 6.94 (d, *J*=8.5 Hz, 2H), 7.10 (d, *J*= 8.5 Hz, 2H).

^{13}C NMR (100 MHz, $CDCl_3$), δ [ppm]: 167.6, 158.5, 155.3, 143.1, 141.5, 131.8, 129.3, 127.9, 121.2, 115.3, 82.6, 65.8, 61.7, 28.0, 14.5.

Elemental analysis: Found: C, 66.17; H, 6.55; N, 6.11. $C_{25}H_{29}BF_2N_2O_3$ requires, C, 66.09, H, 6.43, N, 6.17. FAB-MS (m/z); 454 [M^+].

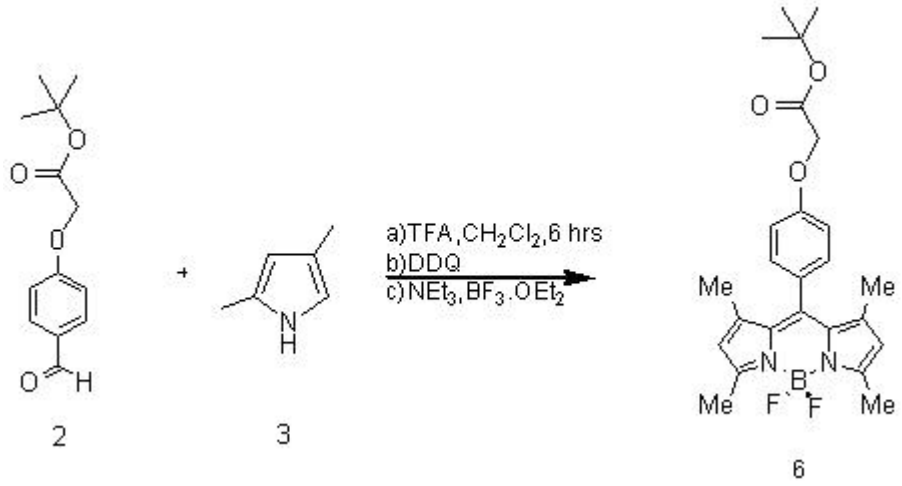

Figure 32: Synthesis of BODIPY dye **6**

2.7. Bromination of the BODIPY dye 6

Compound **6** (0.784 g, 1.73 mmol), AIBN (0.57 g, 3.46 mmol) and NBS (0.616 g, 3.46 mmol) were refluxed for 40 minutes in CCl_4 (40 ml). Crude product was concentrated under reduced pressure and purified by silica gel column chromatography ($CHCl_3$). The red colored fraction was collected and the solvent was removed under reduced pressure to yield the desired compound (**9**) (761 mg, 72%).

^{1}H NMR (400MHz, $CDCl_3$), δ [ppm]: 1.34 (s, 6H), 1.42 (s, 9H), 2.52 (s, 6H), 4.52 (s, 2H), 6.96 (d, *J*= 8.5 Hz, 2H), 7.08 (d, *J*=8.5 Hz, 2H).

^{13}C NMR (100 MHz, $CDCl_3$), δ [ppm]: 167.5, 158.9, 153.9, 143.0, 140.6, 130.7, 129.2, 127.2, 115.6, 111.7, 82.7, 82.7, 82.6, 68.0, 65.8, 28.0, 13.8.

Elemental analysis: Found: C, 49.02; H, 4.49; N, 4.49. $C_{25}H_{27}BBr_2F_2N_2O_3$ requires, C, 49.05, H, 4.45, N, 4.58, O, 7.84 FAB-MS (m/z); 612 [M^+].

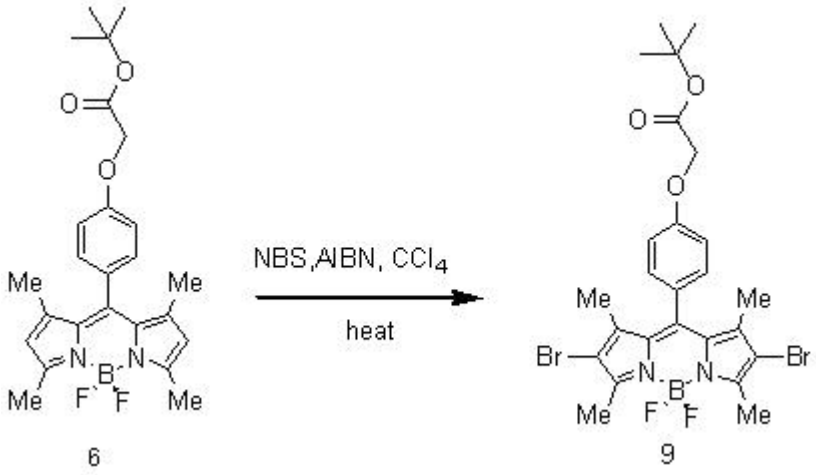

Figure 33: Synthesis of BODIPY dye **9**

2.8. Synthesis of monostyryl and distyryl-BODIPY dyes (12 and 13)

The applied procedure was very similar to the synthesis of other syryl dyes in this study. The dibromo compound **9** (0.761 g, 1.24 mmol), **2** (0.587 g, 2.49 mmol), piperidine (11.2 mL) and acetic acid (0.93 mL) were used in this reaction. Following the usual work-up, the reaction mixture was purified by silica gel column chromotagraphy ($CHCl_3$-Hexane, 5:1). The blue colored fraction was collected and the solvent was removed under reduced pressure to yield the desired compound **12** (0.154 g, 15%).

^{1}H NMR (400 MHz, $CDCl_3$), δ [ppm]: 1.35 (s, 3H), 1.37(S, 3H), 1.38 (s, 9H), 1.47 (s, 9H), 2.58 (s, 3H), 4.47 (s, 2H), 4.53 (s, 2H), 6.83 (d, *J*= 8.7, 2H), 6.98 (d, *J*= 8.5, 2H), 7.12 (d, *J*= 8.5, 2H), 7.54-7.45 (m, 3H), 8.1 (d, *J*= 15.5, 1H).

^{13}C NMR (100 MHz, $CDCl_3$) ,δ [ppm]: 167.6, 166.5, 159.1, 158.3, 156.2, 148.6, 143.0, 141.5, 138.3, 132.9, 129.5, 128.3, 126.9, 121.0, 115.5, 114.9, 82.7, 80.3, 65.8, 61.5, 39.3, 28.0, 23.2, 13.3.

Elemental analysis Found: C, 54.86; H, 4.88; N, 3.43. $C_{38}H_{41}BBr_2F_2N_2O_6$ requires, C, 54.97, H, 4.98, N, 3.37. ESI-MS (m/z); 830 [M^+].

The green colored fraction was collected and then the solvent was removed under reduced pressure to yield the desired compound **13** (0.248 g, 20%).

^{1}H NMR (400 MHz, $CDCl_3$), δ [ppm]: 1.39 (s, 6H), 1.43 (s, 18H), 1.5 (s, 9H), 4.49 (s, 4H), 4.54 (s, 2H), 6.85 (d, *J*= 8.6, 4H), 6.96 (d, *J*= 8.5, 2H), 7.11 (d, *J*= 8.6, 2H), 7.5 (m, 6H), 8.0 (d, *J*= 16.6, 2H).

^{13}C NMR (100 MHz, $CDCl_3$), δ [ppm]: 166.7, 166.5, 157.9, 157.8, 147.3, 139.9, 137.6, 131.3, 129.5, 128.6, 128.3, 126.7, 115.4, 115.4, 114.5, 113.9, 109.1, 81.7, 81.6, 64.7, 64.6, 27.0, 27.0, 12.9.

Elemental analysis: Found: C, 58.46; H, 5.35; N, 2.68. $C_{51}H_{55}BBr_2F_2N_2O_9$ requires, C, 58.42, H, 5.29, N, 2.67. ESI-MS (m/z); 1048 [M^+].

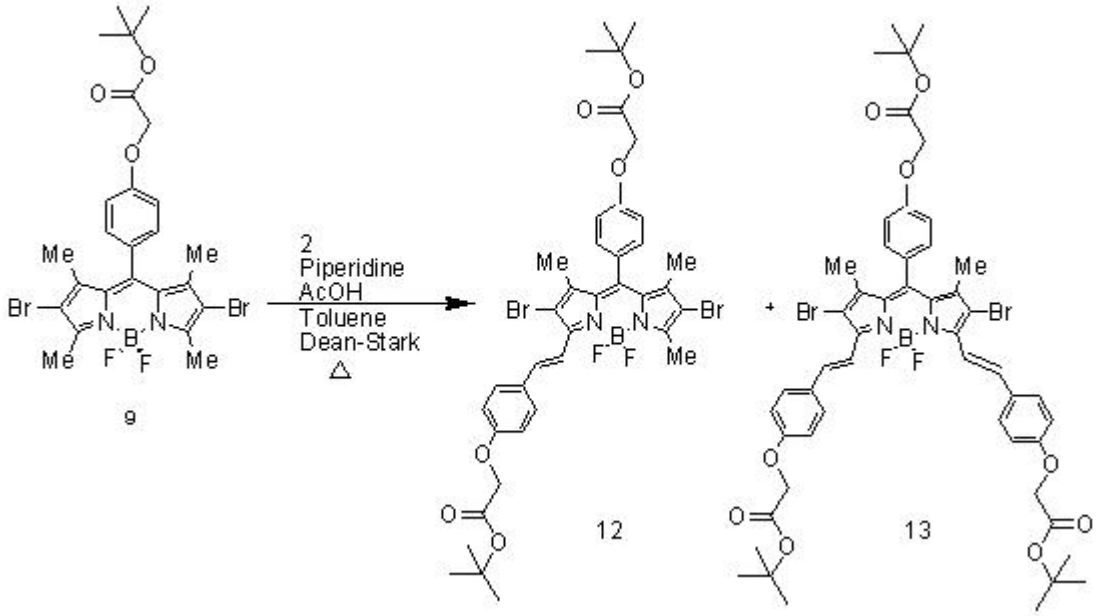

Figure 34: Synthesis of monostyryl and distyryl-BODIPY dyes (**12 and 13**)

CHAPTER III

RESULT AND DISCUSSION

In the first part of study, the synthesis of the dyes **11**, **13** and **15** started with the preparation of the standard BODIPY dyes **5**, **8** and **9**. 8-Phenyl and 8-*t*-butyloxycarbonylmethoxyphenyl-derivatives were synthesized using appropriate aldehydes and purified by a standard work-up. These dyes were then treated with the aldehyde **2** under reflux with azeotropic removal of water. In the other compounds, additional bromine substituents were placed as auxochromic groups. The reaction with the aldehyde, produced both single and double condensation products which can be separated by silica gel column chromatography. The presence of *tert*-butyl groups improved organic solubility to a great extent as expected. Here, we are reporting the first synthesis of doubly styryl substituted boradiazaindacenes (DS-BODIPY's), starting from 3,5-dimethyl-boradiazaindacene derivatives. The condensation reactions seem not to be limited with dialkylamino substituted aromatic aldehydes, which is an important finding for the broader applicability of the derivatization reaction.

In second part, we measured singlet oxygen generation capacities of distyryl BODIPY dyes in isopropanol at 7.5 nM and we compared our singlet oxygen generators with compounds known and used in PDT.

In the last part, we measured absorbances, emissions and calculated their quantum yields of synthesized BODIPY dyes.

3.1. Singlet Oxygen Generation by of monostyryl and distyryl-BODIPY dyes

Singlet oxygen generation capacities of these novel monostyryl and distyryl-BODIPY dyes were studied in isopropanol at 7.5×10^{-9} M concentration. The experiments were performed in such a sensitizers were unequivocally established. Red light from LED lamps was used to excite BODIPY dyes. The light intensity was

determined to be 2.5 mW/cm^2. Firstly, the change in the absorption of the selective singlet oxygen trap 1,3-diphenyl-isobenzofuran [64, 71] (5xl0^{-5} mM) in the aerated for 5 minutes was measured before the irradiation started. During irradiation, the absorbance was measured in every 5 minutes in dark and also under red light. Under these experimental conditions, the absorbance at the peak absorbance wavelength of 1,3-diphenyl-iso-benzofuran Figure [38- 46] (415 nm) did not change whereas, the solutions containing BODIPY dyes showed significant decreases in absorbance. In order to eliminate any contribution to the absorbance changes from dark reactions or check the toxicity of distyryl BODIPY dyes, we also recorded absorbance under the same conditions for 20 minutes in dark. None of the compounds studied resulted in any absorbance changes in the reaction mixture. Only when the light was turned on, the degradation of the sing1et oxygen trap started.

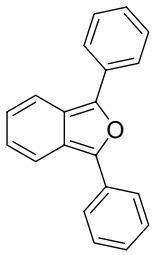

Figure 35: Structure of the singlet oxygen trap 1,3-diphenyl-*iso*-benzofuran.

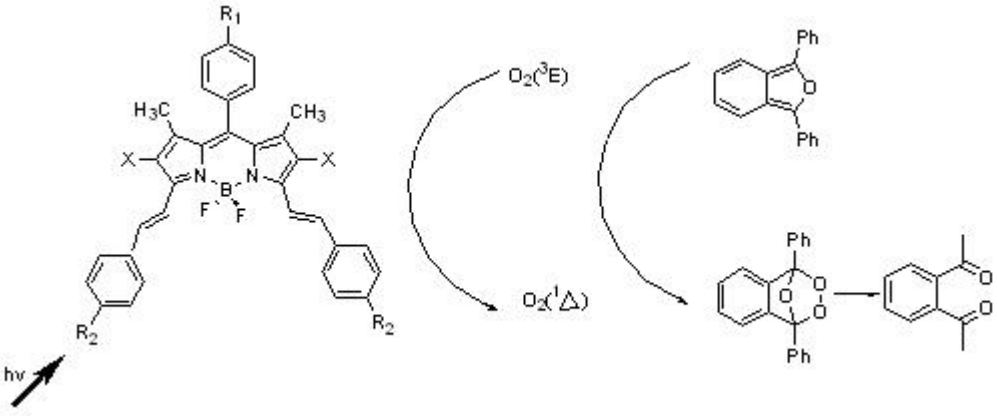

Figure 36: Mechanism of the change in absorbance of singlet oxygen trap.

3.2. Degradation of styryl-BODIPY dyes and 1,3-diphenyl-iso-benzofuran under red light

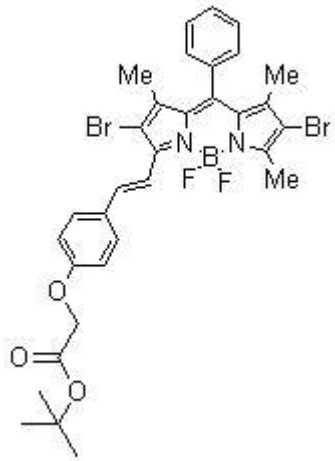

Figure 37: Structure of monostyryl BODIPY dyes **(10)**

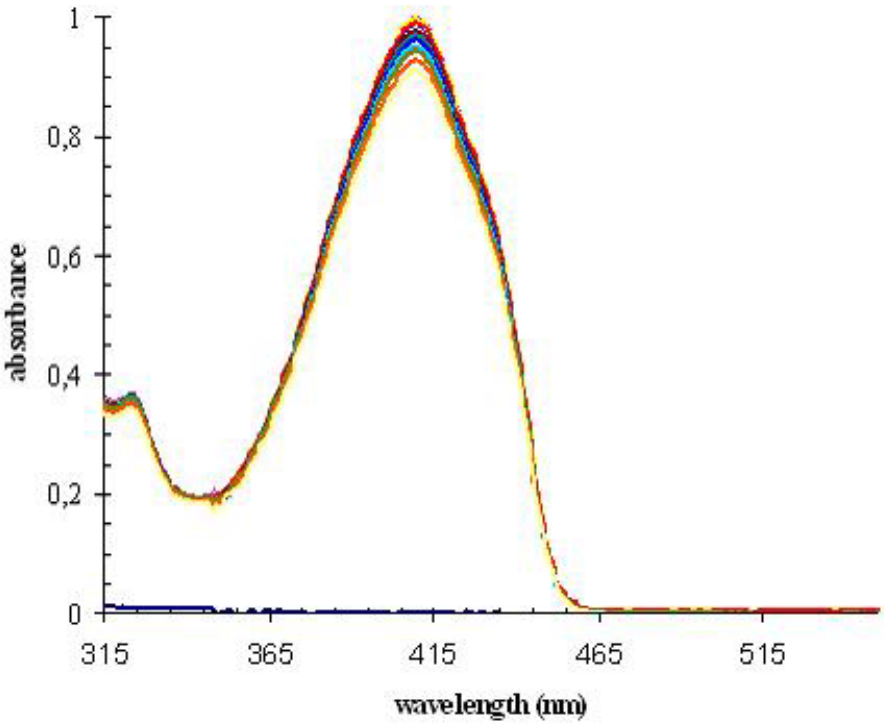

Figure 38: The change in the absorbance spectrum of 1,3-diphenyl-*iso*-benzofuran and compound **(10)** mixture on irradiation with light (625 nm)

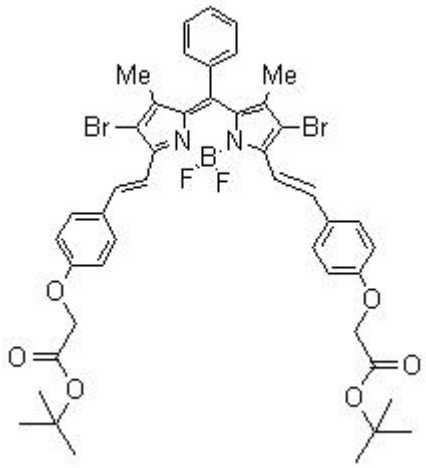

Figure 39: Structure of distyryl BODIPY dyes **(11)**

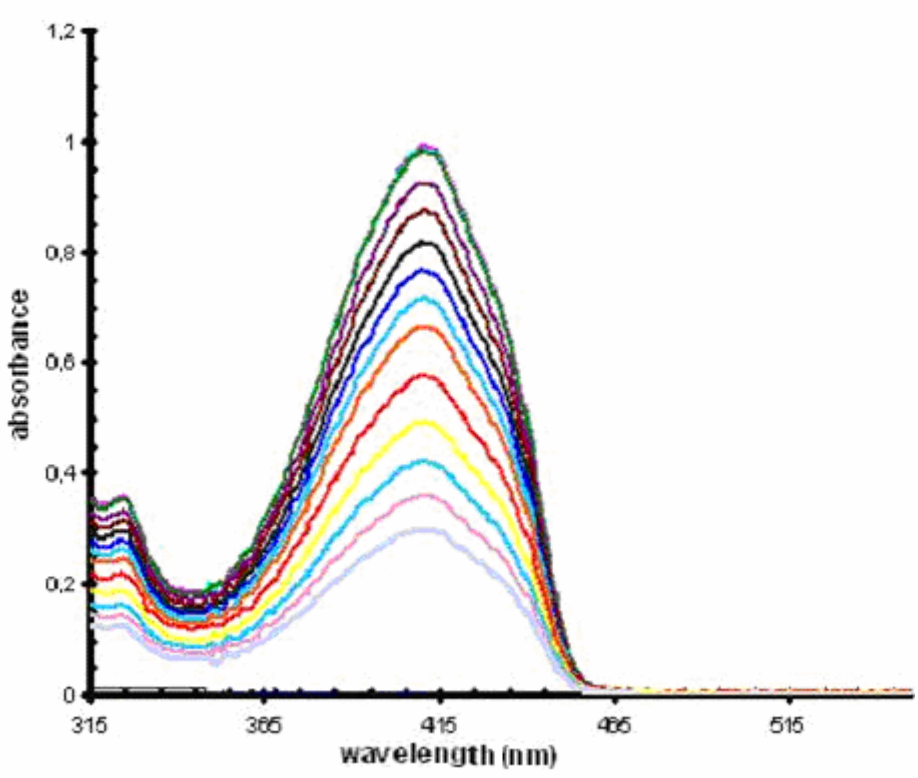

Figure 40: The change in the absorbance spectrum of 1,3-diphenyl-*iso*-benzofuran and compound **(11)** mixture on irradiation with light (625 nm)

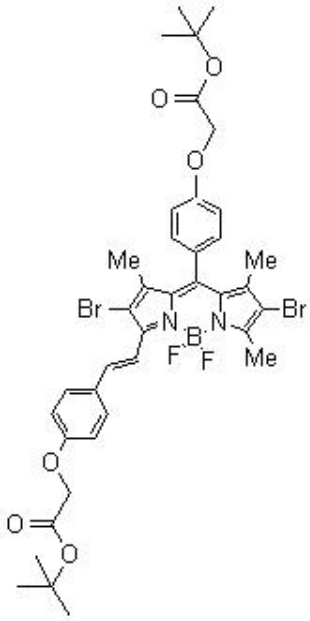

Figure 41: Structure of monostyryl BODIPY dyes **(12)**

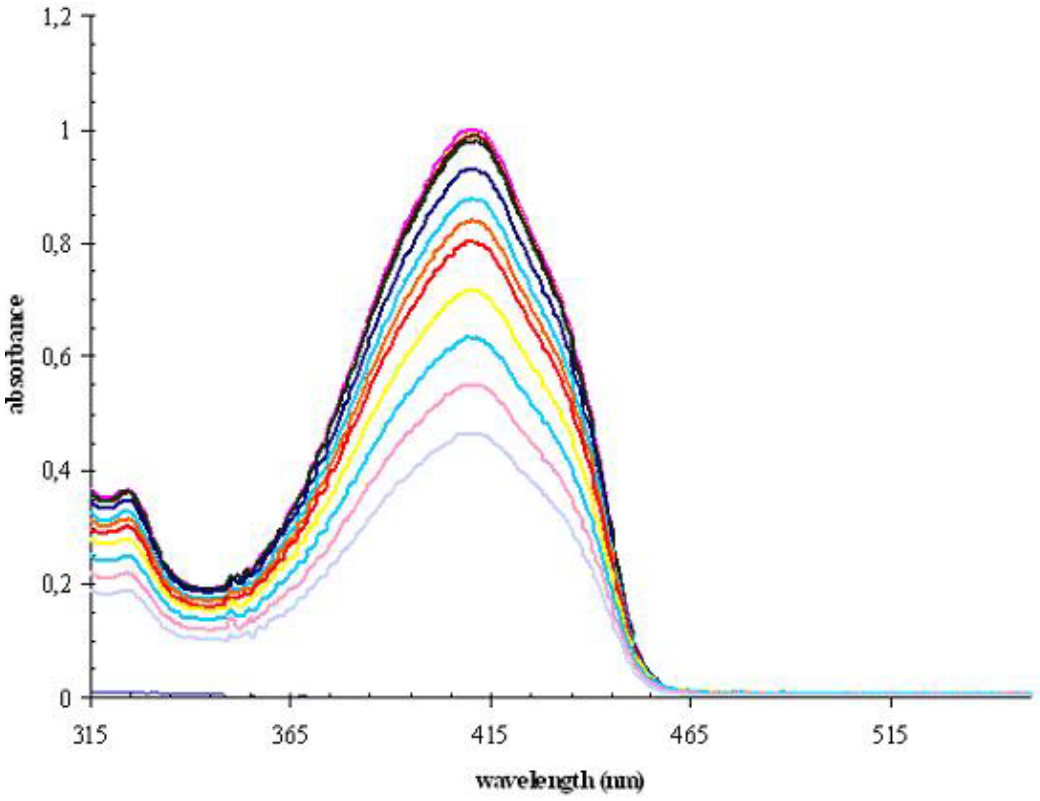

Figure 42: The change in the absorbance spectrum of 1,3-diphenyl-*iso*-benzofuran and compound **(12)** mixture on irradiation with light (625 nm)

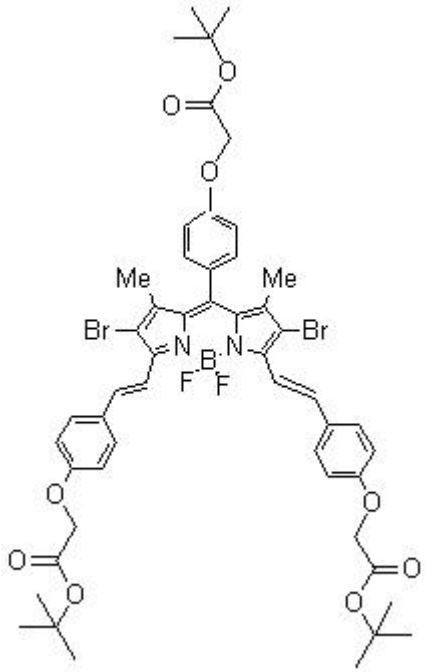

Figure 43: Structure of distyryl BODIPY dyes **(13)**

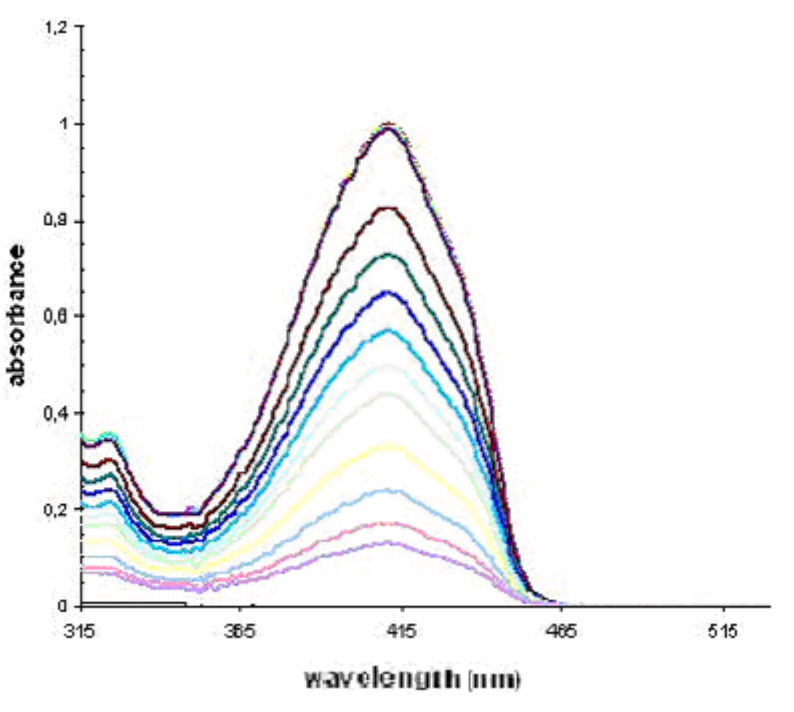

Figure 44: the change in the absorbance spectrum of 1,3-diphenyl-*iso*-benzofuran and compound **(13)** mixture on irradiation with light (625 nm)

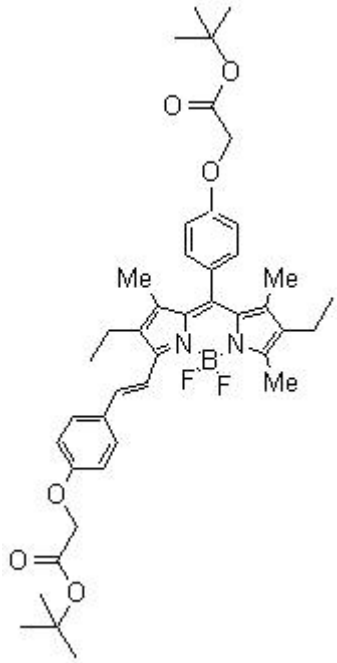

Figure 45: Structure of monostyryl BODIPY dyes **(14)**

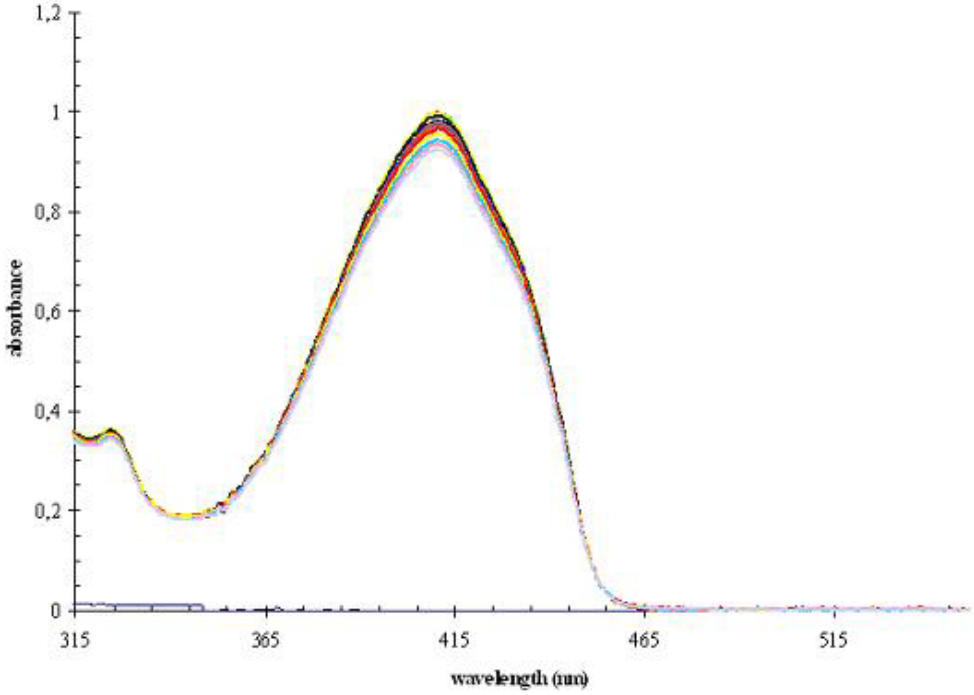

Figure 46: The change in the absorbance spectrum of 1,3-diphenyl-*iso*-benzofuran and compound **(14)** mixture on irradiation with light (625 nm)

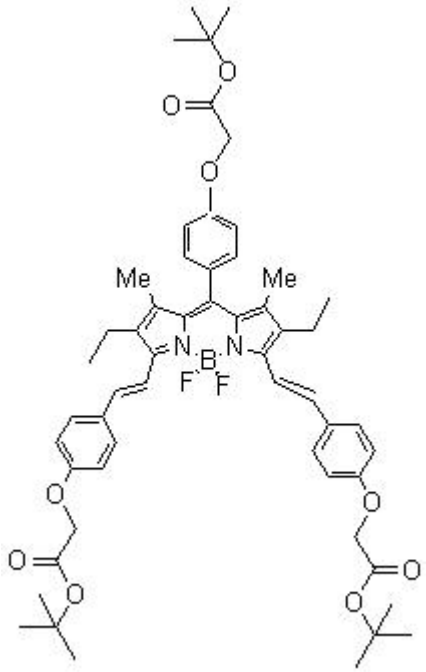

Figure 47: Structure of distyryl BODIPY dyes **(15)**

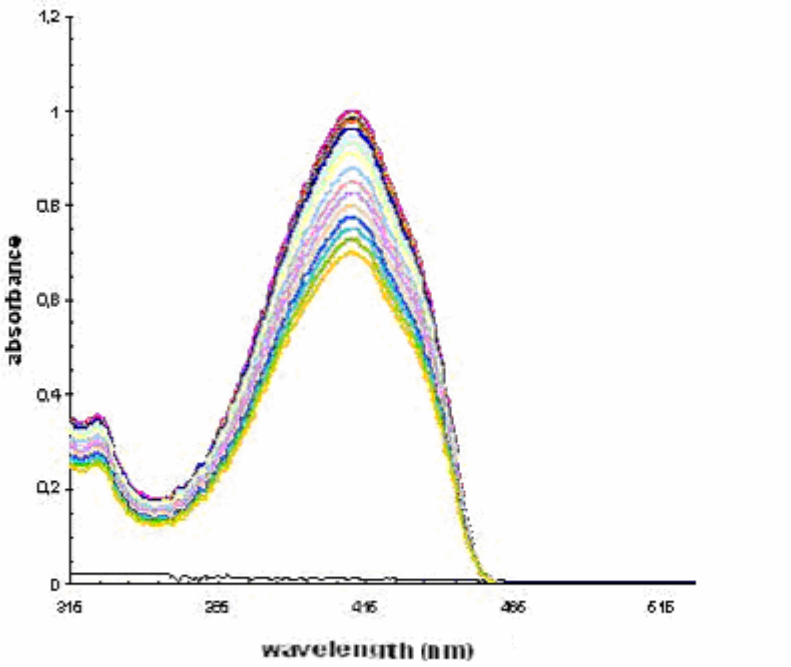

Figure 48: The change in the absorbance spectrum of 1,3-diphenyl-*iso*-benzofuran and compound **(15)** mixture on irradiation with light (625 nm)

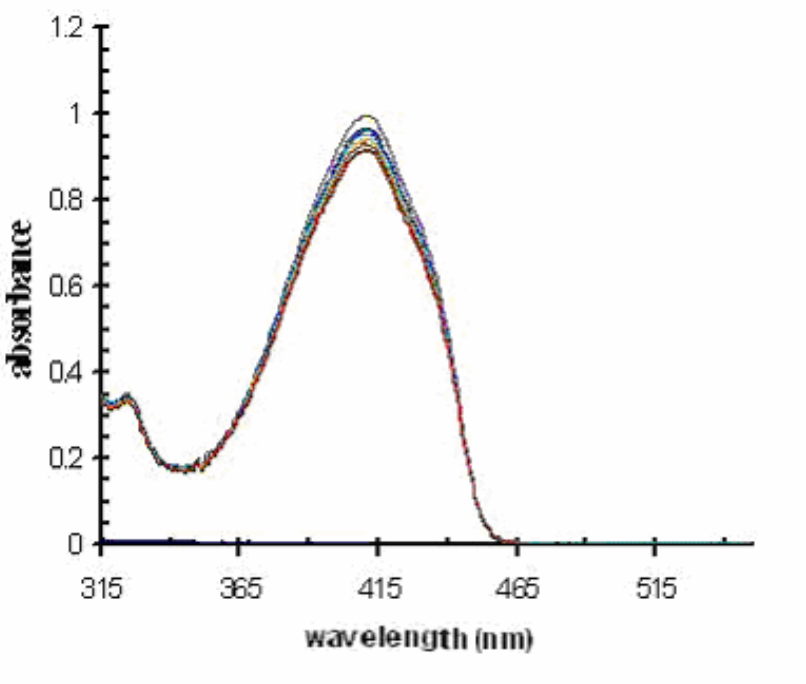

Figure 49: The change in the absorbance spectrum of 1,3-diphenyl-*iso*-benzofuran and compound **TPPS4** mixture on irradiation with light (625 nm)

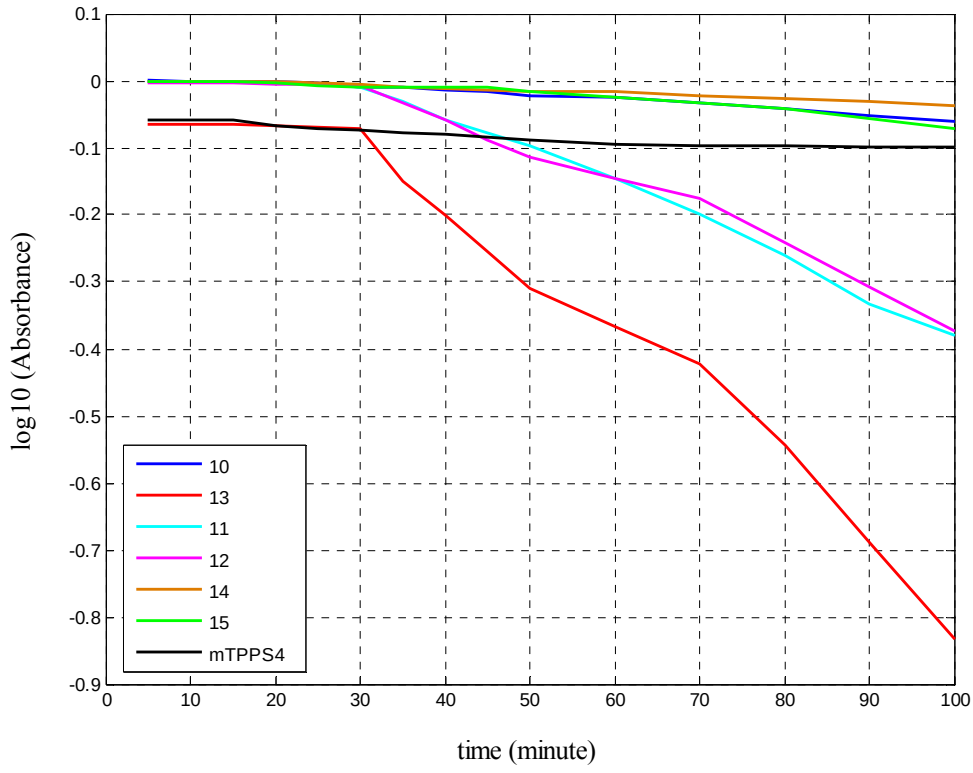

Figure 50: Comparative singlet oxygen generation of compounds 10-15 in $CHCl_3$ at 7.5 μM concentration.

TPPS4 is used in PDT. We measured the change in the absorbance spectra of 1,3-diphenyl-*iso*-benzofuran and BODIPY dyes mixtures [Figure 38, 40, 42, 44, 46, 48] and TPPS4 mixture at same concentration (7.5 nM) and compared these results. We could say that distyryl BODIPY dyes are better singlet oxygen generator than TPPS4.[Figure 50]

Recently, many novel sensitizers for PDT have been synthesized. Squarene 1d [Figure 22] is one of them. Figure 23 shows time evolution of the UV-VIS spectrum of a DPBF and 1d in CH_2Cl_2 solution. By using results in figure 23 and 24, it is said that 1d compound has toxicity and its singlet oxygen generation capacity is lower than that of distyryl BODIPY dyes.

Perylenediimide dyes [Figure 25] and 2I-BODIPY [Figure 27] are good sensitizers. However, their concentrations used in singlet oxygen generation are higher than distyryl BODIPY's. Also, absorbance of 2I-BODIPY is at 540 nm and has high energy. Thus, skin depth or penetration depth is low. The higher penetration depth is, the better sensitizer for PDT is.

3.3. Normalized absorbance and emission spectra of synthesized BODIPY dyes

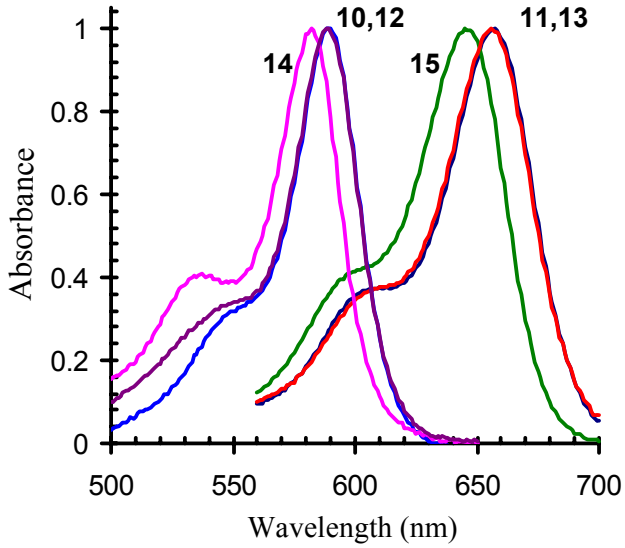

Figure 51: Normalized absorption spectra of extended conjugation BODIPY dyes in isopropanol. Compounds **10**, **12** and **14** are monostyryl derivatives, whereas, **11**, **13** and **15** are distyryl compounds

The presence of *tert*-butyl groups improved organic solubility to a great extent as expected. The absorption spectra of the dyes **10-15** were obtained in a polar protic solvent, isopropanol. The spectra are shown in Figure 51. The second styryl group causes a bathochromic shift of about 100 nm. The bromine substitution at the pyrrolic positions result in an additional 11 nm of shift towards the red end of the visible spectrum. These dyes show remarkable red fluorescence even under ambient light.

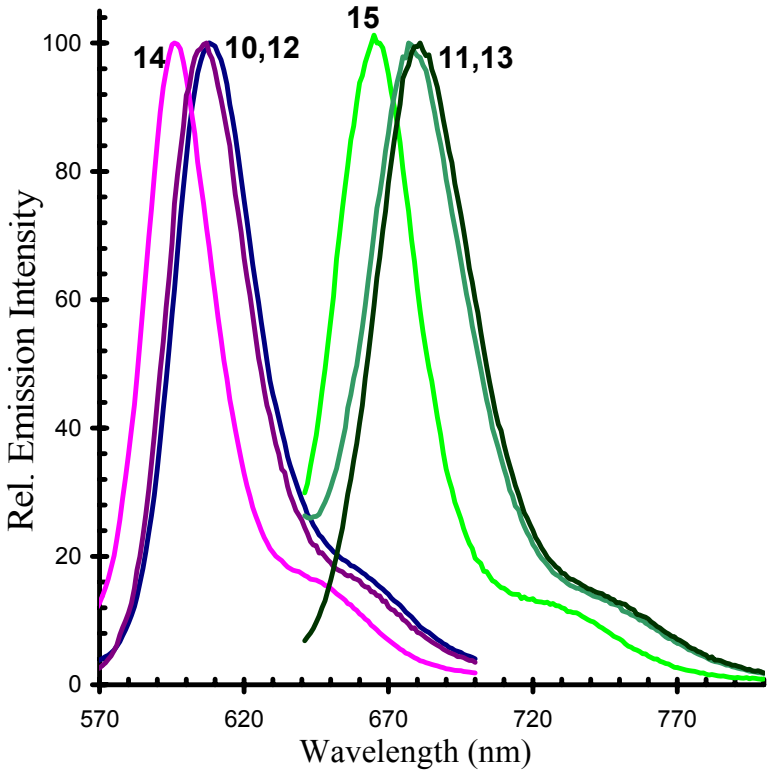

Figure 52: Normalized emission spectra of extended conjugation BODIPY dyes in isopropanol. Compounds **10**, **12** and **14** are monostyryl derivatives, whereas, **11**, **13** and **15** are distyryl compounds. The excitation wavelength was 530 nm for the monostyryl dyes and 610 nm for the distyryl dyes. Slit widths were 5 nm.

The novel fluorophores had relatively small Stokes' shifts of 15 nm, with sharp emission peaks (Figure 52). Compound **11** had the most red shifted emission peak at 679 nm. More importantly however, the fluorophores had only very little internal charge transfer characteristics, the emission peak position was only slightly moved bathochromically on changing the solvent from toluene to DMSO (Figure 52). The quantum yield of emission for the dyes **11**, **13** and **15** were determined

using bis[4-(dimethylamino)-2-hydroxyphenyl]squaraine as a reference [72] (Table 2). Extinction coefficients are also very large (log ε 4.94-5.00), thus the brightness factor (ϕ_f x ε) for these novel fluorophores is in fact larger than fluorescein. This straightforward derivatization of parent boradiazaindacene structures to yield near IR emitting dyes is not only important for the development of new biologically relevant fluorescent labels, but may very well transform these dyes into building blocks in functional supramolecular systems. We are at present investigating such paths for further development.

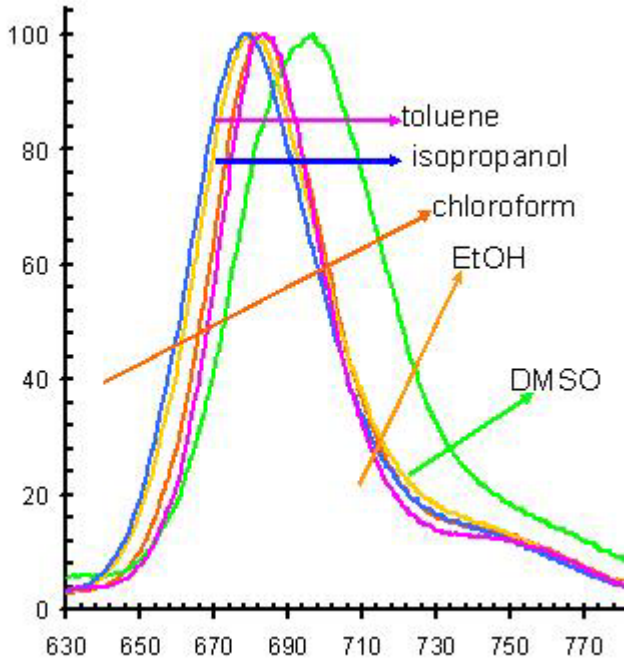

Figure 53: Normalized emission spectra of distyryl-BODIPY dye **13** in solvents of varying polarities. Excitation was at 610 nm, with 5 nm slit widths.

Distyryl-BODIPY	**11**	**13**	**15**
λ_{max} (abs)	657 nm	646 nm	656 nm
λ_{max} (em)	679 nm	668 nm	678 nm
fwhm	41 nm	36 nm	43 nm
ε ($M^{-1}cm^{-1}$)	1.01 x 10^5	8.85 x 10^4	8.79 x 10^4
Φ_{em}	0.42	0.44	0.40

Table 2: Selected spectral data of distyryl-BODIPY compounds **11**, **13** and **15**.

CHAPTER IV

CONCLUSION

We have synthesized and characterized near IR emitting boradiazaindacene dyes in a very straightforward reaction. This is the first report of the double condensation reaction 3,5-dimethylboradiazaindacenes. The use of Dean-Stark apparatus seems to be critical in removing any water formed in the reaction and thus shifting the equilibrium to the double condensation products, which are the distyrl-BODIPY dyes. The simplicity of the modification would allow facile synthesis of many other BODIPY dyes with desired functional groups. The synthesis has definitely a modular character. With the well known advantages of working with red or near IR emitting fluorophores, we have no doubt that this series of boradiazaindacenes will be attractive candidates for practical applications

REFERENCES

1. Lehn, J. *Angew. Chem., Int. Ed. Engl*. **1998**, *27*, 89-112
2. Lehn, J. *Proc. Natl. Acad. Sci. U.S.A.* **2002**, *99*, 4763-4768
3. Pandey, R. K.; Zhang, G. *Porphyrin Handbook*; Kadish, K. M., Smith, K. M., Guilard, R., Eds.; *Academic Press: San Diego, CA*, **2000**; Vol. 6
4. Dougherty, T. J.; Gomer, C. J.; Henderson, B. W.; Jori, G.; Kessel, D. Korbelik, M.; Moan, J.; Peng, Q. *J. Natl. Cancer Inst.* **1998**, *90*, 889-905.
5. Kato, *J. Photochem. Photobiol. B: Biol.* **1998**, *42*, 96-99.
6. Guillemin, F.; Feintrenie, X.; Lignon, D. *Rev. Pneumol. Clin.* **1992**, *48*, 111-114.
7. Puolakkainen, P.; T. Schroder, *Digestive Diseases* **1992**, *10*, 53-60.
8. Noske, D. P.; Wolbers, J. G.; Sterenborg, H. J. A Review of Literature *Clin. Neurol. Neurosurg.* **1991**, *93*, 293-307.
9. Moesta, K. T.; Schlag, P.; Douglass, H. O., Jr.; Mang, T. S. *Lasers Surg. Med.* **1995**, *16*, 84-92.
10. Neurath, A. R., Strick, N., and Debnath, A. K. *J. Mol.* Recog. **1995** *8*, 345-357.
11. Bonnett, R. *Chem. Soc. Re*V. **1995,** 19- 33.
12. Moor, A. C. E. *J. Photochem. Photobiol., B,* **2000,** *57*, 1-13.
13. Mody, T. D. Pharmaceutical development and medical applications of porphyrin-type macrocycles, *J. Porphyrins Phthalocyanines,* **2000** *4*, 362-367.
14. Jori, G. *J. Photochem. Photobiol., B* **1996,** *36*, 87-93.
15. Yang, S. I., Seth, J., Strachan, J.-P., Gentlemann, S., Kim, D., Holten, D., Lindsey, J. S., and Bocian, D. F. *J. Porphyrins Phthalocyanines.* **1999** *3*, 117-147.
16. Dougherty, T. J. *Photochem. Photobiol.* **1993,** *58*, 895-900.
17. Policard, A., *Compt. Rend. Soc. Biol*., **1924**, 91, 1423-1424
18. Figge, FHJ., *AAAS Research Conf. On Cancer*., **1945**, 117-128
19. Figge, FHJ., *Ann. Int. Med*., **1947**, 24, 143-146.

20. Figge, FHJ., Weiland, GS., Mangeniello, LOJ., *Proc. Soc. Exp. Biol. Med*., **1948**, 68, 143-146
21. Rasmussen-Taxdal, DS., Ward. DE., Figge, FHJ*., Cancer*, **1955**, 8, 78-81.
22. Winkelman, J., *J. Natl. Cancer Inst*., **1961**, 27, 1369-1377.
23. Winkelman, J., *Cancer Res*., **1962**, 22, 589-596.
24. Winkelman, J., *Experimentia*, **1967**, 23, 949-950.
25. Dougherty, TJ., *J.Clin. Laser Med. Surg*., **1996**, 14, 52, 1333-1336.
26. Dougherty, TJ., Gomer, CJ., Henderson, BW. Et al., *J. Natl. Cancer Inst*., **1998**, 90, 889-905.
27. Pandey, RK., Zheng, G., *Porphyrins as Photosensitizers in Photodynamic Therapy*, **2000**, 6.
28. Dougherty, T. J.; Marcus, S. L. Photodynamic Therapy. *Eur. J. Cancer* **1992**, *28A*, 1734-1742.
29. Dougherty, T. J.; Gomer, C. J.; Henderson, B. W.; Jori, G.; Kessel, D.; Korbelik, M.; Moan, J.; Peng, Q. *J. Natl. Cancer Inst.* **1998**, *90*, 889-905Fingar, V. H.; Mang, T. S.; Henderson, B. W. *Cancer Res.* **1988**, *48*, 3350-335
30. Foote., CS., *Porphyrin Localization and Treatment of Tumors*, **1984**, 3-18.
31. Henderson, BW., Dougherty, TJ*., Photochem. Photobiol*., **1992**, 55, 147-157.
32. Weishaupt, KR., Gomer, CJ., Dougherty, TJ., *Cancer Res*., **1976**, 2326-2329.
33. Gilbert, A., Baggort, J., *Essentials of Molecular P hotochemistry*, **1991**, 501-525.
34. Gilbert, A., Baggort, J., *Essentials of Molecular P hotochemistry*, **1991**, 1-10.
35. Turro, NJ., *Modern Molecular Photochemistry*, **1991**, 583-593.
36. Pass, HI., *J. Natl. Cancer Inst*., **1993**, 86, 443-456.
37. Henderson BW., Fingar, VH., *Cancer Res*., **1987**, 47, 3110-3114.
38. Dubbelman, TMAR., Prinsze, C., Penning, LC., Van Steveninck, J., *In Photodynamic Therapy: Basic Principles and Clinical Applications*, **1992,** 37-46.
39. See, KL., Forbes, IJ., Betts, WH*., Photochem. Photobiol*., **1984,** 39, 631-634.
40. Dennis, E. J.; Dolmans, G. C.; Fukumura, D.; Jain, R. K. *Nat. Rev. Cancer* **2003**, *3*, 380-387.
41. Dougherty, T. J. *Photochem. Photobiol.* **1983**, *38*, 377-379.

42. Dougherty, T. J.; Potter, W. R.; Weishaupt, K. R. *Prog. Clin. Biol. Res.* **1984**, *170*, 301-314.
43. Sharman, W. M.; Allen, C. M.; van Lier, J. E. *Drug Discovery Today* **1999**, *4*, 507-517.
44. Bellnier, D. A.; Dougherty, T. J. *J. Clin. Laser Med. Surg.* **1996**, *14*, 311-314.
45. Sternberg, E. D.; Dolphin, D.; Bru¨ ckner, C. *Tetrahedron* **1998**, *54*, 4151-4202.
46. Wilkinson, F.; Helman, W. P.; Ross, A. *J. Phys. Chem. Ref. Data* **1993**, *22*, 113-262.
47. Kessel, D.; Thompson, P.; Saatio, K.; Nantwi, K. D. *Photochem. Photobiol.* **1987**, *45*, 787-790.
48. Sema, A. A. F.; Kennedy, J. C.; Blakeslee, D.; Robertson, D. M. *Can. J. Neurol. Sci.* **1981**, *8*, 105-114.
49. Winkelman, J. W.; Collins, G. H. *Photochem. Photobiol.* **1987**, *46*, 801-807.
50. Harth, E. M.; Hecht, S.; Helms, B.; Malmstrom, E. E.; Fre´chet, J. M. J.; Hawker, C. J. *J. Am. Chem. Soc.* **2002**, *124*, 3926-3938.
51. Nishiyama, N.; Stapert, H. R.; Zhang, G.-D.; Takasu, D.; Jiang, D.-L.; Nagano, T.; Aida, T.; Kataoka, K. *Bioconjugate Chem.* **2003**, *14*, 58-66.
52. Kostenich, G. A.; Zhuravkin, I. N.; Zhavrid, E. A. *J. Photochem. Photobiol., B* **1994**, *22*, 211-217.
53. Wong, T.-W.; Aizawa, K.; Sheyhedin, I.; Wushur, C.; Kato, H. *J. Pharmacol. Sci.* **2003**, *93*, 136-142.
54. Walt, H.; Degen, A.; Fehr, M. K. *Int. J. Cancer* **2001**, *93*, 720 724.
55. Schmidt, A. H. In *Oxocarbons*; West, R., Ed.; *Academic Press: New York*, **1980**, p 185.
56. Law, K. Y. *J. Phys. Chem.* **1987**, *91*, 5184. (b) Law, K. Y. *Chem. Re*V. **1993**, *93*, 449.
57. (a) Dolmans, D. E. J. G. J.; Fukumura, D.; Jain, R. K. *Nat. Re*V. *Cancer* **2003**, *3*, 380. (b) Bonnett, R. *Chem. Soc. Re*V. **1995**, *24*, 19.
58. Luca B.; Alessandro A.; Mirko L.; Michele C.; Riccardo T.; Francesco M.; Silvia B.; Giorgio A. P. *Org. Lett*. **2005** *Vol. 7, No. 19,* 4257-4260
59. Law, K. Y. *Chem. Re*V. **1993**, *93*, 449.

60. (a) Dotcheva, D.; Klapper, M.; Mullen, K. *Macromol. Chem. Phys.* **1994**, *195*, 1905-1911. (b) Wurthner, F.; Thalacker, C.; Sautter, A. *Ad*V. *Mater.* **1999**, *11*, 754- 758.
61. (a) Qu, J.; Kohl, C.; Pottek, M.; Mullen, K. *Angew. Chem., Int. Ed*. **2004**, *43*, 1528-1531. (b) Margineanu, A. et al. *J. Phys. Chem. B* **2004**, *108*, 12242-12251.
62. (a) Langhals, H.; Schonmann, G.; Feiler, L. *Tetrahedron Lett.* **1995**, *36*, 6423-6424. (b) Holtrup, F. O.; Muller, G. R. J.; Quante, H.; De Feyter, S.; De Schryver, F. C.; Mullen, K. *Chem.*s*Eur. J.* **1997**, *3*, 219-225. (c) Kohl, C.; Becker, S.; Mullen, K. *Chem. Commun.* **2002**, 2778-2779.
63. Zhao, Y.; Wasielewski, M. R. *Tetrahedron Lett*. **1999**, *40*, 7047- 7050.
64. Sugiyasu, K.; Fujita, N.; Shinkai, S. *Angew. Chem., Int. Ed*. **2004**, *43*, 1229-1233.
65. Yukruk F.; Dogan A.L.; Canpinar H.; Guc D.; Akaya E.U**.** *Org. Lett*. **2005,** *Vol. 7, No. 14*, 2885-2887
66. Guiraud, H. J.; Foote, C. S. *J. Am. Chem. Soc*. **1976**, *98*, 1984- 1986.
67. McClure, D. S. *J. Chem. Phys*. **1949**, *17*, 905.
68. Krasnovsky, A. A. *Chem. Phys. Lett.* **1981**, *81*, 443-445.
69. Yuster, P.; Weissman, S. I. *J. Chem. Phys.* **1949**, *17*, 1182.
70. Mitzel, F., FitzGerald, S., Beeby, A., Faust, R., *Chem. Commun.,* **1943**, 596.
71. Law, K.-Y. *J. Phys. Chem.* **1987**, *91*, 5184-5193.

APPENDIX

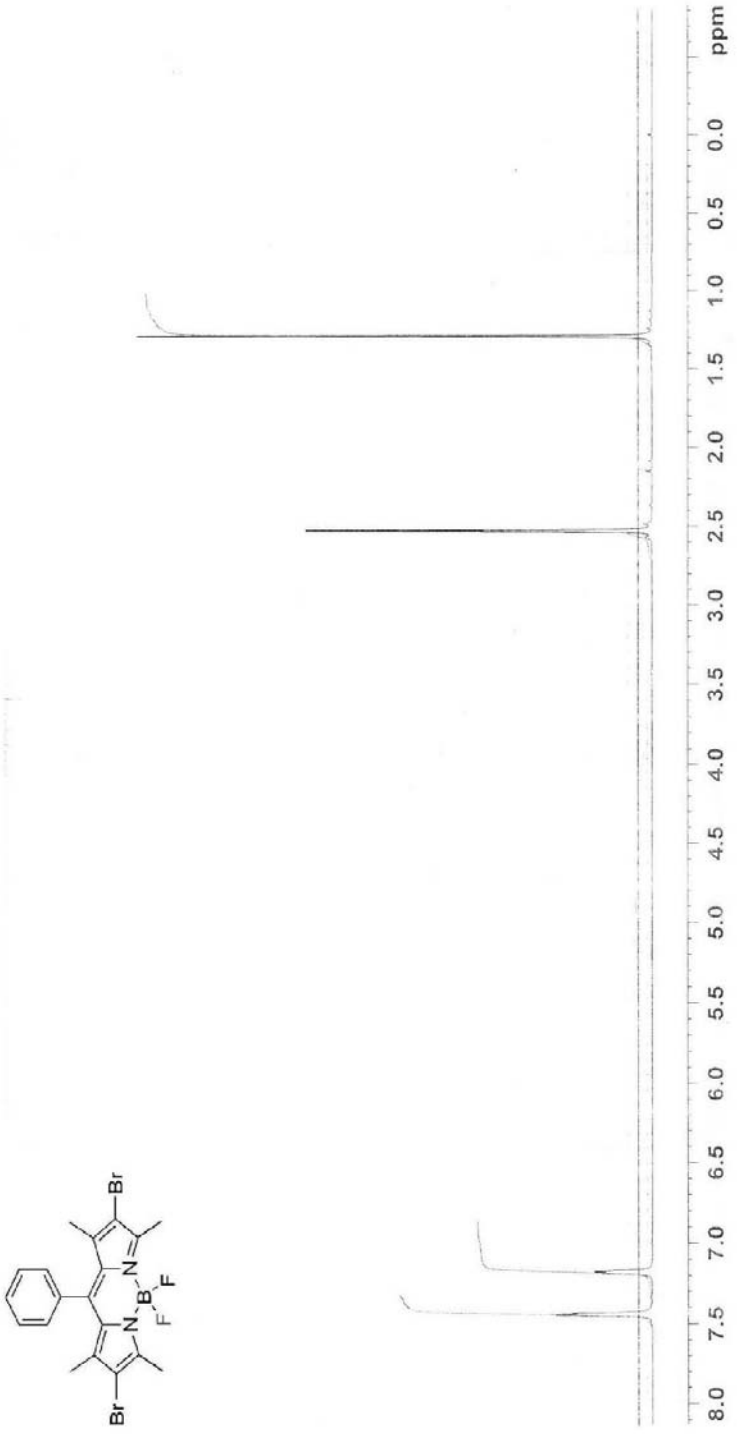

Figure 53: H NMR Spectrum of 8

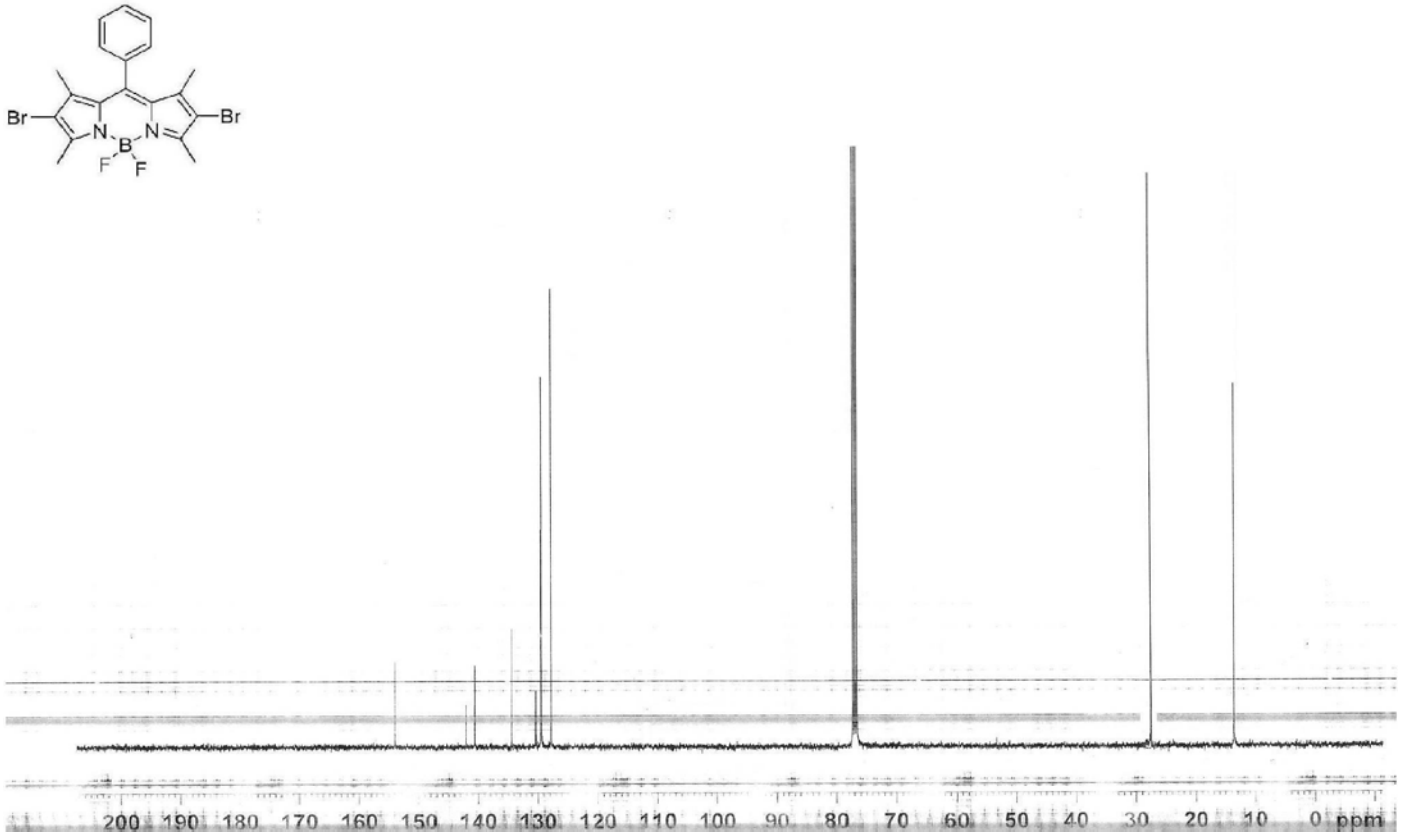

Figure 54: C NMR Spectrum of 8

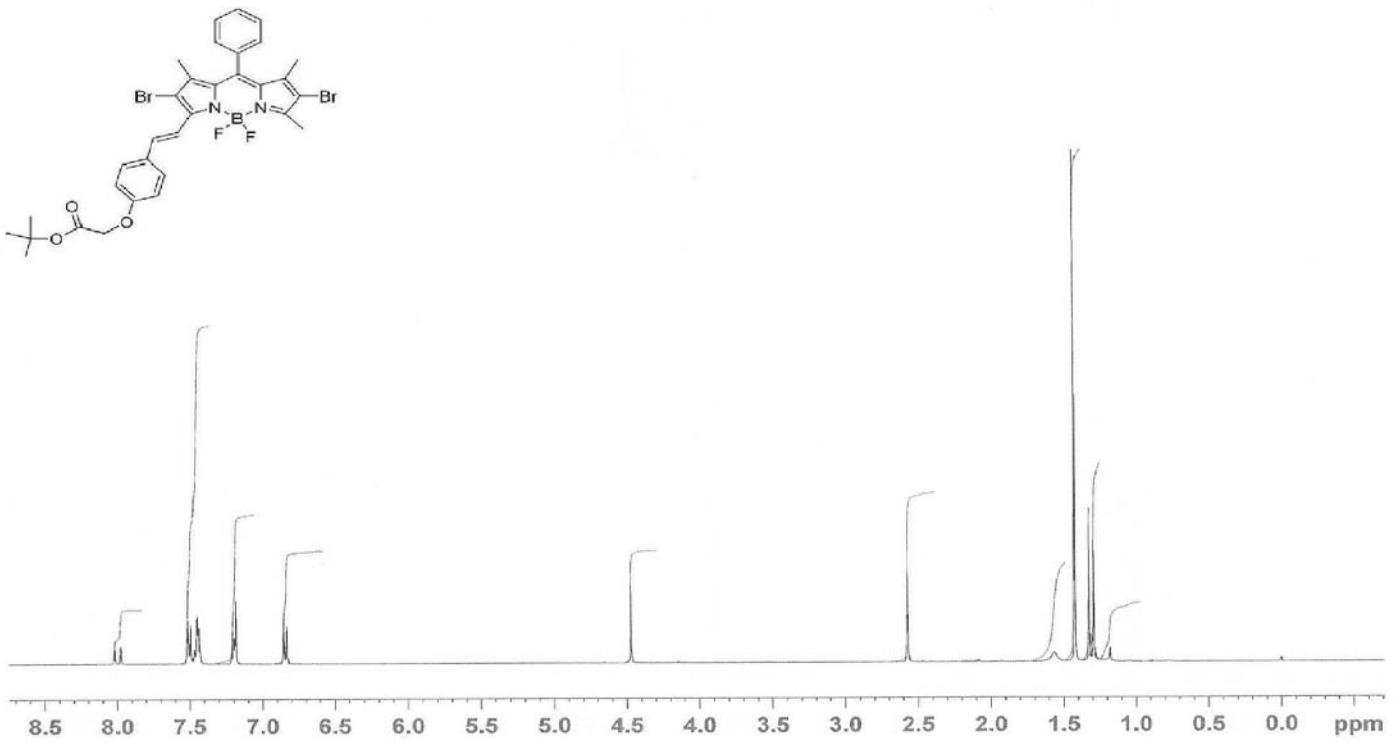

Figure 55: H NMR Spectrum of 10

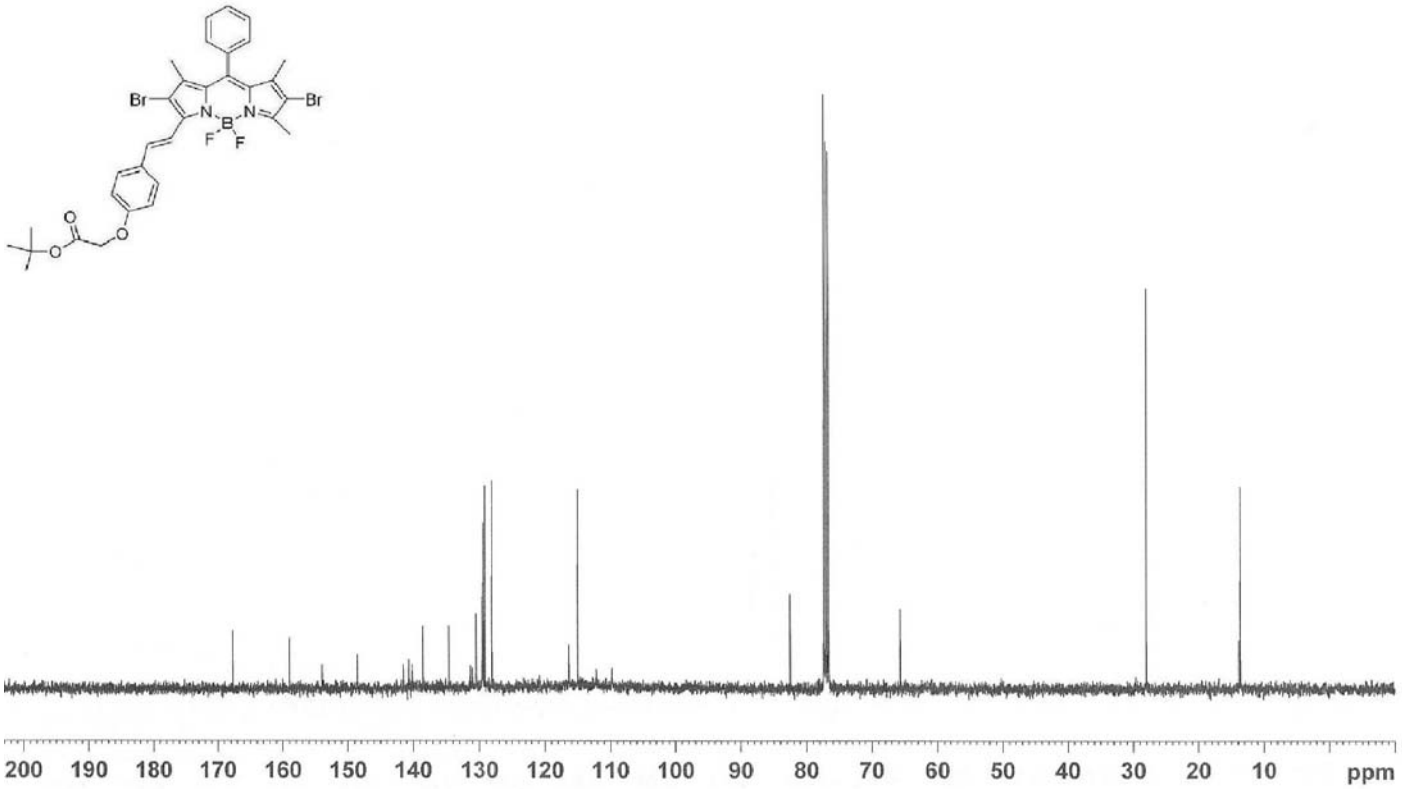

Figure 56: C NMR Spectrum of 10

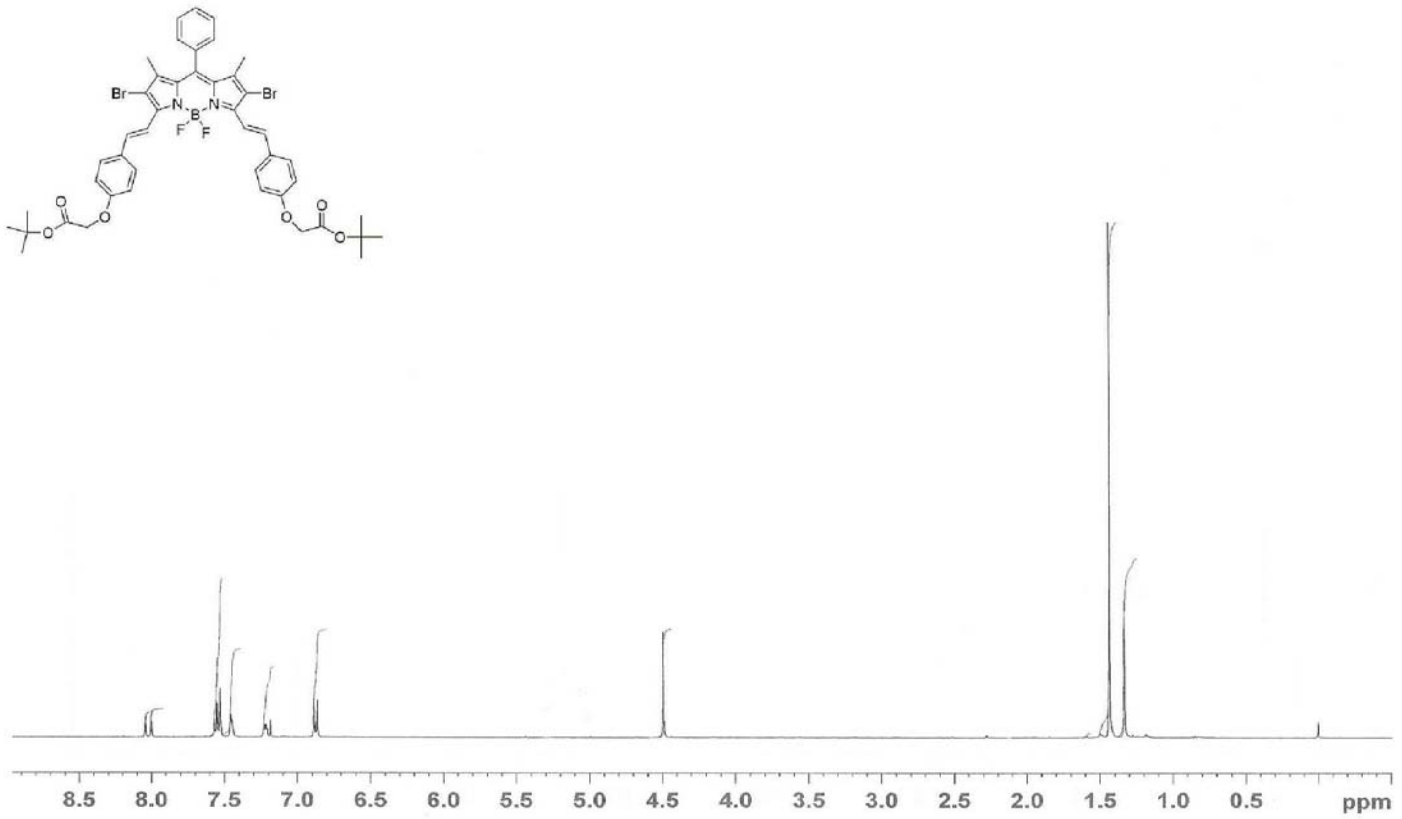

Figure 57: H NMR Spectrum of 11

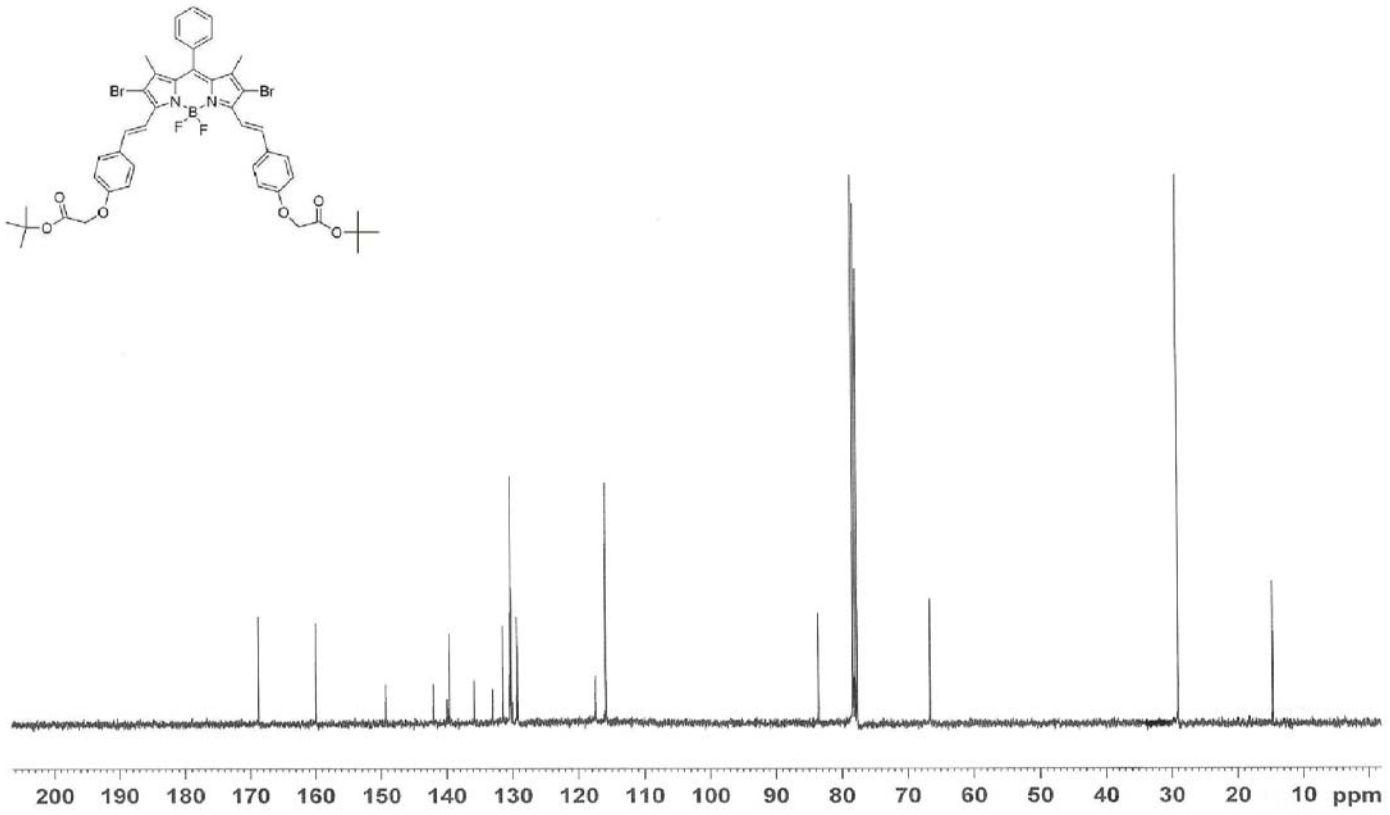

Figure 58: C NMR Spectrum of 11

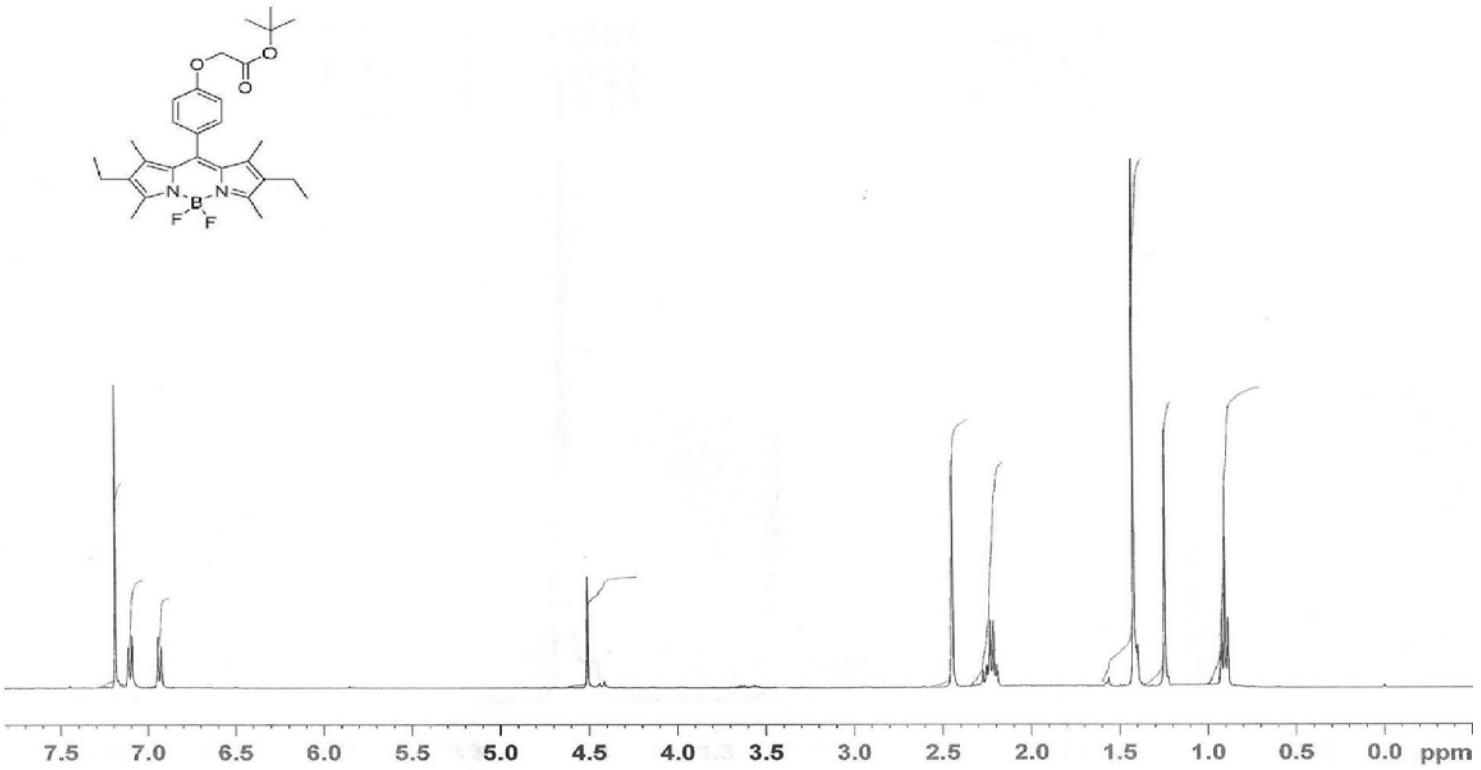

Figure 59: H NMR Spectrum of 7

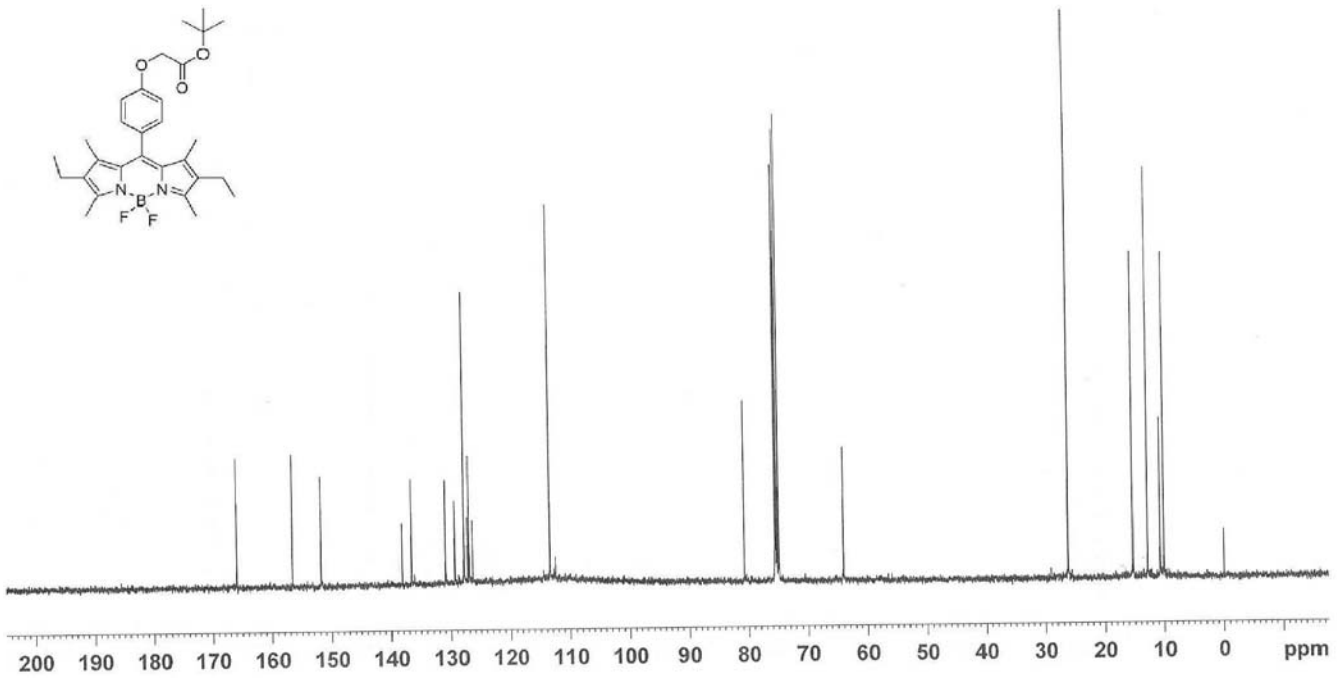

Figure 60: C NMR Spectrum of 7

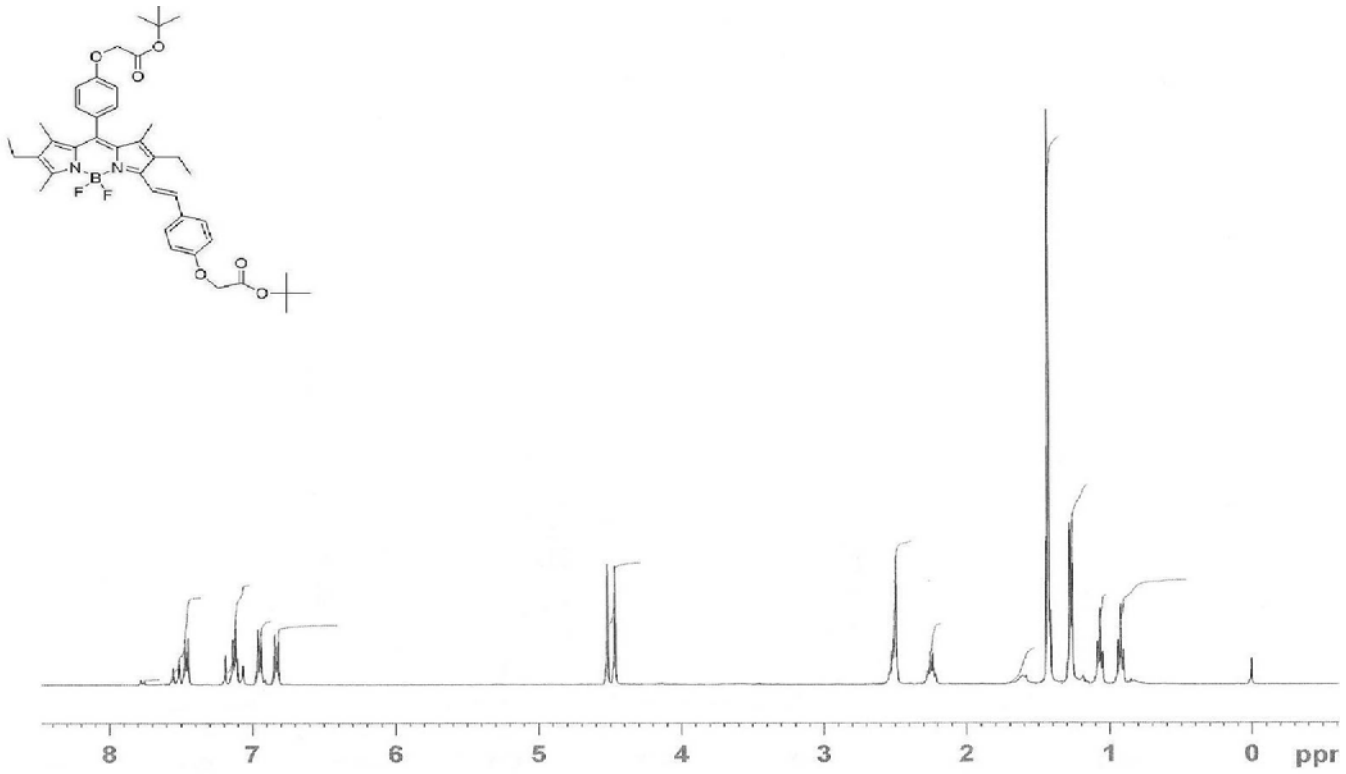

Figure 61: H NMR Spectrum of 14

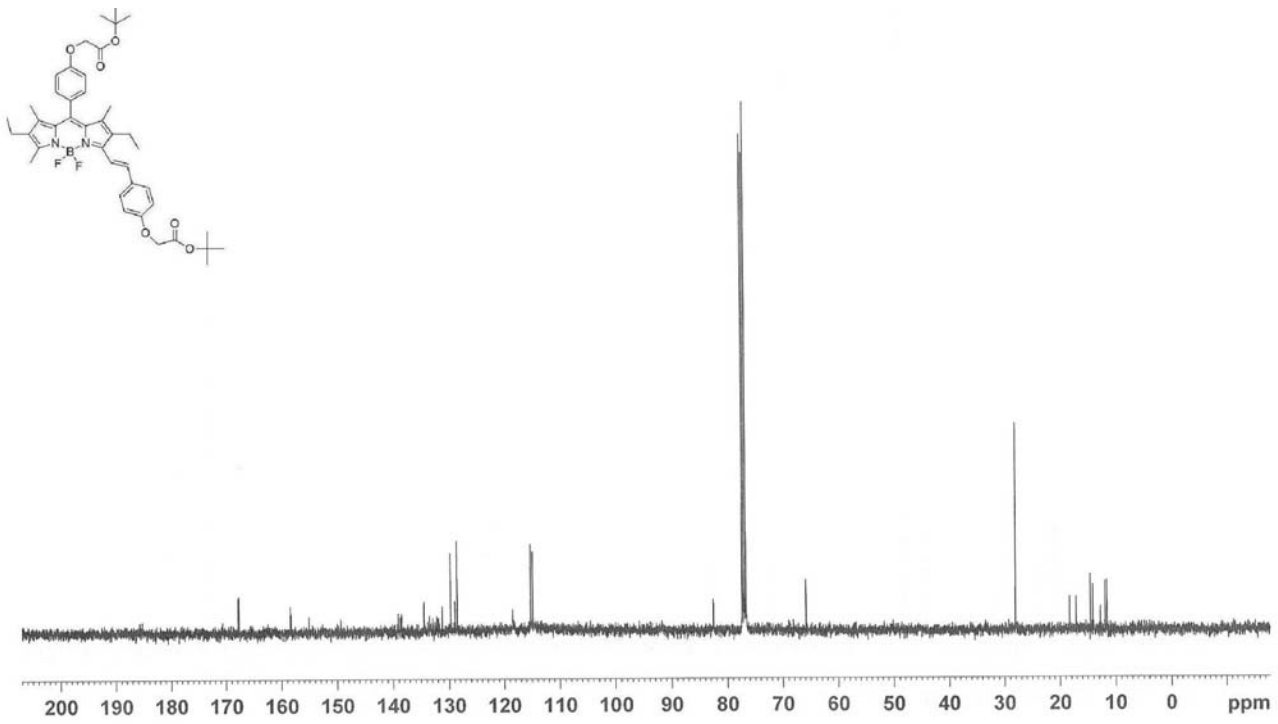

Figure 62: C NMR Spectrum of 14

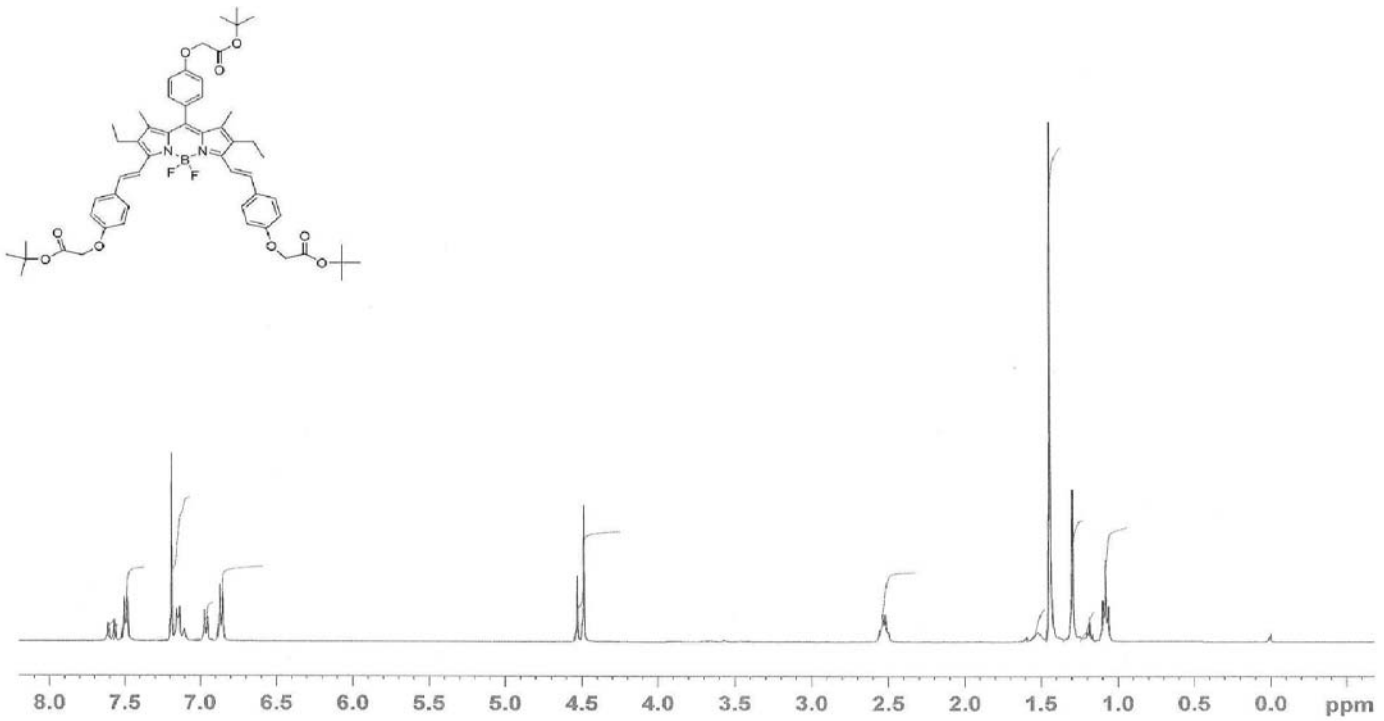

Figure 63: H NMR Spectrum of 15

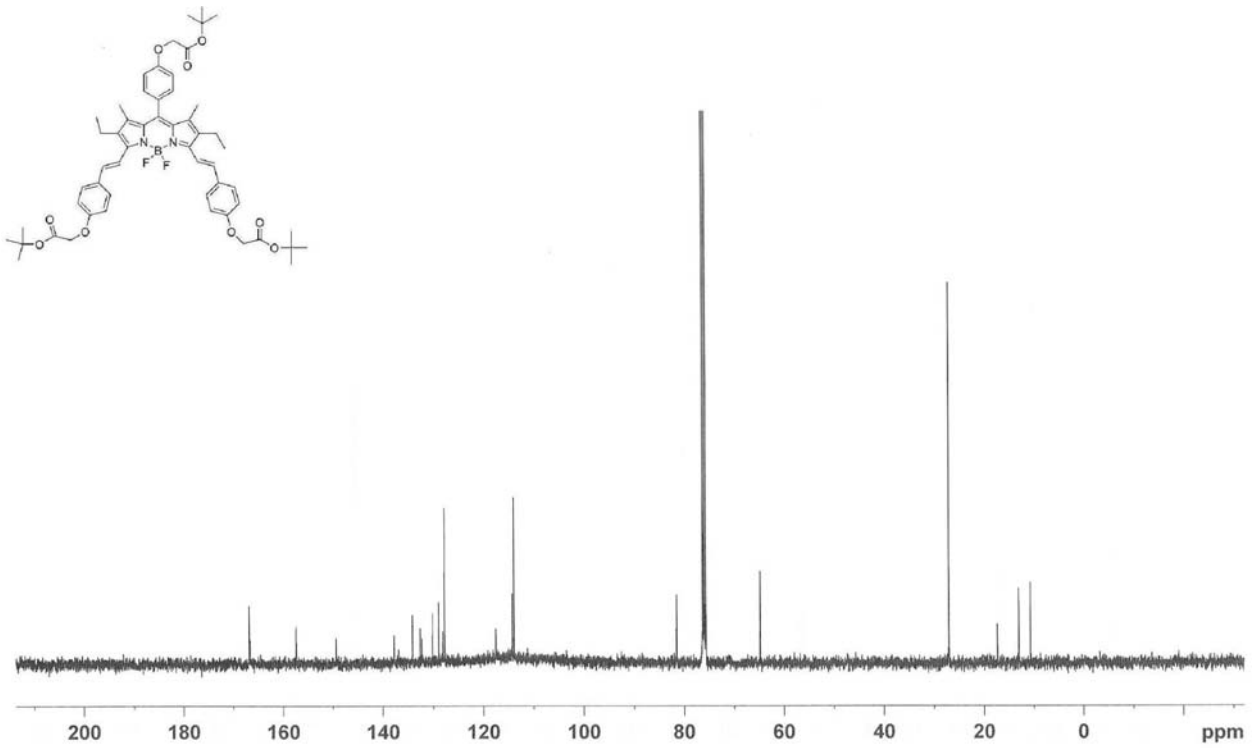

Figure 64: C NMR Spectrum of 15

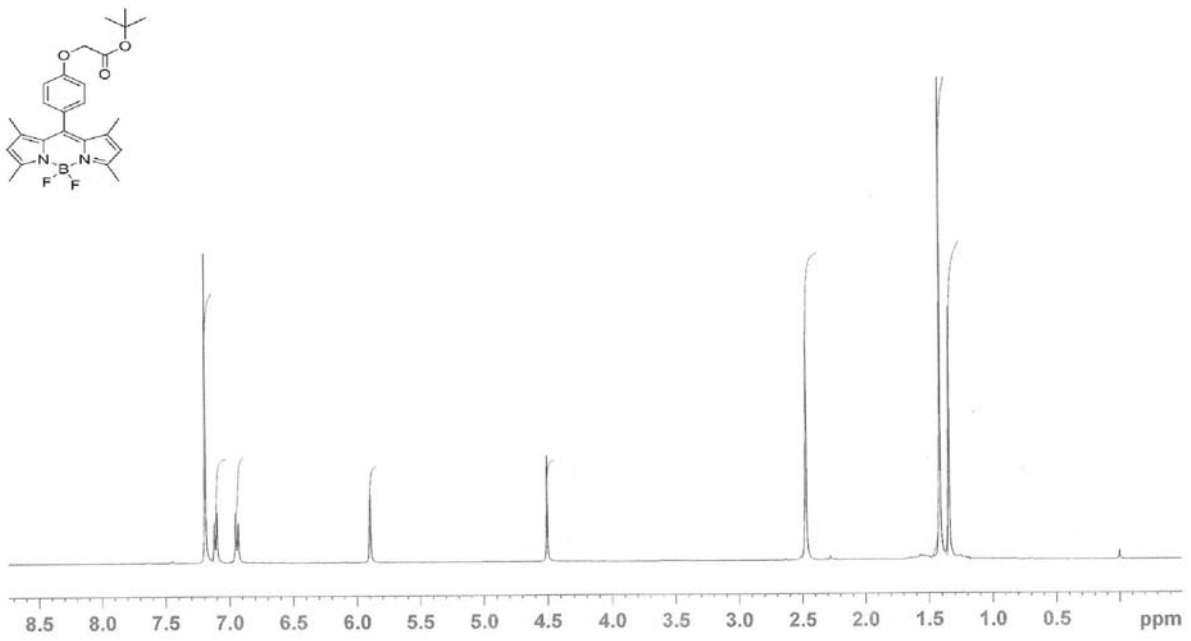

Figure 65: H NMR Spectrum of 6

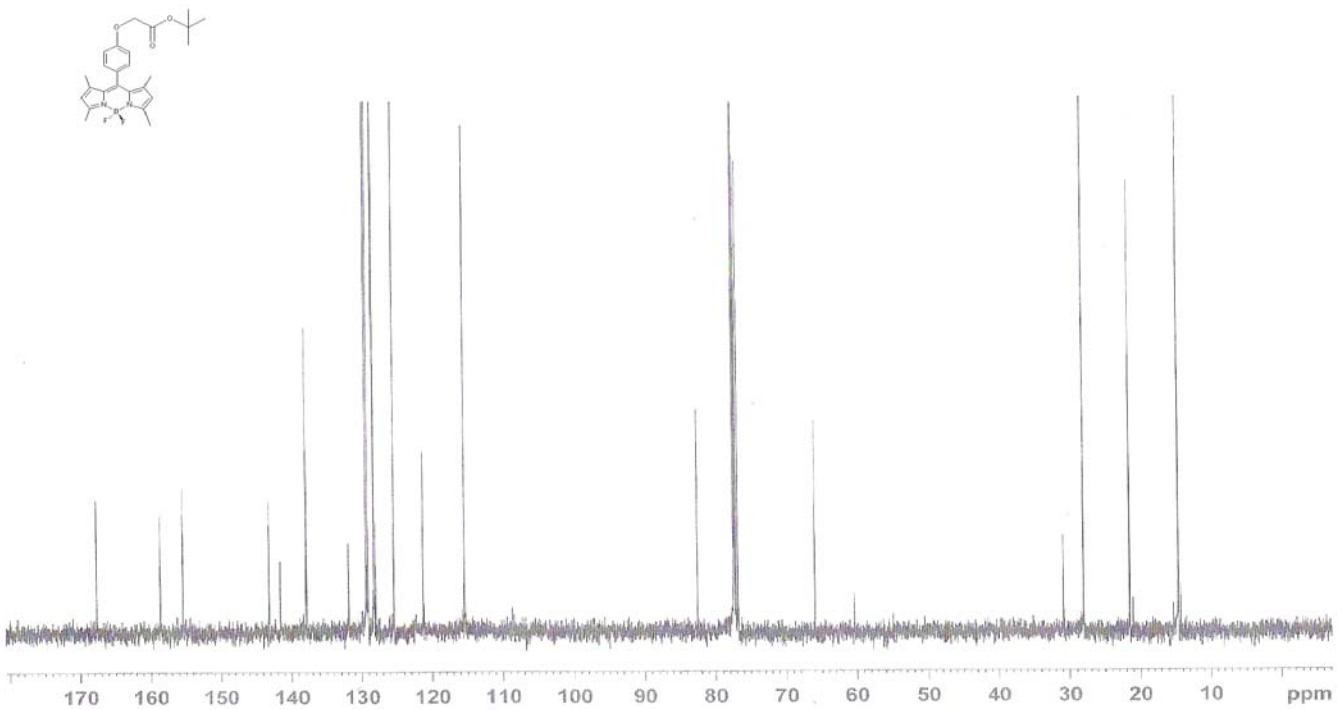

Figure 66: C NMR Spectrum of 6

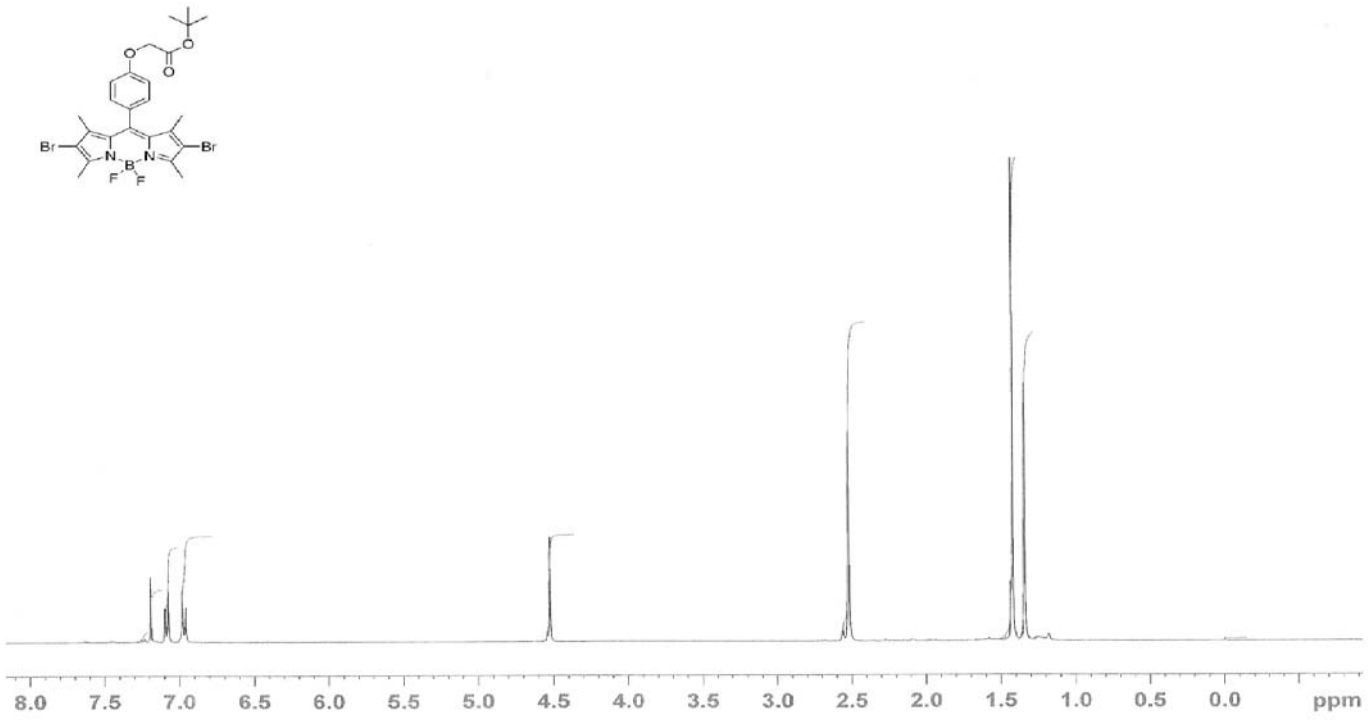

Figure 67: H NMR Spectrum of 9

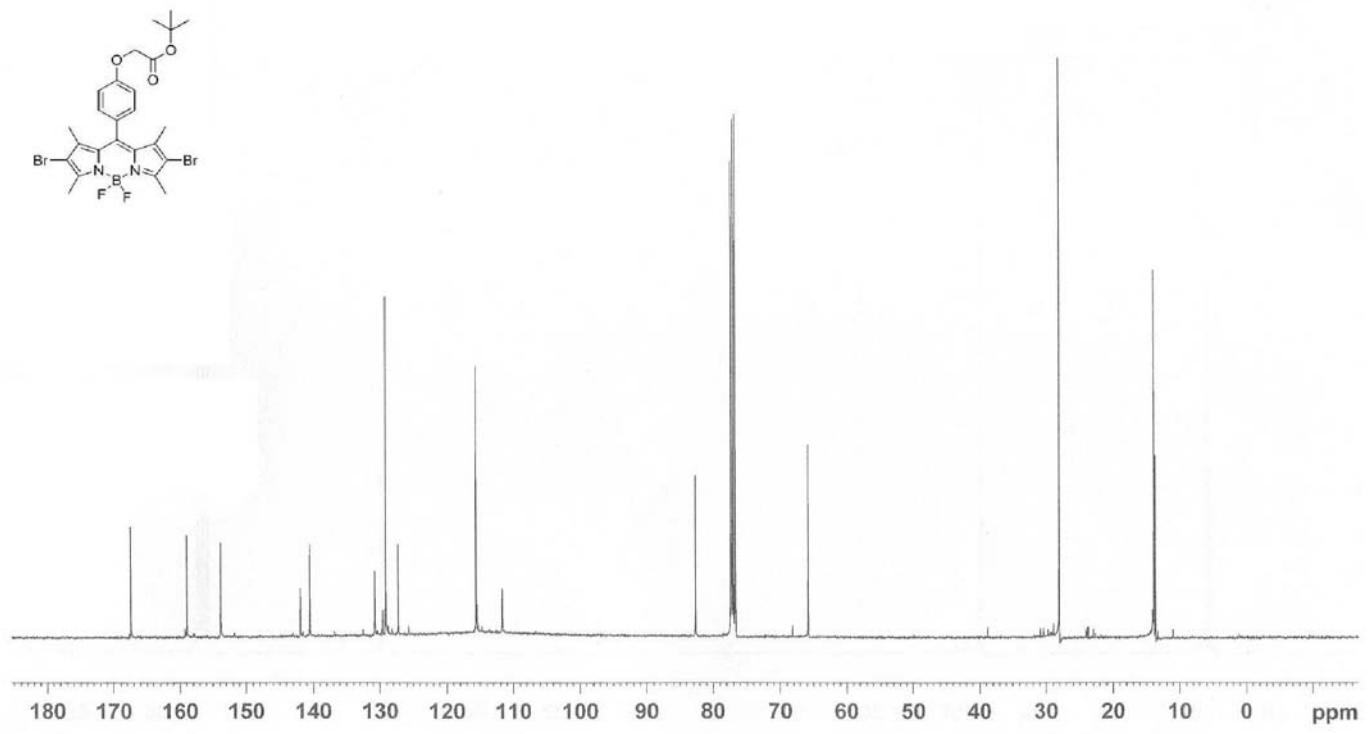

Figure 68: C NMR Spectrum of 9

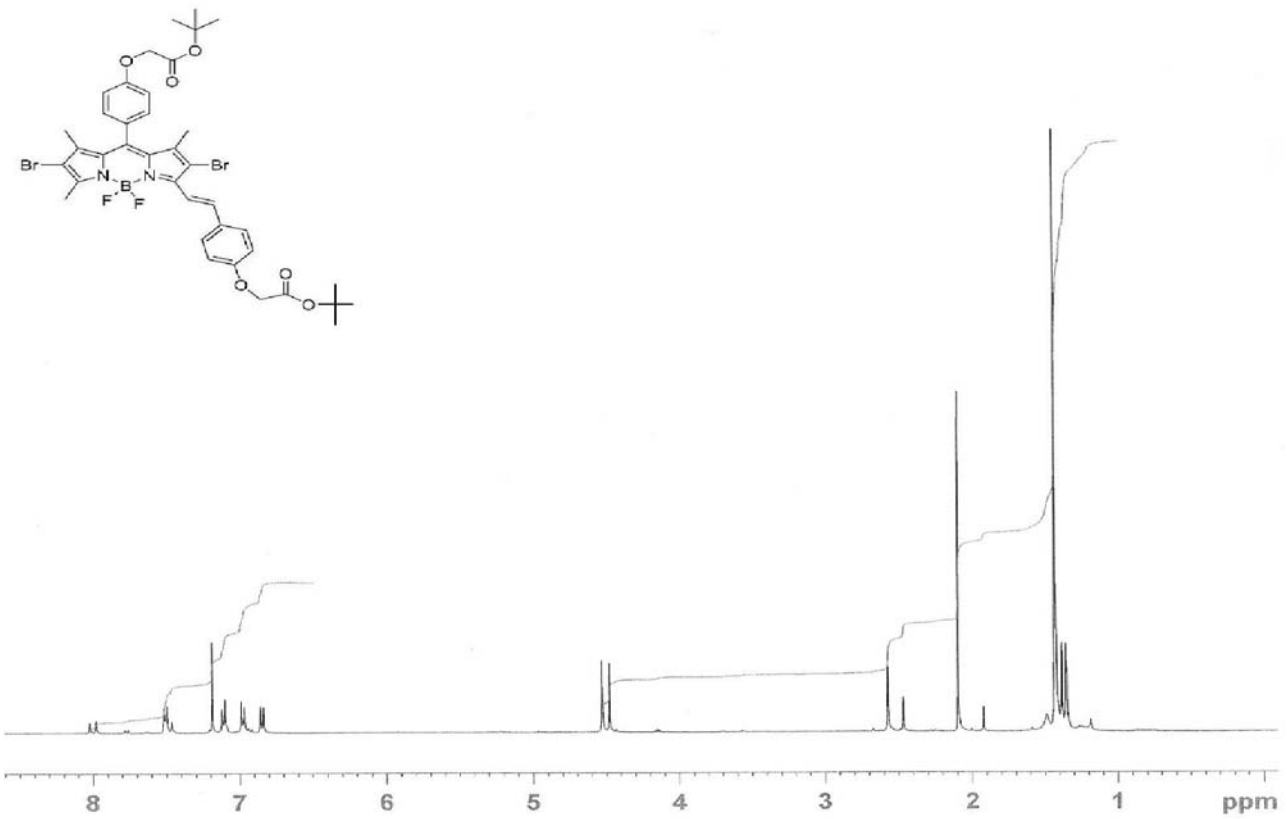

Figure 69: H NMR Spectrum of 12

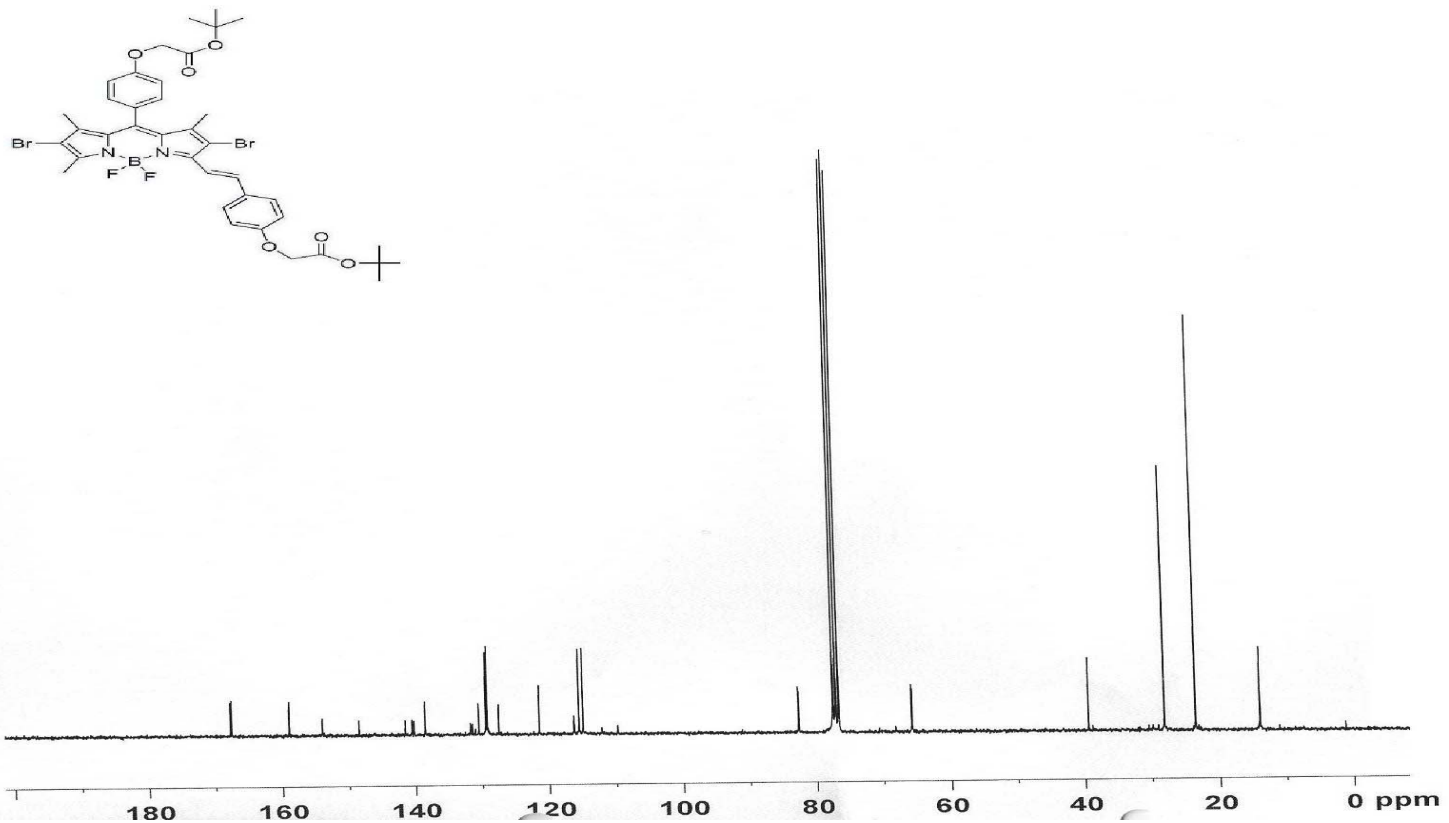

Figure 70: C NMR Spectrum of 12

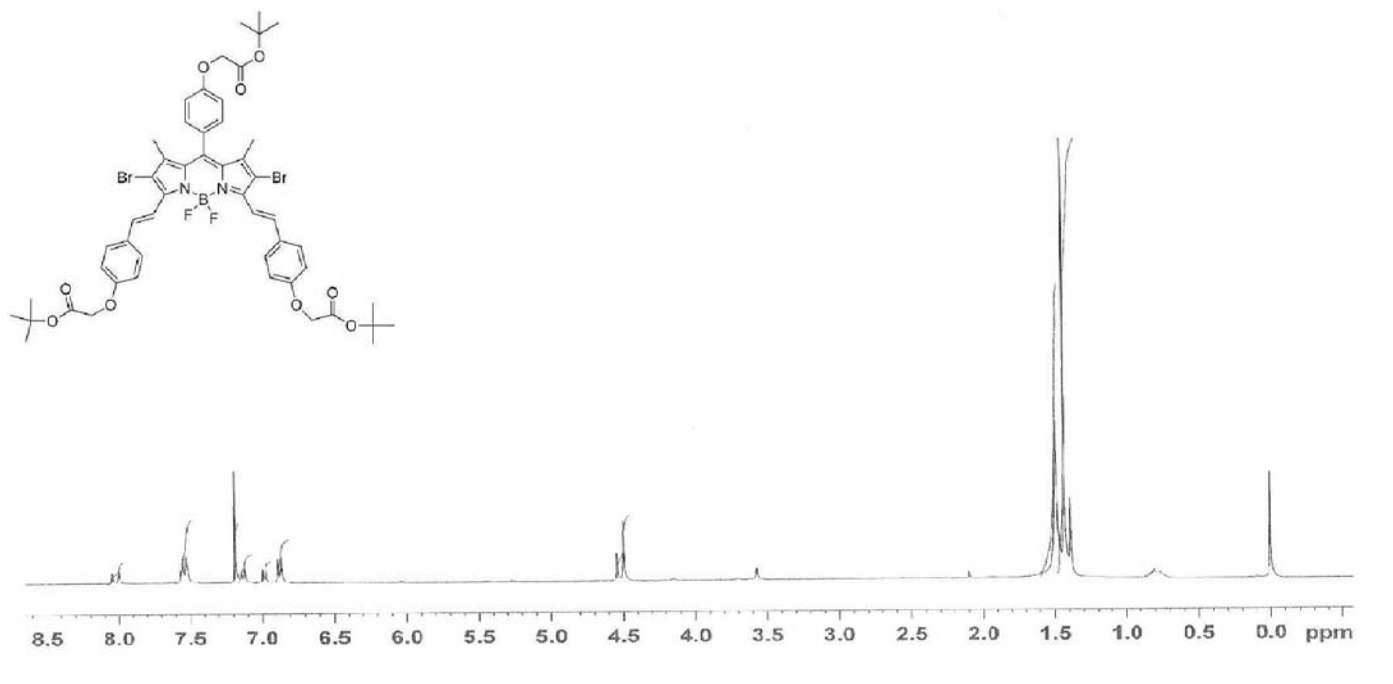

Figure 71: H NMR Spectrum of 13

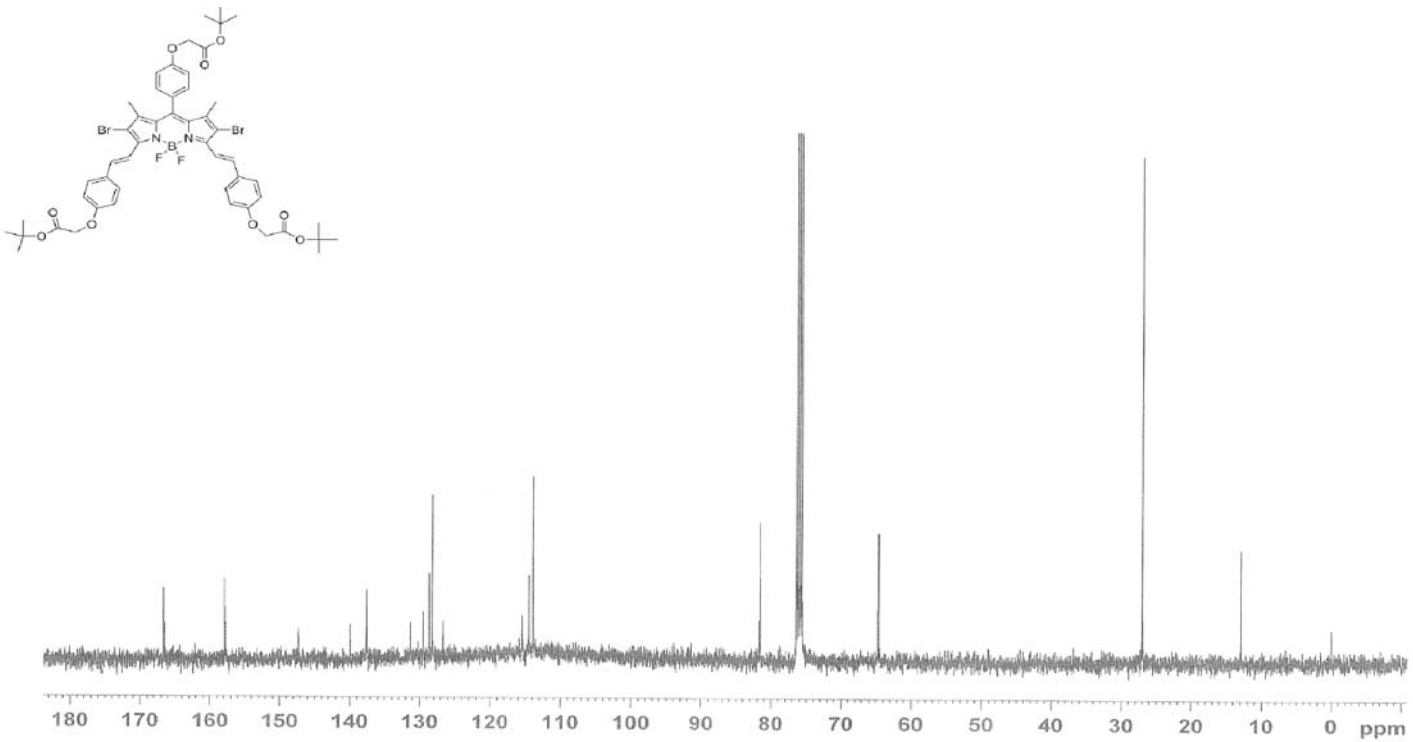

Figure 72: C NMR Spectrum of 13